FINAL REPORT

TECHNICAL TASK DIRECTIVE NO. VA-1039
CONTRACT NO. DTRS-57-89-D-00006

on

STRESS ANALYSIS OF STUB SILL TANK CARS

to

VOLPE NATIONAL TRANSPORTATION SYSTEMS CENTER
RESEARCH AND SPECIAL PROGRAMS ADMINISTRATION
U.S. DEPARTMENT OF TRANSPORTATION

December 15, 1993

by

Charles R. Miele and Richard C. Rice

Battelle
505 King Ave
Columbus, Ohio 43201

NOTICE

NOTICE

PREFACE

This report summarizes the results of a detailed stress analysis and fatigue assessment of two stub sill tank car designs often used for the transport of hazardous materials. This particular class of railroad cars has come under scrutiny by the Federal Railroad Administration in recent years because of occasional stub sill tank car failures that have led to the release of hazardous materials. The United States and Canadian governments asked the tank car industry to inspect at least 1,100 tank cars, perform a theoretical analysis of the stub sill problem, and then evaluate the inspection results compared with theoretical calculations.

In line with these actions, the FRA decided that an independent, detailed stress analysis of several common stub sill tank car designs was needed to assist in the determination of whether certain corrective actions taken by the industry would help reduce the incidence of stub sill fatigue cracking and to help the parties involved evaluate the criticality of cracks found during routine inspections.

The shell of a stub sill tank car is a primary structural element, since any buff or draft forces incurred in service are transmitted through the tank shell. The most critical site, in terms of stress concentration and the likelihood of fatigue cracking, tends to be the welded region where the stub sill is welded to the tank shell. That stub sill/tank shell transition region was the primary focus of the study described in this report.

This work was sponsored by the FRA Office of Research and Development in Washington, D.C. under the guidance of Mr. Jose Pena. The technical effort was monitored by the Volpe National Transportation Systems Center (VNTSC) in Cambridge, MA. The key individuals at VNTSC were Ms. Yim Har Tang and Dr. Oscar Orringer. The ongoing technical reviews and guidance provided by these individuals is gratefully acknowledged by the authors.

An integral part of this study was the comparison of stress analysis predictions with actual test results on a strain-gaged stub sill tank car tested at the Transportation Test Center in Pueblo, CO. The cooperation and assistance of Mr. David Cackovic of TTC is very much appreciated.

TABLE OF CONTENTS

Section	Page
1.0 INTRODUCTION	1
2.0 ANALYSIS PROCEDURE	9
2.1 Mesh Generation and Modeling Assumptions	9
2.1.1 Model Validation and Quality Assurance	10
2.2 Load Applications and Boundary Conditions	10
2.3 Stress Analysis	19
2.4 Assumed Field Loading Spectra	21
2.5 Crack Initiation Analysis Methodology	22
2.6 Crack Growth Analysis Methodology	23
3.0 Evaluation of Cracking Potential and Criticality	25
3.1 North American Tank Car; NATX 34081 Series	25
3.1.1 Crack Initiation Potentials	26
3.1.2 Potentially Dangerous Cracks	29
3.2 Trinity Car Class TK-S, ATSF 98600-94749	34
3.2.1 Crack Initiation Potentials	34
3.2.2 Potentially Dangerous Cracks	37
4.0 Evaluation of Stub Sill Inspection Procedure	39
5.0 Correlation of Analytical and Experimental Results	41
6.0 Discussion of Results	59
6.1 Crack Initiation Potentials	59
6.2 Potentially Dangerous Cracks	64
7.0 Conclusions	66
8.0 References	67
APPENDICES	
A Von Mises Plots for Potentially Critical Locations	A-1
B Local Stress Plots for Each Potentially Critical Location	B-1
C Stress Plots Supporting the Stub Sill Inspection Procedure	C-1

LIST OF ILLUSTRATIONS

Figure		Page
1.	FINITE ELEMENT MODEL FOR THE NATX 34081 SERIES CAR	2
2.	FINITE ELEMENT MODEL FOR THE TRINITY CAR, CLASS TK-S	3
3.	DETAILED FINITE ELEMENT MODEL OF NATX CAR WITH HEAD BRACE	5
4.	DETAILED FINITE ELEMENT MODEL OF NATX CAR WITHOUT HEAD BRACE	6
5.	DETAILED FINITE ELEMENT MODEL OF TRINITY CAR WITH HEAD BRACE	7
6.	DETAILED FINITE ELEMENT MODEL OF TRINITY CAR WITHOUT HEAD BRACE	8
7.	VNTSC SHELL PROGRAM RESULTS FOR THE NATX CAR IN COMPARISON WITH FINITE ELEMENT RESULTS	11
8.	QUARTER SYMMETRIC MODEL	12
9.	HALF SYMMETRIC MODEL	13
10.	COMPRESSION BUFF LOADS AND BOUNDARY CONDITIONS	14
11.	UPWARD VERTICAL LOAD AND BOUNDARY CONDITIONS	15
12.	OFFSET VERTICAL (INSPECTION PROCEDURE) LOAD AND BOUNDARY CONDITIONS - EMPTY TANK	16
13.	OFFSET VERTICAL (INSPECTION PROCEDURE) LOAD AND BOUNDARY CONDITIONS - FULL TANK	17
14.	PURE TORSION (ROLLOVER DERAILMENT) LOAD AND BOUNDARY CONDITIONS	18
15.	EXAGGERATED DISPLACEMENT PLOT OF NATX CAR - COMPRESSION BUFF LOAD	20
16.	AAR DESIGNATED CRITICAL AREAS	32
17.	ADDITIONAL AREAS OF OBSERVED CRACKING	33
18.	GENERAL VIEW OF STRAIN GAGED AREA ADJACENT TO THE STUB SILL ON THE TRINITY CAR	42
19.	CLOSEUP VIEW OF STRAIN GAGED AREA ON THE TRINITY CAR	43
20.	ILLUSTRATION OF EQUIVALENT UPWARD VERTICAL MOMENTS APPLIED IN THE FIELD AND IN THE ANALYSIS	45
21.	LONGITUDINAL STRAIN CONTOURS IN THE STRAIN GAGED AREA FOR THE UPWARD VERTICAL LOADING CASE	48
22.	CIRCUMFERENTIAL STRAIN CONTOURS IN THE STRAIN GAGED AREA FOR THE UPWARD VERTICAL LOADING CASE	49
23.	LONGITUDINAL STRESS CONTOURS IN THE STRAIN GAGED AREA FOR THE UPWARD VERTICAL LOADING CASE	51
24.	CIRCUMFERENTIAL STRESS CONTOURS IN THE STRAIN GAGED AREA FOR THE UPWARD VERTICAL LOADING CASE	52
25.	MAXIMUM PRINCIPAL STRESS CONTOURS IN THE STRAIN GAGED AREA FOR THE UPWARD VERTICAL LOADING CASE	53
26.	MINIMUM PRINCIPAL STRESS CONTOURS IN THE STRAIN GAGED AREA FOR THE UPWARD VERTICAL LOADING CASE	54

LIST OF ILLUSTRATIONS (Continued)

Figure		Page
27.	LONGITUDINAL STRESS CONTOURS IN THE STRAIN GAGED AREA FOR THE COMPRESSION BUFF LOADING CASE	55
28.	CIRCUMFERENTIAL STRESS CONTOURS IN THE STRAIN GAGED AREA FOR THE COMPRESSION BUFF LOADING CASE	56
29.	MAXIMUM PRINCIPAL STRESS CONTOURS IN THE STRAIN GAGED AREA FOR THE COMPRESSION BUFF LOADING CASE	57
30.	MINIMUM PRINCIPAL STRESS CONTOURS IN THE STRAIN GAGED AREA FOR THE COMPRESSION BUFF LOADING CASE	58
31.	VON MISES STRESS CONTOURS - NATX CAR WITH HEAD BRACE	60
32.	VON MISES STRESS CONTOURS - NATX CAR WITHOUT HEAD BRACE	61
33.	VON MISES STRESS CONTOURS - TRINITY CAR WITH HEAD BRACE	62
34.	VON MISES STRESS CONTOURS - TRINITY CAR WITHOUT HEAD BRACE	63

LIST OF TABLES

Table		Page
1.	Stub Sill Tank Car Load Cases	4
2.	Assumed Frequency and Severity of Field Loads for the Stub Sill Tank Car Fatigue Analysis	21
3.	Estimated Fatigue Properties From Reference [1]	23
4.	Summary of Maximum Von Mises Stresses for Potentially Critical Stub Sill Locations, North American Tank Car; NATX 34081 Series	27
5.	Summary of Highest Stress Sites in the NATX Car for each Load Case	30
6.	Summary of Orthogonal Stress Components in the NATX Car at Potentially Critical Sites Identified in Appendix A	31
7.	Summary of Maximum Von Mises Stresses for Potentially Critical Stub Sill Locations, Trinity Car Class TK-S; ATSF 98600-94749	35
8.	Summary of Highest Stress Sites in the Trinity Car for each Load Case	38
9.	Summary of Orthogonal Stress Components in the Trinity Car at Potentially Critical Sites Identified in Appendix A	40
10.	Comparison of TTC Strain Gage Results with Battelle Finite Element Analysis Results	46

LIST OF ABBREVIATIONS AND SYMBOLS

$2N_f$	Reversals to failure
A	Crack growth rate coefficient, also cross-sectional area
a	Crack length
AAR	Association of American Railroads
AE	Acoustic emission test
b	Fatigue strength exponent
c	Fatigue ductility exponent, also length in bending stress calculation
da/dN	Crack growth rate
DOT	Department of Transportation
FEA	Finite element analysis
FEEST	Freight Equipment Environmental Sampling Test
FRA	Federal Railroad Administration
HAZ	Heat affected zone
I	Moment of inertia
K	Cyclic strength coefficient
kips	Thousands of pounds
LCF	Longitudinal coupler force
M	Moment
m	Crack growth rate exponent
NATX	North American Car Company
P	Load
R	Stress ratio
SG	Strain gage
S_{max}	Maximum stress
S_{min}	Minimum stress
S_U	Ultimate strength
TTC	Transportation Test Center
VCF	Vertical coupler force
VNTSC	Volpe National Transportation Systems Center, or Volpe Center
X	Lateral (width) dimension
Y	Vertical (height) dimension, also geometry dependent factor in stress intensity solution
Z	Fore-aft (length) dimension

Greek Symbols

ΔK	Stress intensity range
ΔS	Stress range
$\Delta\varepsilon/2$	Strain amplitude
ε_{circ}	Local circumferential strain
ε'_f	Fatigue ductility coefficient
ε_{long}	Local longitudinal strain
μ	Local strain
η'	Cyclic strain hardening exponent
σ_{circ}	Circumferential stress
σ'_f	Fatigue strength coefficient

LIST OF ABBREVIATIONS AND SYMBOLS (Continued)

σ_{long}	Longitudinal stress
σ_m	Mean stress
σ_{max}	Maximum stress
σ_{min}	Minimum stress
σ_N	Nominal stress
σ_x	Longitudinal stress
σ'_y	Cyclic yield strength

EXECUTIVE SUMMARY

A detailed stress analysis of two stub sill tank car designs was completed to gain an improved understanding of the local stresses in these structures due to typical service loadings and to use this information to better understand the fatigue cracking problems that have recurred in the past few years. The primary area of concern in this investigation was the stub sill attachment region including the welds on the underside of the tank car. Stress distributions due to ten specific reference loading conditions were evaluated. The analytical results for two of these load cases were also compared with experimental results developed at the Transportation Test Center (TTC) in Pueblo, CO.

The potentially critical stub sill locations are illustrated in Appendix A, where color plots of the Von Mises stress contours are shown for each high stress location and loading combination. Appendix B includes numerous local stress plots for each potentially critical location and Appendix C shows detailed stress patterns resulting from the loading used as a part of the stub sill inspection procedure.

One of the load cases examined for this study was the "Offset Vertical" case, which represents the "Acoustic Emissions" test. The loading and boundary conditions given to Battelle for this case were based on verbal descriptions and calculated estimates; no measurements or test data were made available for the initial analyses. Several months later, after submission of the task final report, Dr. Henry Fowler of Monsanto provided a better description of the loading and support conditions for the Acoustic Emissions test. This information suggested that the boundary conditions and the load magnitudes used in the initial model for the Offset Vertical (Acoustic Emissions test) load case led to unrealistically high predicted stresses in the sill-to-tank interface area.

To assess the effect of these new boundary conditions on stress results, the Offset Vertical load case was rerun with a reduced vertical load, a shortened offset (twist bar) and no restraint at the truck pivot for the Trinity car with a full tank and no head brace. These new loads and boundary conditions were estimates based on followup conversations with Dr. Fowler.

The peak Von Mises stress in the Sill-to-Tank-Pad interface area were reduced substantially from 87 ksi to 45 ksi with these new boundary conditions applied. However, the **distribution** of stresses in the most critical regions remained essentially unchanged, i.e., the highest stress sites remained the same, with only the magnitude of the stresses changing. The reduced maximum principal stresses in the sill-to-tank area on the side in tension was 25 ksi, and the minimum principal stress in this same area on the side in compression (loaded side) was reduced in magnitude to -53 ksi.

Through scaling of the Von Mises stress results for the NATX car Offset Vertical load case by the ratio of 45/87, the highest estimated stress for the linear elastic analysis (originally 157 ksi) was reduced to 81 ksi.

Tables 5 and 8, which summarize the Von Mises stress results for the Offset Vertical load case, have been modified to reflect these estimated reductions in Von Mises stress for the NATX and Trinity cars. **No other tables, color contour plots, or captions for the Offset Vertical load case stress results have been modified**. The ratio of 45/87 may be applied to the other unmodified results for the Offset Vertical load case to estimate the reduction in stress levels.

These new results for the Offset Vertical load case probably offer a better estimate of the stresses typically induced by the Acoustic Emissions test. However, these results are still based on estimates and verbal information. If a true assessment of the stresses induced by the Acoustic Emissions test is required, additional analyses that are based on documented experimental data should be run on both cars for this loading condition.

In summary, based on this analytical effort there is significant evidence that:

- Both the NATX and Trinity tank cars showed that head braces significantly lower the stresses in the tank shell area with head braces installed - which suggests that the likelihood of fatigue cracking in these stub sill designs would be significantly reduced compared with tank cars without head braces.
- The head brace is less beneficial for reducing stresses in the Z-section lug area.
- The likelihood of fatigue damage due to compression buff loads is not diminished by the installation of a head brace.
- The effects of a draft load on the structure should be the same as the buff load, except opposite in sign. The draft load case was not run as a load case because we made the assumption that the stresses from the draft load will be the same as those produced by the buff load except opposite in sign. This should be verified experimentally or analytically.

1.0 INTRODUCTION

Stub sill tank cars are used to carry a variety of liquid chemicals and products. Many of these substances are considered hazardous. The safe transport of these materials depends to a large extent on tank car structural integrity. In a stub sill tank car, the tank is the main load carrying structural member with short (stub) sills at each end to attach the wheel truck and coupler. The stub sill - tank shell region is an area of particular concern because of the significant fluctuating stresses and the consequent potential for fatigue cracking and subsequent leakage.

Cracks in the tank car shell or weldment can develop from fatigue, corrosion or other causes. Service, maintenance, inspection, or derailment loads will induce stresses of various magnitudes and directions in the structure. Tensile stresses resulting from these loading conditions that are normal to any of these cracks will tend to open and propagate them.

The likelihood of fatigue cracking at potentially critical locations in two different stub sill tank car designs was evaluated in this study:

- North American Car Company, NATX 34081 Series, 33,800 gallon capacity, and
- Trinity Industries TK-S Class, DOT-111A100W1, 26,000 gallon capacity.

Figures 1 and 2 show overall views of the NATX and Trinity car finite element models.

The NATX car analysis was completed first because Battelle had done a previous study on this car, and drawings were immediately available[1]*. The Trinity car was also chosen for analysis because the Federal Railroad Administration and the Volpe National Transportation Systems Center (VNTSC) had a testing program underway at the Transportation Test Center (TTC) using a Trinity car[2]. As a result, the finite element results could be used as a supplement to their test data. In addition, correlation of the two provided a good validation of the analytical results.

The objectives of this study were to:

1) perform a detailed stress analysis of existing stub sill tank cars,
2) evaluate the stub sill inspection procedure,
3) evaluate service/design loads, and
4) characterize stresses for service life prediction.

The ten load cases chosen for this study are summarized in Table 1. The compression buff and upward vertical load cases represent common service loads. The pure torsion loading case was used to simulate the loading that might occur in a rollover derailment of a stub sill tank car. The

* References are listed on page 67.

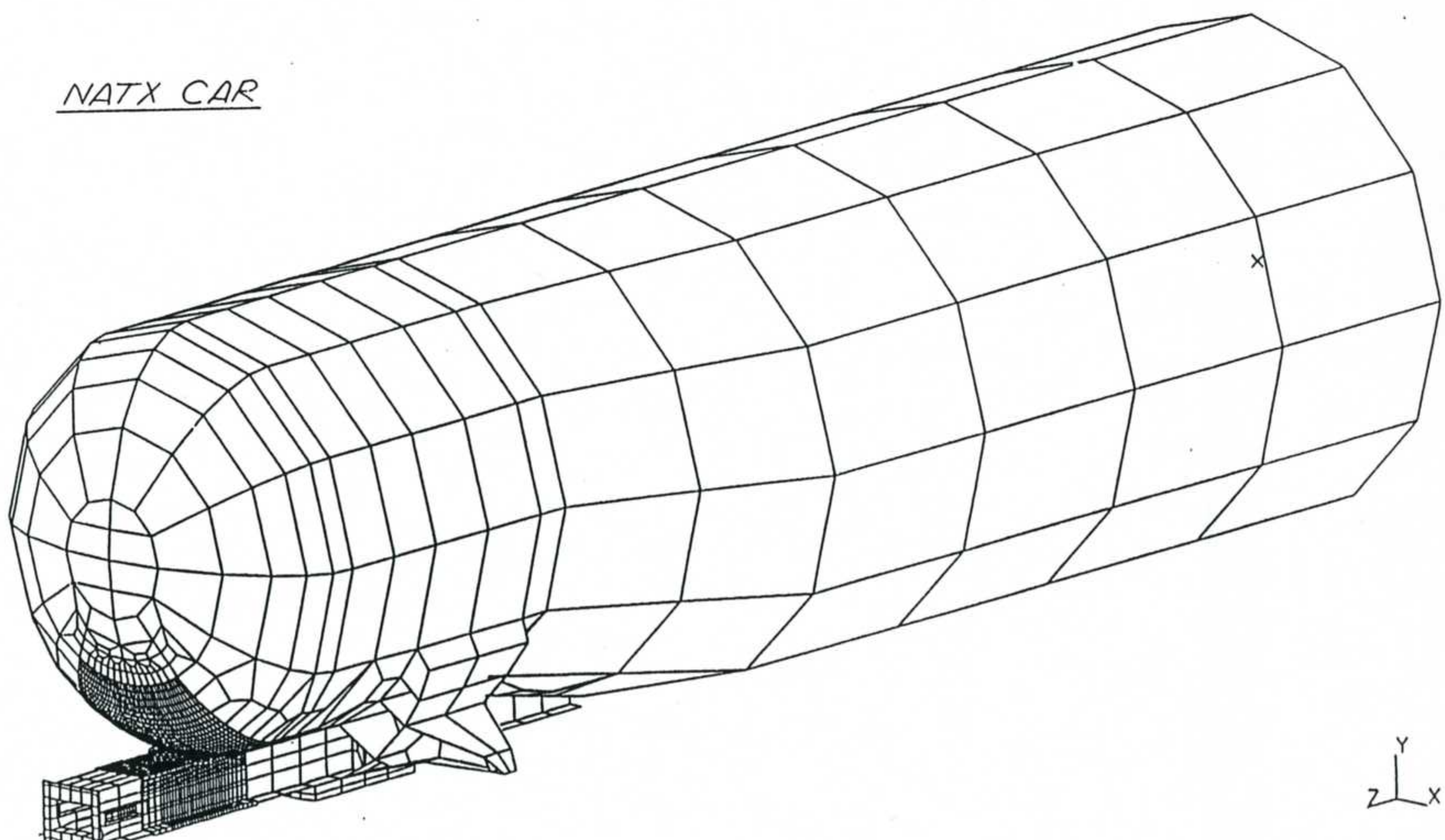

FIGURE 1. FINITE ELEMENT MODEL FOR THE NATX 34081 SERIES CAR

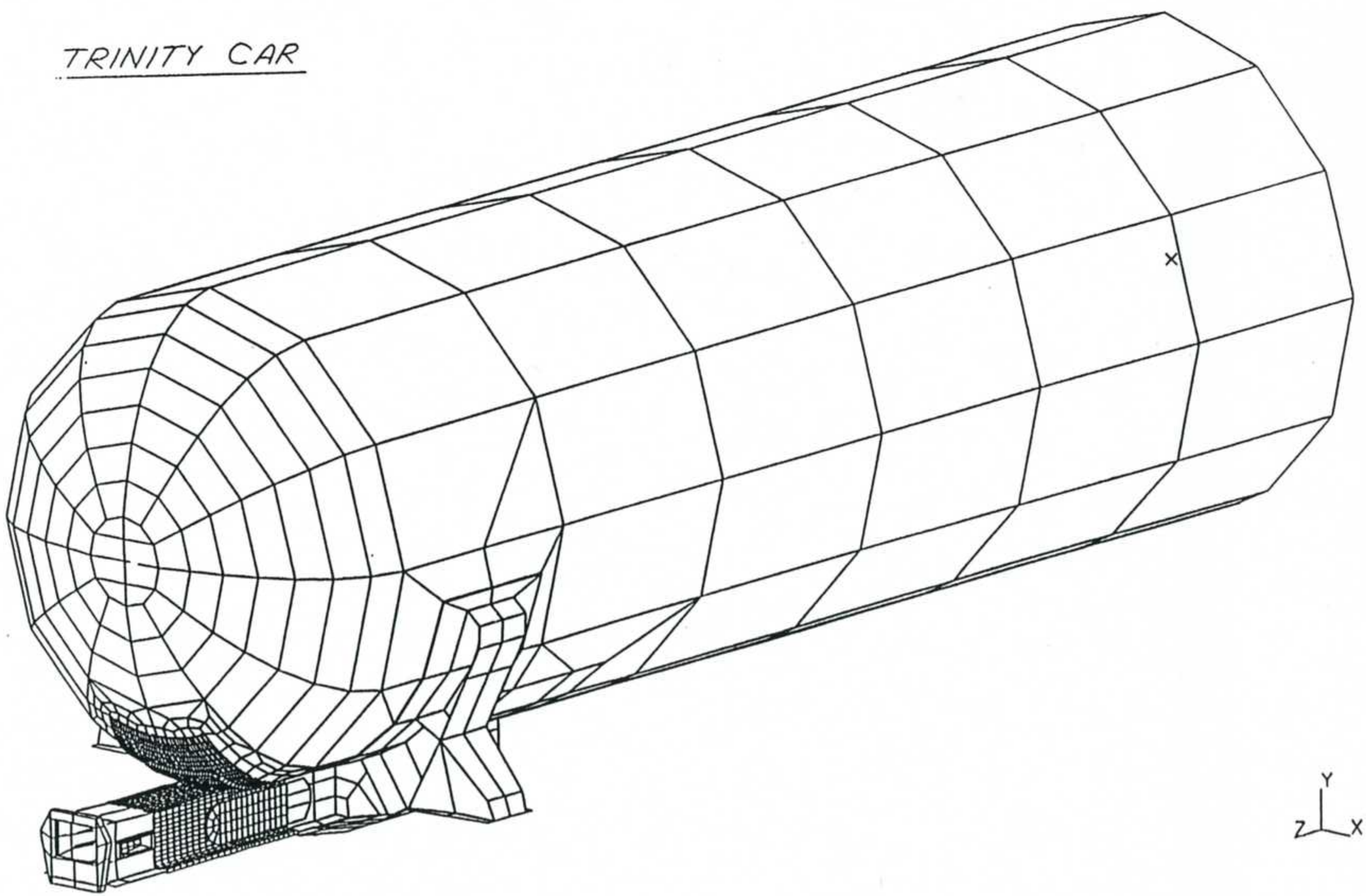

FIGURE 2. FINITE ELEMENT MODEL FOR THE TRINITY CAR, CLASS TK-S

offset vertical loading case was included to model the loading that has been applied to stub sill tank cars at TTC as part of a nondestructive ("Acoustic Emissions") inspection test. The upward vertical loading case was meant to simulate the significant vertical loads seen in service. As Table 1 illustrates, comparative analyses between head brace/no head brace and full tank/empty tank conditions were also completed. Figures 3 through 6 show close up views of the stub sill area for both cars with and without head braces.

Table 1. Stub Sill Tank Car Load Cases

LOAD	CONFIGURATION	
Compression Buff	Full Tank	Head Brace
Compression Buff	Full Tank	No Head Brace
Upward Vertical	Full Tank	Head Brace
Upward Vertical	Full Tank	No Head Brace
Pure Torsion	Full Tank	Head Brace
Pure Torsion	Full Tank	No Head Brace
Offset Vertical	Full Tank	Head Brace
Offset Vertical	Full Tank	No Head Brace
Offset Vertical	Empty Tank	Head Brace
Offset Vertical	Empty Tank	No Head Brace

FIGURE 3. DETAILED FINITE ELEMENT MODEL OF NATX CAR WITH HEAD BRACE

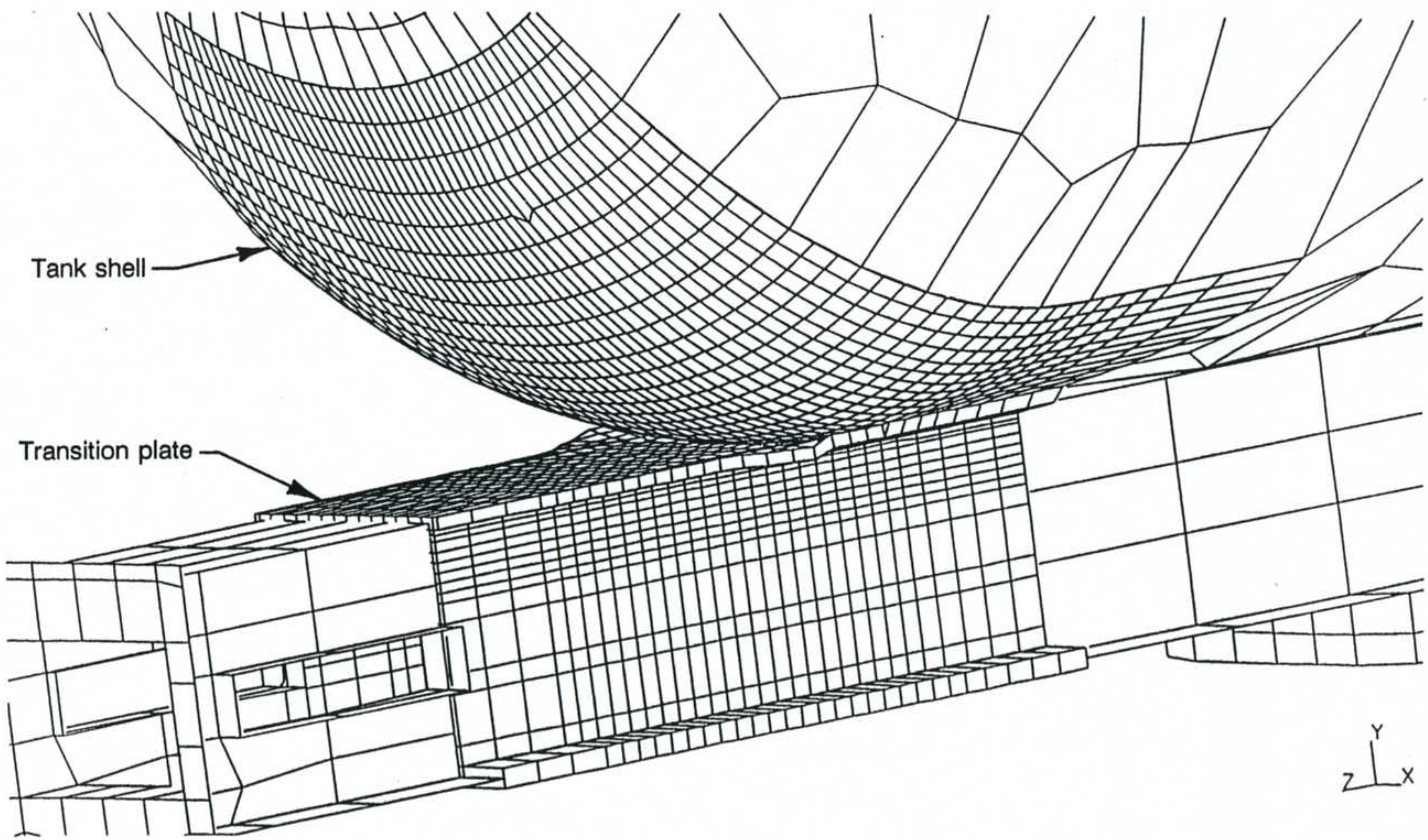

FIGURE 4. DETAILED FINITE ELEMENT MODEL OF NATX CAR WITHOUT HEAD BRACE

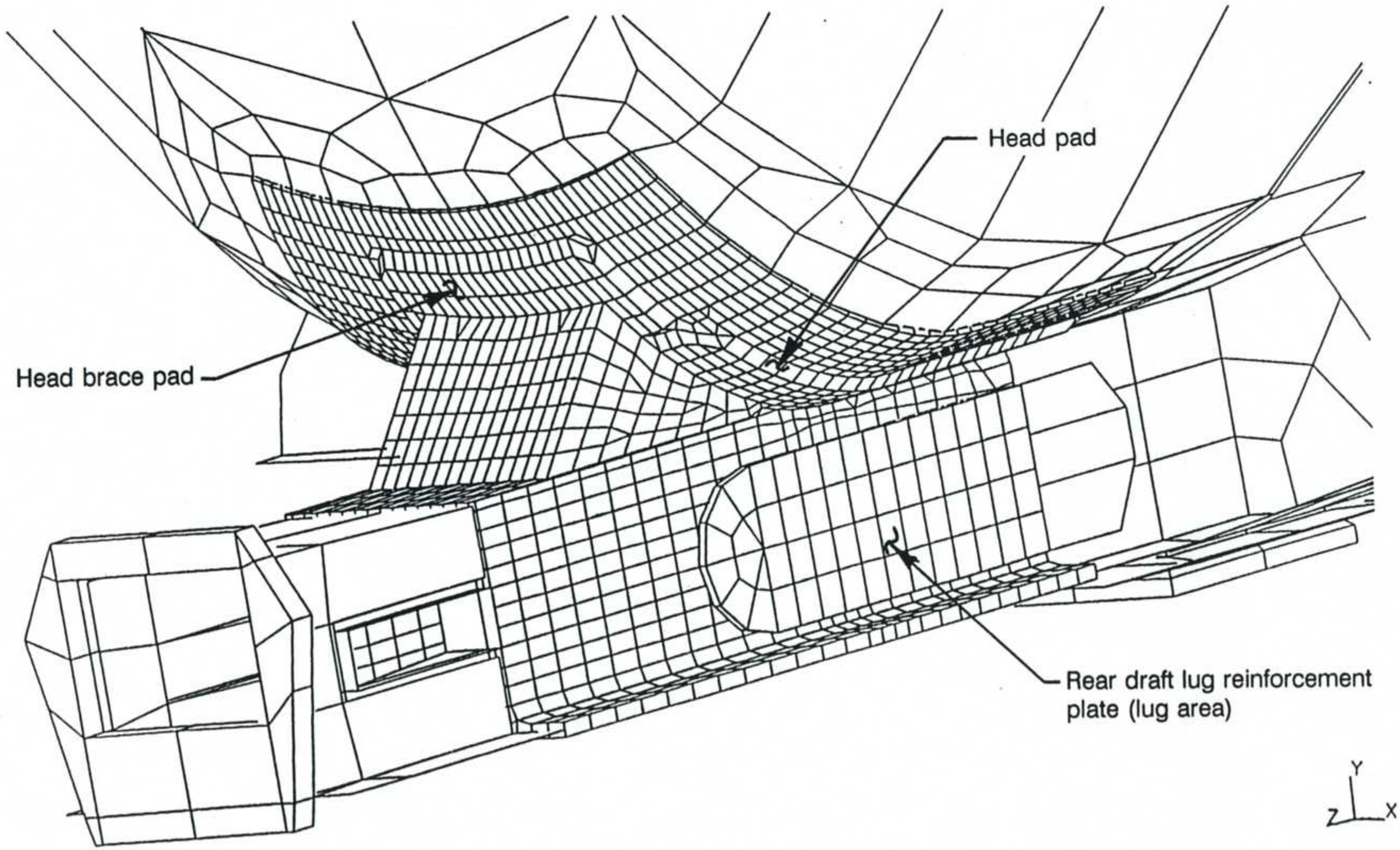

FIGURE 5. DETAILED FINITE ELEMENT MODEL OF TRINITY CAR WITH HEAD BRACE

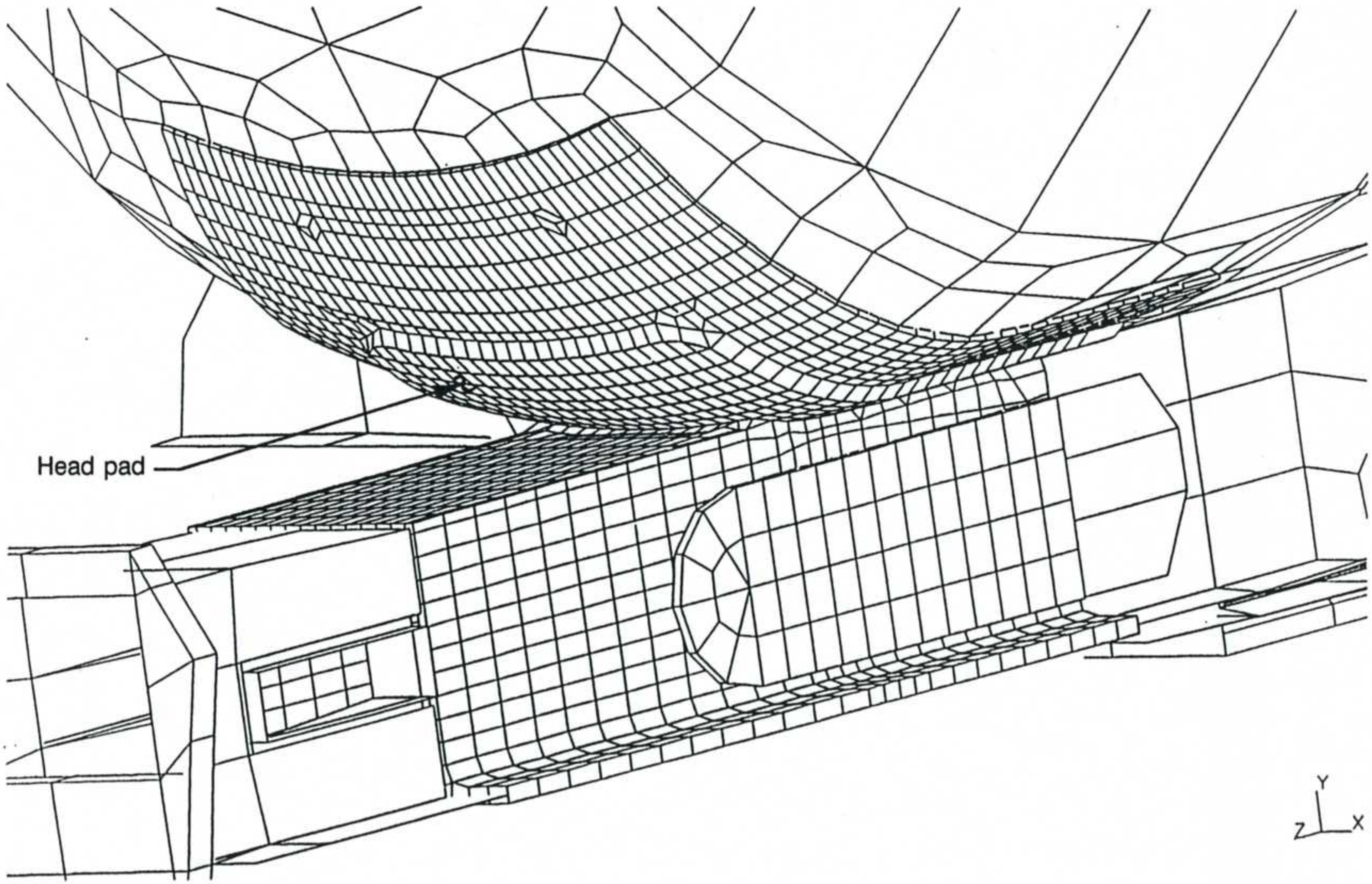

FIGURE 6. DETAILED FINITE ELEMENT MODEL OF TRINITY CAR WITHOUT HEAD BRACE

2.0 ANALYSIS PROCEDURE

A detailed finite element analysis was performed on two different stub sill tank car designs. Sections 2.1 through 2.3 detail the finite element methodology that was used, assumed loading configurations and boundary conditions, and key assumptions and areas of uncertainty. Sections 2.4 through 2.6 describe assumptions made concerning field service loads and the methodology used for the fatigue crack initiation and crack growth estimates.

2.1 Mesh Generation and Modeling Assumptions

The SDRC I-DEAS program[3] was used to develop both of the models. The models consisted of approximately 1000 linear, thin shell quadrilateral and triangular elements, 4000 linear solid brick and wedge elements, 90 rigid elements, a few beam elements, and a total of about 7000 nodes. Figures 1 and 2 showed the overall car models and coordinate system orientation. Note that X is the lateral (width) dimension, Y is the vertical (height) dimension, and Z is the fore-aft (length) dimension.

The basic modeling approach was to develop a detailed solid model in the tank shell and draft sill intersection areas surrounded by a coarse shell model of the rest of the car. This method provided detailed stress results in the areas of concern and a good stiffness representation for each tank car in areas where stress results were not required.

In each case, the coarse model was connected to the refined model using rigid elements. The rigid elements were specified so that all displacement degrees of freedom were the same at the intersection of the dissimilar (solid and shell) meshes. The rigid elements were also configured to transmit all forces and moments at the interface.

Most welds in the coarse region were same-node connections since the shell elements that were used have rotational degrees of freedom. Some weld connections were also made using rigid elements. Welds in the refined region were modeled explicitly wherever possible. Solid wedge elements were used for fillet welds, and solid brick elements were used for butt welds. Rigid elements were used for some welded connections when mesh dissimilarities complicated the modeling.

2.1.1 Model Validation and Quality Assurance

The finite element models of both the NATX and the Trinity Car were checked for validity and accuracy in several ways. The weight of the car components that were listed on the engineering drawings were compared with the weight that the finite element program calculated.

Weld locations and plate thicknesses in the finite element model were independently checked at Battelle by a knowledgeable person other than the person who built the finite element model. Plots of the weld locations were routed through VNTSC to the Trinity Car Co. and to the North American Car Co. for further confirmation. Sketches of loading and boundary conditions as understood by Battelle were sent to VNTSC to confirm that these conditions were represented properly. Exaggerated deformation plots were produced for each load case to confirm that the structure was reacting realistically to the applied loadings.

Finite element analysis stress results along the bottom of the tank shell from the Compression Buff load case were compared with a closed-form shell-theory analytical solution developed by VNTSC. A comparison of finite element results with the output from the shell program is shown in Figure 7. The results of the finite element analysis agreed with the VNTSC shell theory results within about 14 percent near the load application point, and within 10 percent in areas away from the load application point. The purpose of this comparison was not to achieve exact correlation; it was done to provide a reasonability check for the finite element calculations.

2.2 Load Applications and Boundary Conditions

There were two different boundary conditions used, depending on load symmetry. The "Quarter-Symmetric" load cases were the Compression Buff load and the Upward Vertical load. The "Half-Symmetric" load cases were the Offset Vertical load cases (as used in the acoustic emission inspections) with Full Tank and Empty Tank, and the Pure Torsion load case (simulating loading that might occur in a tank car derailment). Figure 8 shows a quarter symmetric model, and Figure 9 shows a half symmetric model.

There were a total of ten load cases which represented a combination of full tank/empty tank, and head brace/no head brace configurations (as detailed earlier in Table 1). Figures 10 through 14 are illustrations of the loading conditions shown on the NATX car. The loading conditions were the

2.1.1 Model Validation and Quality Assurance

The finite element models of both the NATX and the Trinity Car were checked for validity and accuracy in several ways. The weight of the car components that were listed on the engineering drawings were compared with the weight that the finite element program calculated.

Weld locations and plate thicknesses in the finite element model were independently checked at Battelle by a knowledgeable person other than the person who built the finite element model. Plots of the weld locations were routed through VNTSC to the Trinity Car Co. and to the North American Car Co. for further confirmation. Sketches of loading and boundary conditions as understood by Battelle were sent to VNTSC to confirm that these conditions were represented properly. Exaggerated deformation plots were produced for each load case to confirm that the structure was reacting realistically to the applied loadings.

Finite element analysis stress results along the bottom of the tank shell from the Compression Buff load case were compared with a closed-form shell-theory analytical solution developed by VNTSC. A comparison of finite element results with the output from the shell program is shown in Figure 7. The results of the finite element analysis agreed with the VNTSC shell theory results within about 14 percent near the load application point, and within 10 percent in areas away from the load application point. The purpose of this comparison was not to achieve exact correlation; it was done to provide a reasonability check for the finite element calculations.

2.2 Load Applications and Boundary Conditions

There were two different boundary conditions used, depending on load symmetry. The "Quarter-Symmetric" load cases were the Compression Buff load and the Upward Vertical load. The "Half-Symmetric" load cases were the Offset Vertical load cases (as used in the acoustic emission inspections) with Full Tank and Empty Tank, and the Pure Torsion load case (simulating loading that might occur in a tank car derailment). Figure 8 shows a quarter symmetric model, and Figure 9 shows a half symmetric model.

There were a total of ten load cases which represented a combination of full tank/empty tank, and head brace/no head brace configurations (as detailed earlier in Table 1). Figures 10 through 14 are illustrations of the loading conditions shown on the NATX car. The loading conditions were the

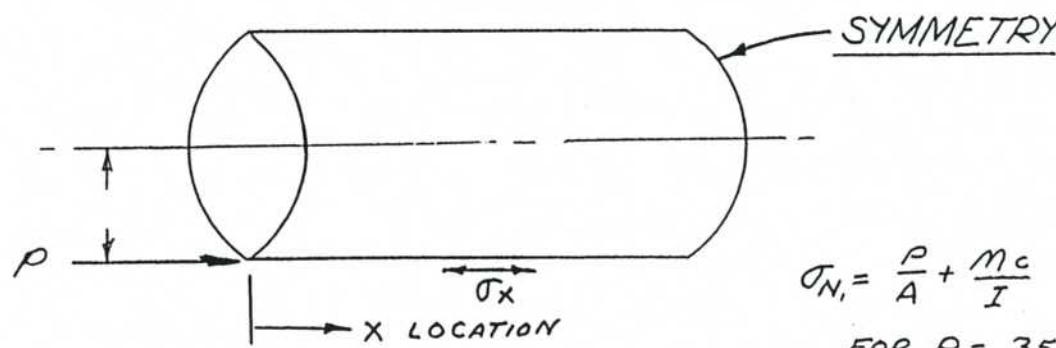

$$\sigma_{N_1} = \frac{P}{A} + \frac{Mc}{I} \qquad \sigma_{N_2} = \frac{P}{A}$$

FOR $P = 350{,}000$

$\sigma_{N_1} = 4100$ PSI $\sigma_{N_2} = 1350$ PSI

2 BOUNDING CASES
DUE TO VERTICAL RESTRAINT

OUTPUT FROM TSC SHELL PROGRAM

X LOCATION	BNX
25.930	4.666
51.860	3.282
77.790	2.745
103.720	2.442
129.650	2.241
155.580	2.096
181.510	1.985
207.440	1.896

MULTIPLY σ_N BY BNX TO GET σ_x

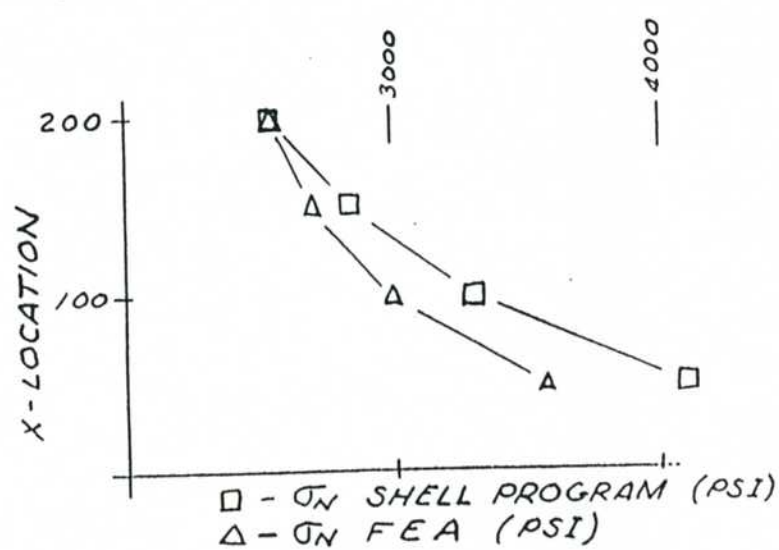

FIGURE 7. VNTSC SHELL PROGRAM RESULTS FOR THE NATX CAR IN COMPARISON WITH FINITE ELEMENT RESULTS

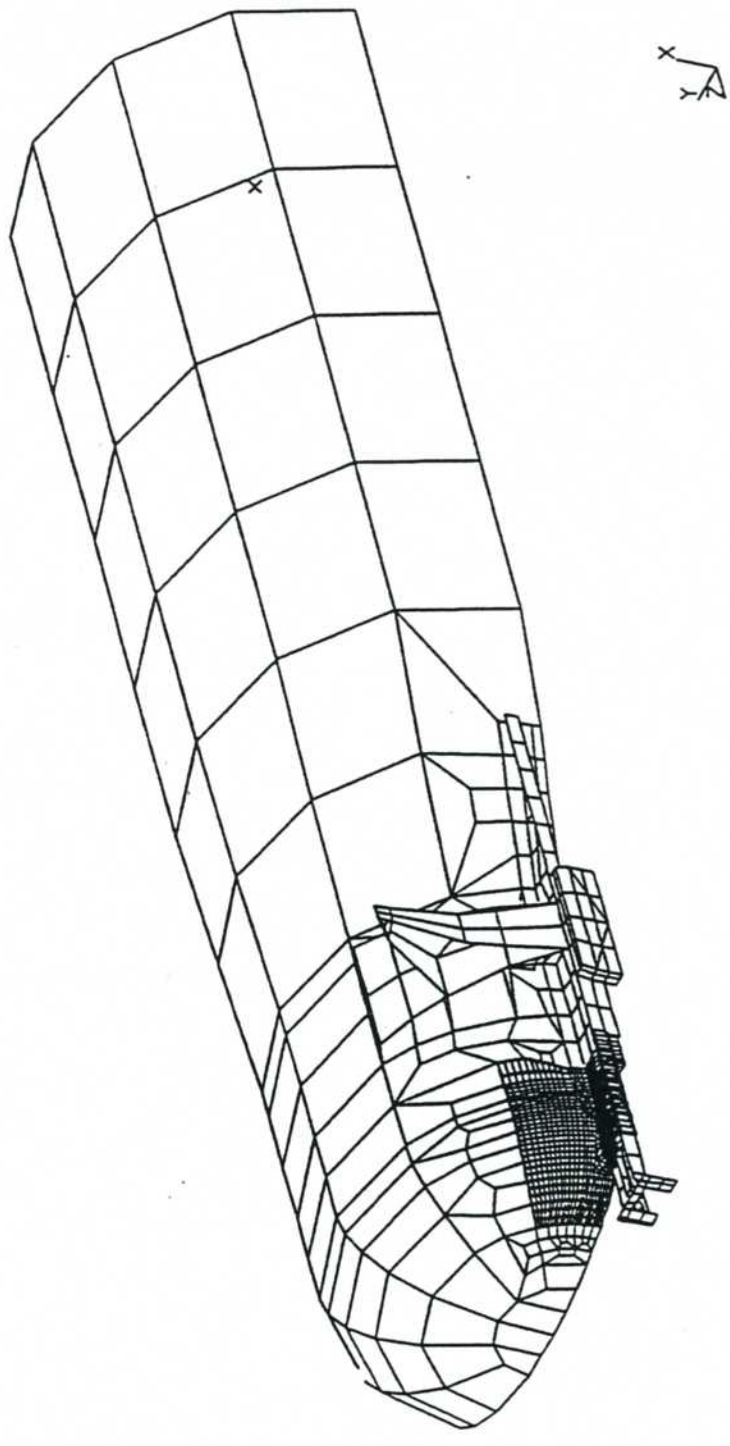

FIGURE 8. QUARTER SYMMETRIC MODEL

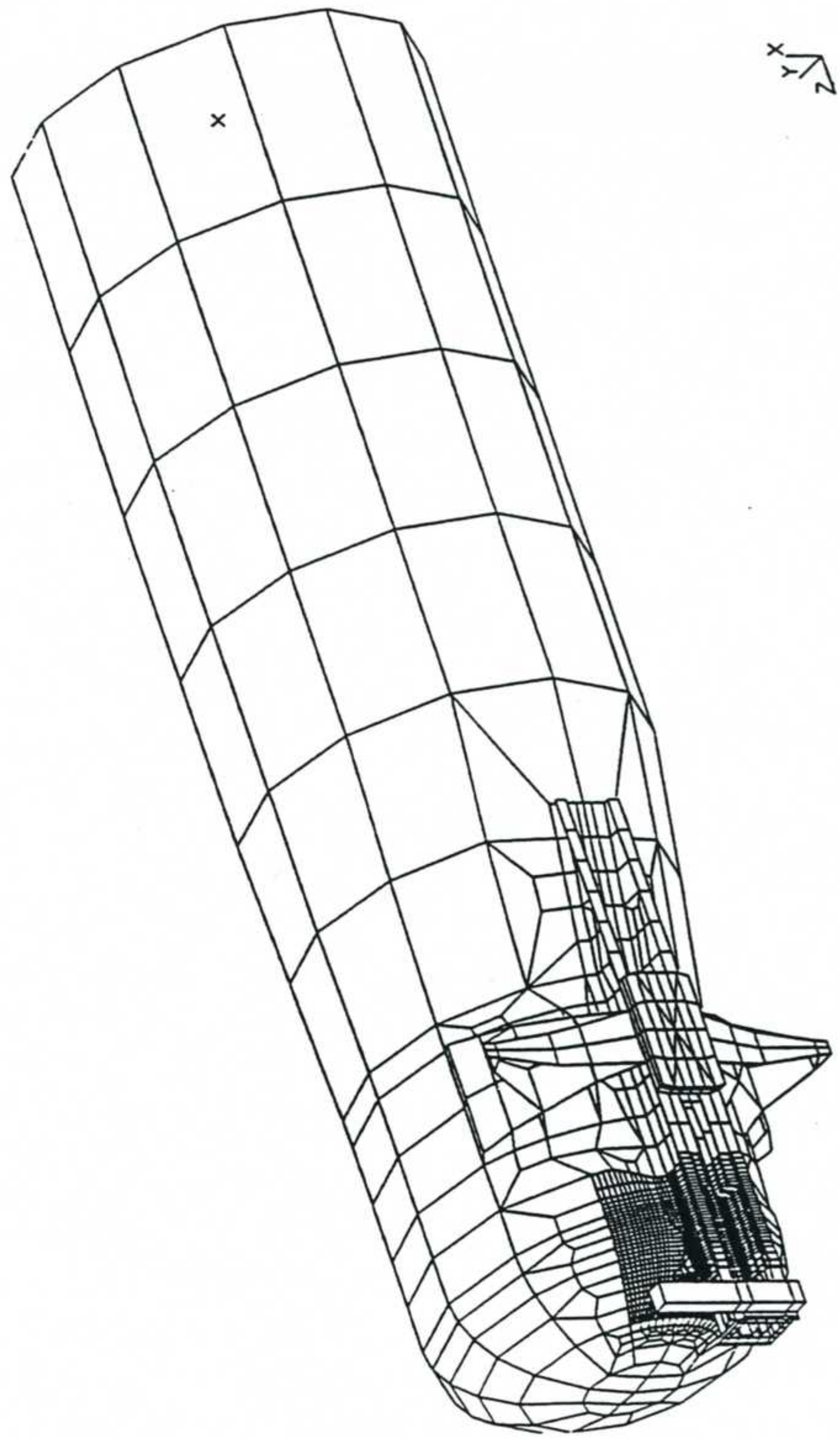

FIGURE 9.   HALF SYMMETRIC MODEL

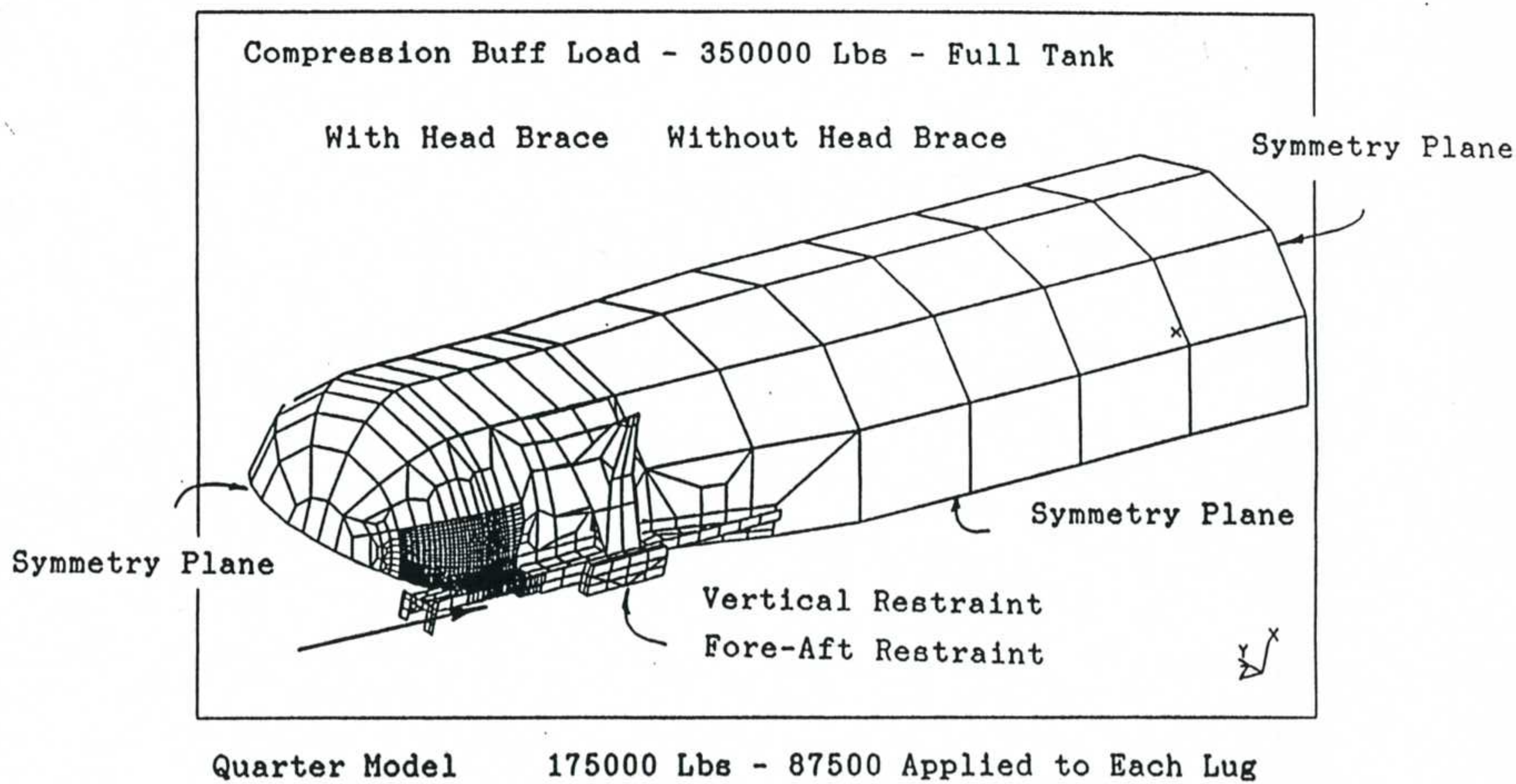

FIGURE 10. COMPRESSION BUFF LOADS AND BOUNDARY CONDITIONS

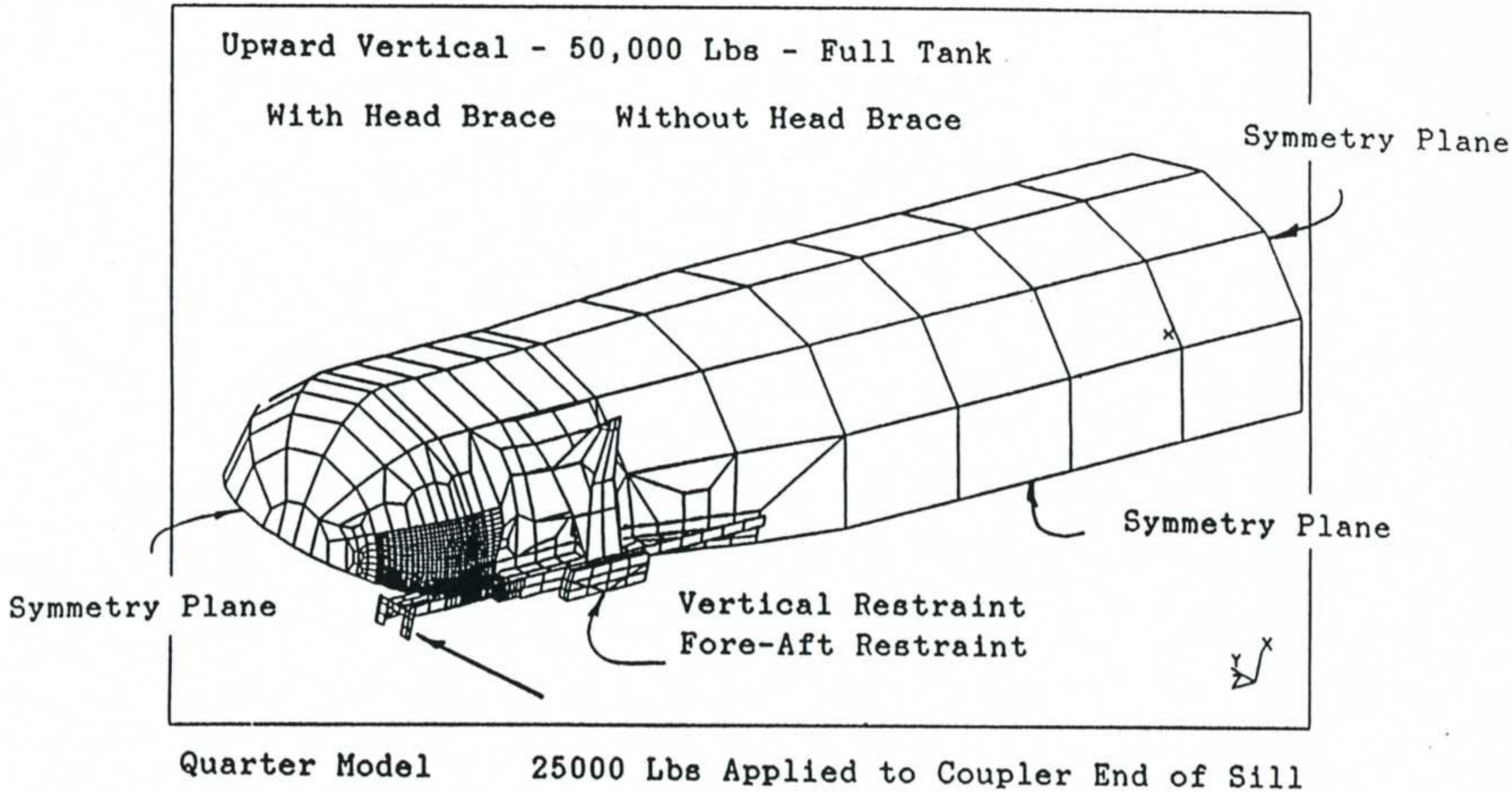

FIGURE 11. UPWARD VERTICAL LOAD AND BOUNDARY CONDITIONS

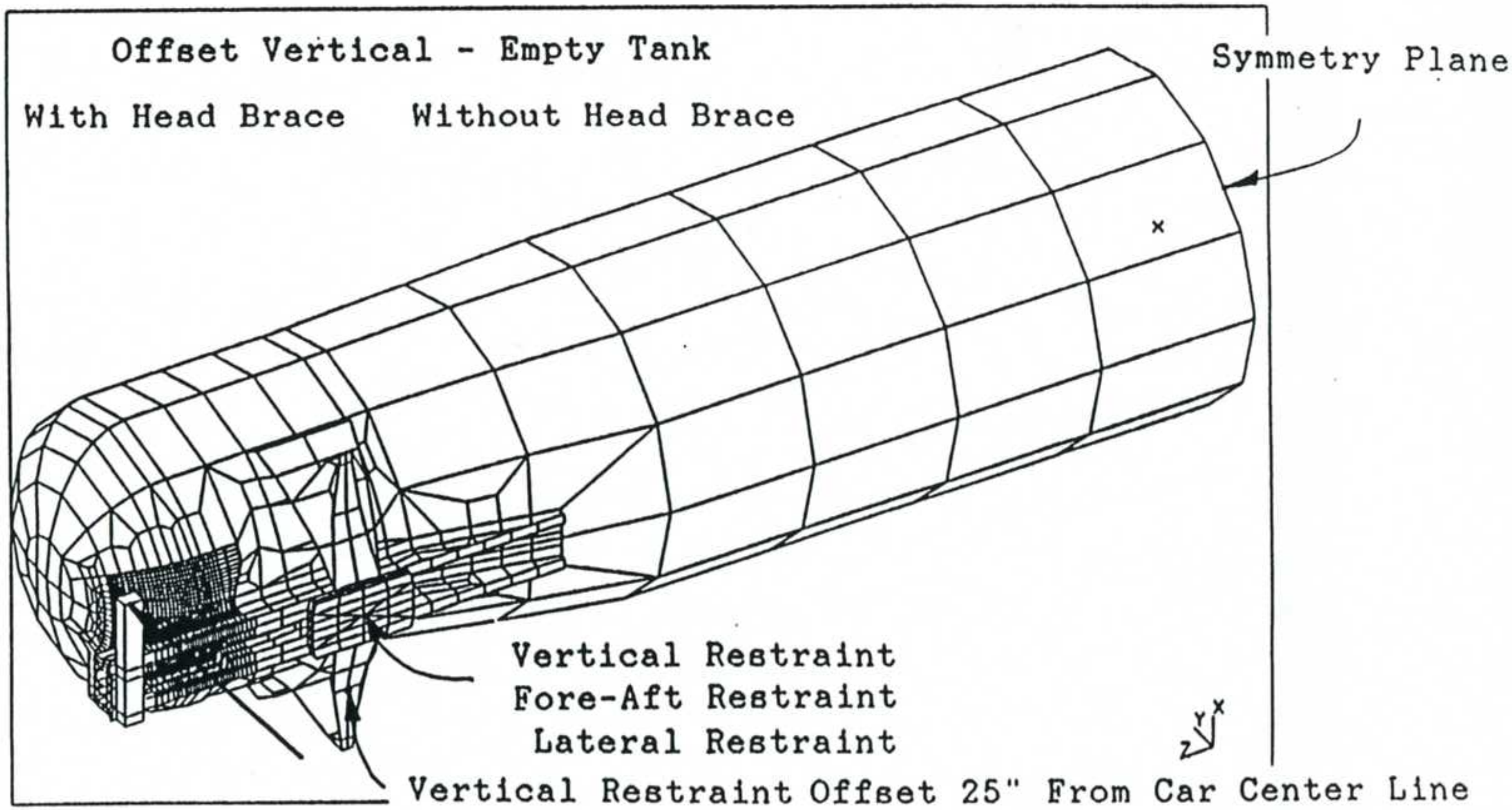

NATX: 7826 Lbs (1/8 Weight of Car) Applied at End of 36" Rigid Bar

Trinity Car: 4892 Lbs

FIGURE 12. OFFSET VERTICAL (INSPECTION PROCEDURE) LOAD AND BOUNDARY CONDITIONS - EMPTY TANK

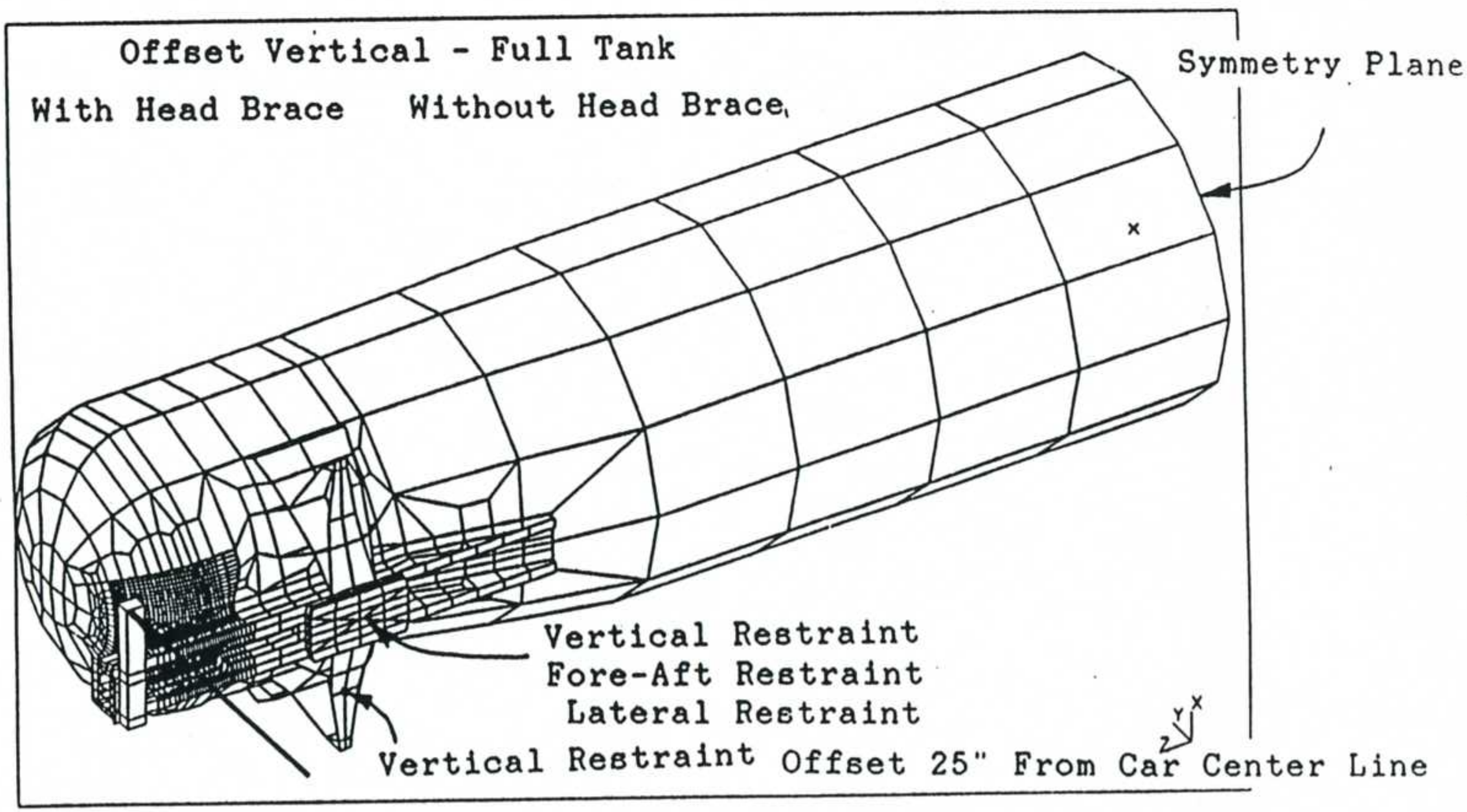

NATX: 27123.5 Lbs (1/8 Weight of Car+Load) Applied at End of 36" Rigid Bar

Trinity Car: 19681.4 Lbs

FIGURE 13. OFFSET VERTICAL (INSPECTION PROCEDURE) LOAD AND BOUNDARY CONDITIONS - FULL TANK

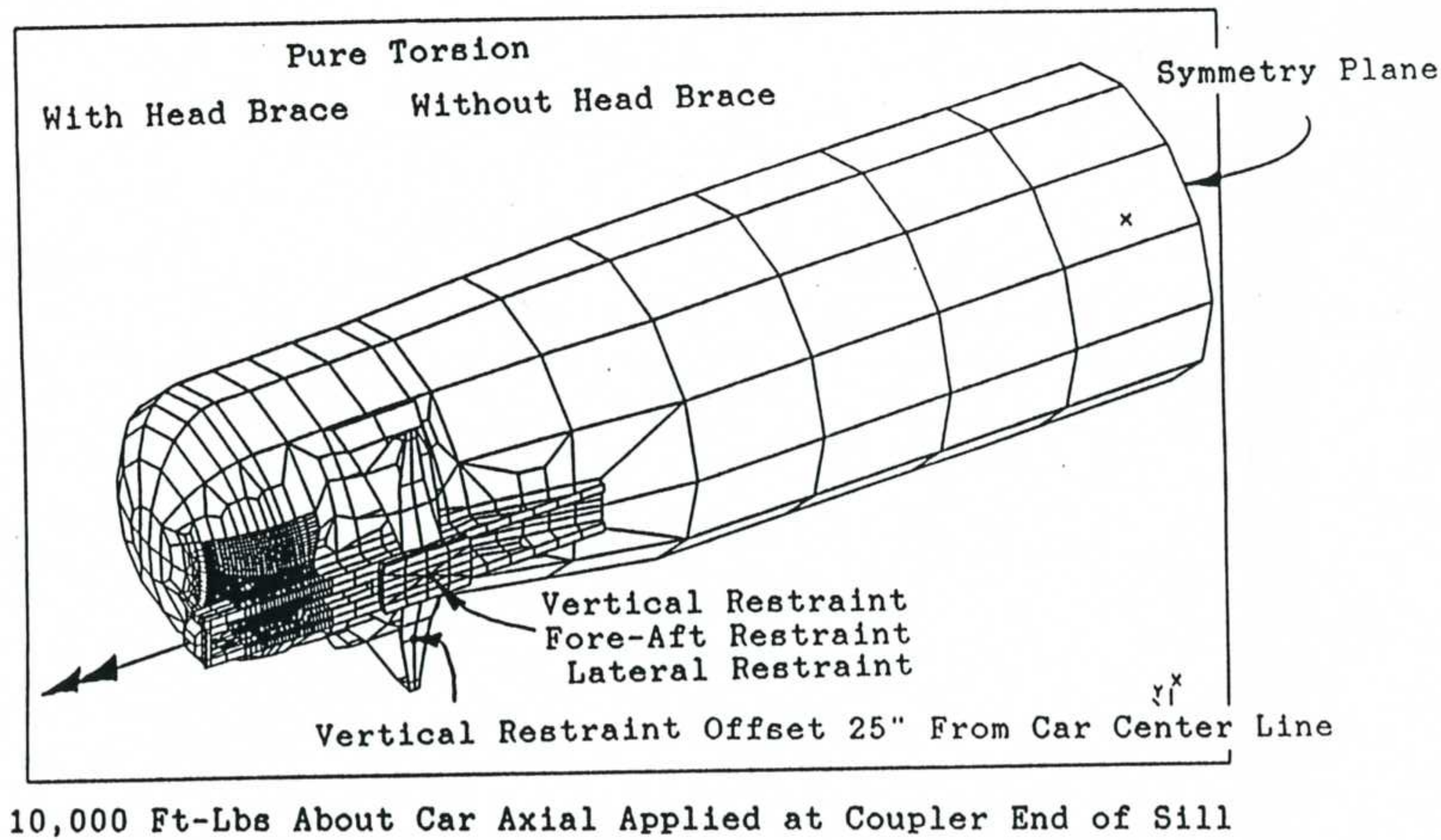

FIGURE 14. PURE TORSION (ROLLOVER DERAILMENT) LOAD AND BOUNDARY CONDITIONS

same on the Trinity car except for the different magnitudes, as indicated.

Detailed stress results were produced for all the loading conditions described earlier. In general, they showed the beneficial effect of adding a head brace on a fully loaded or empty car, as well as a relative comparison, car to car, of a rollover derailment. It should be noted that the magnitude of the pure torsion moment that was stipulated for these analyses was an arbitrary "unit load" of 10,000 ft-lbs. Based on simple statics hand calculations, about 800,000 ft-lbs of pure torsion at the coupler would be required to lift all the wheels on one side of a tank car off the rail. In reality, this much torque on one coupler would cause plastic deformation and probably lead to stub sill fracture. In a linear elastic analysis, this extreme load magnitude would result in unrealistically high stresses (millions of psi), so the "unit load" was used for relative comparisons. Within the limits of this linear elastic analysis, larger moments could be expected to produce proportionately larger stresses in areas of concern.

The offset vertical loading does not represent a field service loading. It represents the loading applied during occasional nondestructive inspections of selected tank cars. The test is done by attaching a 3-foot-long rigid bar near the coupler end of the draft sill and raising the end of the bar with a jack until one wheel just lifts off the rail. The jacking force magnitude has never been measured. The load given to us by VNTSC for the acoustic emissions test inspection procedure load case was based on their estimate of the force required to lift one wheel off the rail.

2.3 Stress Analysis

The SDRC I-DEAS program was used for all finite element analyses. This software package was used for all pre-processing, solving, and post-processing. All analyses were static and linear elastic.

Continuity across the solid/shell interface was checked by plotting the deformations for the entire model and checking the deformation continuity. (Figure 15 includes a plot of the deformations in this area for the Compression Buff load). The nearly continuous deformation lines on this plot indicate reasonable load transfer. However, because of the mesh discontinuity between the solid and shell elements, the stresses local to this discontinuity are not valid.

At the beginning of this project VNTSC suggested that Battelle assume the lading to be liquid propane. This lading produced typical, but not "worst case" tank car loads, since liquid propane has a

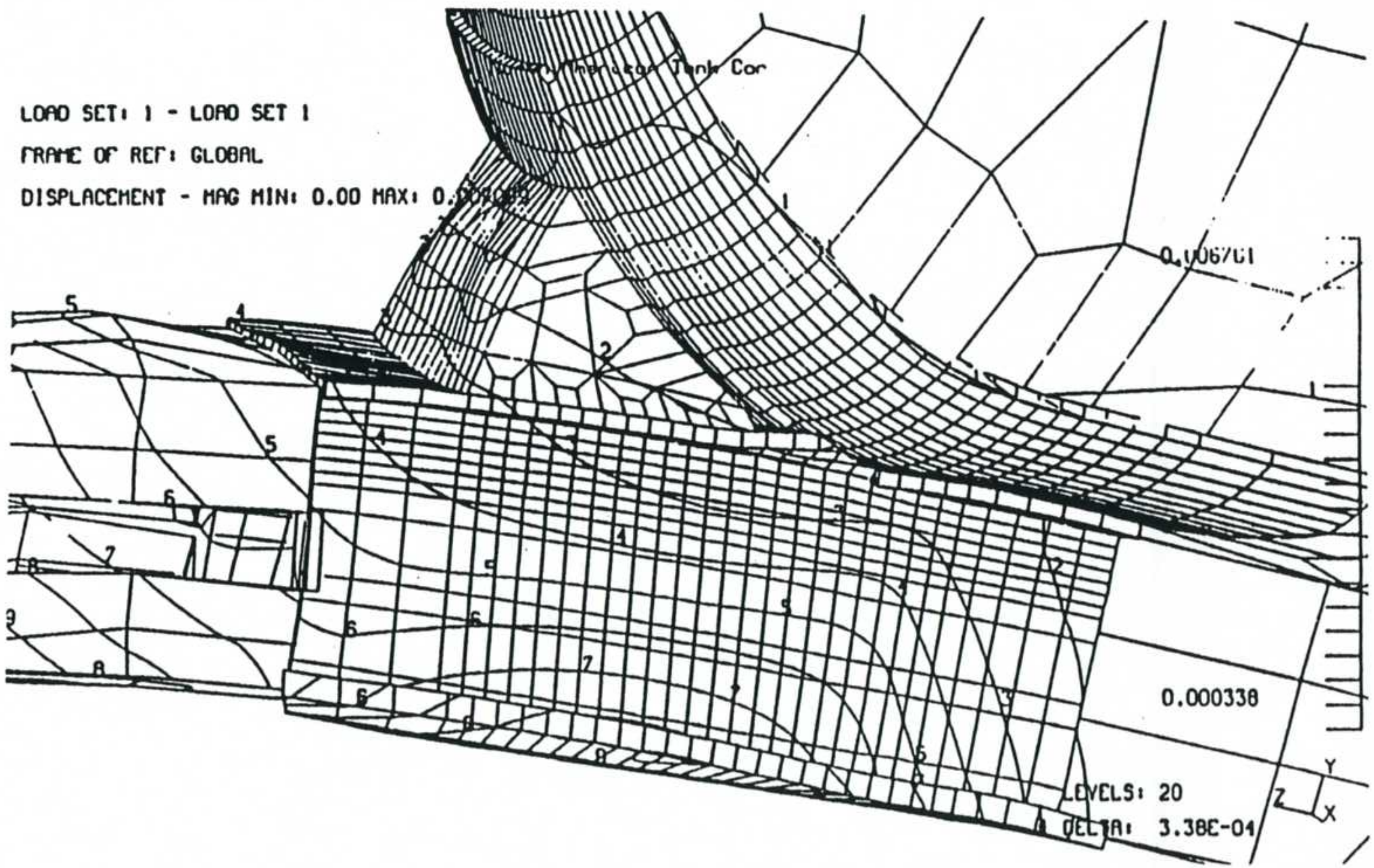

FIGURE 15. EXAGGERATED DISPLACEMENT PLOT OF NATX CAR - COMPRESSION BUFF LOAD

specific gravity of only 0.54. If we had assumed another more dense lading, such as oil, the stress results would have been proportionately higher in the load cases which included vertical components. Since this was a linear, static analysis the horizontal inertial effects of the load's mass (in a draft or buff load case) were not directly solved for as part of the analysis. However, inertial effects were included in the "static" load magnitudes for each particular load case, as defined by TTC[2]. The effect of gravity was included in all load cases. The dead weight of the tank car load was simulated by modifying (increasing) the density of tank elements.

2.4 Assumed Field Loading Spectra

Assumptions regarding the relationship between the modeled loads and typical field loads were based on an earlier, related study by Battelle for the FRA[1]. These data are summarized in Table 2 for the compression buff and upward vertical load cases. The compression buff loading spectrum was reasonably well defined based on AAR data developed under the FEEST program[4]. The upward vertical loading spectrum was not as well defined. The estimates that are included in Table 2 are based on the use of F Interlocking couplers; the limited data available[5] suggest the possibility of

Table 2. Assumed Frequency and Severity of Field Loads for the Stub Sill Tank Car Fatigue Analysis

Loading Frequency (Exceedances per Mile)	**Compression Buff Loading (kips)**	**Upward Vertical (kips)**
1	200	8
0.1	250	25
0.01	350	50
0.001	400	--
0.0001	500	--

vertical loads (with shelf couplers) as high as 50,000 lbs. The AAR Specifications for Design, Fabrication and Construction of Freight Cars[6] also call out these load levels as limits that must be withstood without "yielding the loaded members or exceeding their critical buckling strengths". Each of these spectra were assumed to act independently for this analysis, with the possibility of simultaneous high loadings considered to be remote.

2.5 Crack Initiation Analysis Methodology

Fatigue cracks generally initiate at a geometric discontinuity such as a notch or weld toe. These act as stress concentrations, magnifying the stresses in this region to levels above the nominal levels. Subjecting these regions to cyclic loading may cause repeated plastic deformation that will eventually result in one or more fatigue cracks. Although a reasonably detailed finite element mesh was used in the stub sill/tank interface, the mesh was not fine enough to provide truly accurate estimates of the local stresses at points of highest stress concentration. Therefore, the fatigue calculations included here should be used as a relative measure of the likelihood of fatigue cracking in various locations as a result of the various assumed loadings. Avoidance of fatigue cracking in actual practice with these stub sill designs should be based on a detailed examination of the severity and integrity of the geometric details in the areas of highest predicted stresses, combined with a careful assessment of the actual vehicle loadings. The fatigue calculations that are presented in the following paragraphs should be viewed with these caveats in mind.

Low cycle fatigue strain-life data are often represented by the Coffin-Manson[7] equation, with Morrow's[8] mean stress correction factor as follows:

$$\frac{\Delta\epsilon}{2} = \epsilon'_f \, (2N_f)^c + \frac{(\sigma'_f - \sigma_m)}{E} \, (2N_f)^b \qquad (1)$$

where $\Delta\varepsilon/2$ is the strain amplitude, ε'_f is the fatigue ductility coefficient, σ'_f is the fatigue strength coefficient, σ_m is the mean stress, $2N_f$ is the reversals to failure, c is the fatigue ductility exponent, and b is the fatigue strength exponent. By relating the strain calculated at the notch root to the strain-life data, the number of cycles to initiate a fatigue crack at the notch can be estimated. This is the basis of the initiation life predictions. The strain-life data parameters, ε'_f, σ'_f, c, and b, are obtained either by low cycle fatigue testing or by using estimates.

Hardness measurements are often used to estimate fatigue properties of weldments in place of mechanical testing to determine properties. Since fatigue cracks often initiate in the relatively narrow metallurgical region of the heat affected zone (HAZ), direct testing is difficult. These estimated material fatigue properties were obtained from an earlier Battelle study[1]. The significant parameters are summarized in Table 3.

The fatigue properties for the weld bead were used for crack initiation fatigue life estimates within a specific weld or within the weld's HAZ. The fatigue properties for the sill pad extension were used for crack initiation fatigue life estimates at locations away from welds.

Table 3. Estimated Fatigue Properties From Reference [1]

Identification	Weld Bead	Sill Pad Extension
Material	TC-128B	A515-70
Source	GE[9]	Canadian Transport Commission[10]
Material Properties		
Ultimate Strength, S_U, ksi	127	85
Cyclic Yield Strength, σ'_y, ksi	77	52
Fatigue Strength Coefficient, σ'_f, ksi	174	134
Fatigue Strength Exponent, b	-0.083	-0.094
Fatigue Ductility Coefficient, ε'_f	0.72	0.89
Fatigue Ductility Exponent, c	-0.6	-0.6
Cyclic Strength Coefficient, K, ksi	182	137
Cyclic Strain Hardening Exponent, η'	0.138	0.157

2.6 Crack Growth Analysis Methodology

For cases involving only localized yielding, it was shown over 30 years ago[11] that the growth rate of fatigue cracks is dependent upon the stress intensity associated with the crack tip. The power law relationship is of the form:

$$\frac{da}{dN} = A\ \Delta K^m \tag{2}$$

where da/dN is the fatigue crack growth rate, ΔK is the stress intensity factor range, and A and m are material constants dependent on the environment, stress ratio, temperature and frequency (of the stress excursions). The effects of stress ratio, or mean stress, are at least partially accounted for in the following formulation, first proposed by Forman[12]

$$\frac{da}{dN} = \frac{A\ \Delta K^m}{1 - R} \tag{3}$$

where R is the stress ratio, S_{min}/S_{max}. The crack growth constants A and m used in this analysis were taken from values reported by Rolfe and Barsom[13] as lower bound values for pearlitic steels. These are

$$A = 3.8 \times 10^{-10}$$

$$m = 3$$

The general relationship for the stress intensity factor range can be written as

$$\Delta K = Y\ \Delta S\ \sqrt{\pi a} \tag{4}$$

where Y is a geometry dependent factor, ΔS is the stress range, and a is the crack length. The solution for the stress intensity of a semi-elliptical crack in a plate was used in this analysis to model a fatigue crack growing in Mode I through a plate member[14].

The estimated crack propagation life is strongly dependent on the assumed initial crack size. An initial crack size of 0.25 inch was used for this analysis because it represents the lower limit of what could reasonably be detected in the field[15]. Smaller assumed initial crack sizes would have, of course, produced significantly increased crack growth life estimates. Larger assumed crack sizes would have had the opposite effect. Since this study was done to identify the **relative** likelihood of fatigue cracking at various sites at the stub sill/tank car interface, the selected initial crack size was not a critical issue. This would not be the case in a situation where accurate estimates of remaining life or safe inspection intervals were to be determined; initial crack sizes would have to be closely tied to the reliability of the inspection system and well defined loading conditions.

Crack growth life at a specific location within the stub sill/tank car interface was defined as the service interval within which a 0.25 inch crack would grow to a length of 1.00 inch. Only the cracking sites most commonly seen in service were examined to evaluate relative crack growth lives.

Based on prior studies[16] that showed the strong propensity for fatigue cracks to grow in Mode I (opening mode due to stress excursions orthogonal to the plane of the crack), only the stress components perpendicular to the assumed plane of cracking were considered.

3.0 EVALUATION OF CRACKING POTENTIAL AND CRITICALITY

In order to evaluate the potential for fatigue cracking at various sites within the stub sill designs and to assess the likelihood of unstable cracking at these sites, a simplified fatigue and fracture mechanics analysis was completed. This analysis was accomplished in four steps:

1) For the various load cases and tank car conditions the regions showing the highest Von Mises stresses were identified.

2) Each of these regions were examined to identify the relative likelihood of fatigue crack initiation (for an assumed mix of service loads described earlier).

3) The most probable sites for crack initiation (within the limits of the assumptions required to complete the analysis) were examined to identify their relationship to the regions of most common field cracking.

4) The principal stress components in each of these potentially critical sites were examined to determine the relative likelihood of crack propagation and subsequent fracture instability. The cracking sites with the greatest likelihood of crack growth were deemed to be potentially dangerous (again within the limits of the assumptions required to complete the analysis).

Details of the analysis are included in the following sections for both of the stub sill tank car designs examined in this study.

3.1 North American Tank Car; NATX 34081 Series

The NATX tank car was examined first, and in the greatest detail. Lessons learned from this analysis led to a somewhat more focussed examination of the Trinity car. Both analyses required some basic assumptions regarding the relationship between the modeled loads and typical field service, as well as assumptions concerning the fatigue resistance of the tank car materials.

3.1.1 Crack Initiation Potentials

A summary of the maximum Von Mises stresses for potentially critical stub sill locations in the North American Tank Car, NATX 34081 Series, is included in Table 4. This table was constructed to allow simple comparisons between the maximum Von Mises stresses in various components as a function of tank condition (i.e. tank full or empty, head brace installed or absent). The dramatic (and anticipated) increase in the maximum stress levels between the empty and full condition is also apparent at all locations for the offset vertical load case (the only one considered for both empty and full tank conditions in this study). Similarly, the maximum Von Mises stresses were considerably higher in almost all cases for the NATX tank car without the head brace installed than with it in place. There are a few minor exceptions, such as in the Z-section lug area and weld for the compression buff loading, where the introduction of a head brace actually increased stresses slightly.

Of the four load cases considered, the offset vertical loading produced the highest stresses at most locations in the stub sill/tank car interface area. In fact, for the full tank/no head brace condition some of the computed (linear elastic) stresses far exceeded 80,000 psi, suggesting the possibility of significant inelastic deformation resulting from this tank and loading combination. Table 4[17]. summarizes the relative comparisons between various load cases (with and without head braces) for the various critical locations.

The potentially critical stub sill locations are illustrated in Appendix A. Color plots of the Von Mises stress contours are shown for the high stress locations and loading combinations in appendix A. Note that appendix A does not directly correspond to each location/case in table 4 because appendix A shows only the locations of high or significant stresses. Table A-1 summarizes the locations of those high stresses.

The relative likelihood of fatigue crack initiation at each of these sites can be correlated, at least approximately, with the magnitude of the Von Mises (or octahedral shear) stresses reported in Table 4. Although the detailed calculations are not presented here because the results of this study are meant to be interpreted qualitatively, it can be said that those locations showing Von Mises stresses in excess of the cyclic yield strength for these materials (roughly 50 to 70 ksi) could be expected to initiate fatigue cracks after relatively few of these high loadings (hundreds to thousands of cycles). Locations showing lower Von Mises stresses may also eventually develop fatigue cracks, but the likelihood of their occurrence would depend on the nature and severity of the actual service spectrum. The focus of the crack growth analysis is on the most severe sites depicted in Appendix A.

Table 4. Summary of Maximum Von Mises Stresses for Potentially Critical Stub Sill Locations, North American Tank Car; NATX 34081 Series

Potentially Critical Area	Load Case	Empty Tank		Full Tank	
		Head Brace	No Head Brace	Head Brace	No Head Brace
		Maximum Von Mises Stress, psi			
Z-Section Lug Area	Compression Buff			28560	24200
	Upward Vertical			20500	36700
	Pure Torsion			4100	10600
	Offset Vertical	12000	25400	33300	89000
Transition Plate Radius	Compression Buff			12050	24600
	Upward Vertical			14600	72000
	Pure Torsion			1100	7200
	Offset Vertical	2200	16000	14500	53300
Transition Plate Tank Weld	Compression Buff			7400	19470
	Upward Vertical			10000	64150
	Pure Torsion			4360	20360
	Offset Vertical	7400	37300	25640	131000
Tank Shell	Compression Buff			3820	10420
	Upward Vertical			13740	31540
	Pure Torsion			3800	11300
	Offset Vertical	7080	19360	24650	68340

Table 4. (Cont.)

Potentially Critical Area	Load Case	Empty Tank		Full Tank	
		Head Brace	No Head Brace	Head Brace	No Head Brace
		Maximum Von Mises Stress, psi			
Z Section- Transition Plate Weld	Compression Buff			19600	13900
	Upward Vertical			19340	42330
	Pure Torsion			9200	15600
	Offset Vertical	17540	27540	60830	97170
Z Section Weld	Compression Buff			19600	13900
	Upward Vertical			19340	42330
	Pure Torsion			9200	15600
	Offset Vertical	17540	27540	60830	97170
Head Brace Pad	Compression Buff			8000	--
	Upward Vertical			29200	--
	Pure Torsion			6200	--
	Offset Vertical	15070	--	52870	--
Transition Plate Max (End Of Weld)	Compression Buff			17730	36430
	Upward Vertical			21260	126000
	Pure Torsion			9000	21000
	Offset Vertical	18070	44350	63000	157000

The highest computed Von Mises stresses for each type of loading are summarized in Table 5. Whether the tank was full or empty, and whether a head brace was included or not is also identified. The computed Von Mises stress values are ranked separately for each loading condition, because the criticality of these sites in terms of fatigue crack initiation depends directly on the relative frequency of occurrence of these different types of loading. The first two loading conditions are commonly withstood by tank cars in normal service (at varying severity levels), while the last two loading conditions are not. However, the concern with the offset vertical loading is not so much the introduction of fatigue cracks, as it is the possibility of substantially and permanently deforming the tank car structure. Stresses above the yield strength of the material were calculated in several areas for the case of a full tank car without a head brace.

3.1.2 Potentially Dangerous Cracks

The sites of potentially dangerous cracks were identified by examining the locations where the highest Von Mises stresses were identified (as in Table 5), comparing these locations with sites (and planes) where cracks have been most frequently observed in the field, and then assessing the potential for Mode I crack growth in these potentially critical cracking planes. In order to do this it was necessary to identify the principal stress components at each of the sites identified in Appendix A. A variety of other cases showing relatively high stress levels orthogonal to the commonly observed cracking planes were also examined. These results are compiled in Table 6 and shown in Appendix B. Where two stress components are shown for the same location and stress direction, they represent values at two different potentially critical sites within the component.

For stub sill tank cars like the NATX and Trinity models described in this report the AAR has designated three critical areas as shown in Figure 16. Cracking has also been observed in three other areas as shown in Figure 17. Both of these figures illustrate potentially critical cracking sites for stub sill tank cars with head braces installed. These figures illustrate the point that head braces do not entirely eliminate the potential of fatigue cracking for all load cases, even though they significantly reduce the potential of fatigue cracking for most loadings, as discussed elsewhere in this report.

Based on this analysis, full NATX tank cars without head braces show the greatest potential for dangerous service cracks in the transition plate, near the end of the weld joining it to the tank body. Longitudinal coupler loads would be the primary contributor. If draft and buff loads of equal

Table 5. Summary of Highest Stress Sites in the NATX Car for each Load Case

Load Case	Highest Von Mises Stresses, ksi	Potentially Critical Area	Condition
Compression Buff	36	Transition Plate (End of Weld)	Full, No Head Brace
	29	Z-Section Lug Area	Full, Head Brace
	25	Transition Plate Radius	Full, No Head Brace
Upward Vertical	126	Transition Plate (End of Weld)	Full, No Head Brace
	72	Transition Plate Radius	Full, No Head Brace
	64	Transition Plate Tank Weld	Full, No Head Brace
	42	Z Section- Transition Plate Weld and Z Section Weld	Full, No Head Brace
	37	Z Section Lug Area	Full, No Head Brace
Pure Torsion	21	Transition Plate (End of Weld)	Full, No Head Brace
	20	Transition Plate Tank Weld	Full, No Head Brace
	16	Z Section- Transition Plate Weld and Z Section Weld	Full, No Head Brace
Offset Vertical*	81	Transition Plate (End of Weld)	Full, No Head Brace
	68	Transition Plate Tank Weld	Full, No Head Brace
	50	Z Section- Transition Plate Weld and Z Section Weld	Full, No Head Brace
	46	Z Section Lug Area	Full, No Head Brace
	35	Tank Shell	Full, No Head Brace
	33	Transition Plate (End of Weld)	Full, Head Brace
	32	Z Section- Transition Plate Weld and Z Section Weld	Full, Head Brace

*Stress values for this case have been modified from original values - see Executive Summary.

magnitude are considered, cracking across the transition plate would be most likely (due to draft loads). However, large buff loads could also contribute to the growth of longitudinally oriented cracks in the transition plate at the end of the weld.

Full NATX tank cars with head braces installed are also susceptible to the development of dangerous service cracks, but the analysis suggests that the most likely site would be the Z-section lug

Table 6. Summary of Orthogonal Stress Components in the NATX Car at Potentially Critical Sites Identified in Appendix A

Location(s)	Loading Conditions	Head Brace Installed?	Orthogonal Stress Components	Approx. Maximum Stress, psi
Z-Section Lug Area	Compression Buff Full Tank	Head Brace	Longitudinal Vertical	-32,300 13,500
Transition Plate (End of Weld)		No Head Brace	Longitudinal Vertical	-30,200 16,600
Head Brace Pad	Upward Vertical Full Tank	Head Brace	Longitudinal Circumferential	-27,000 -25,300
Transition Plate (End of Weld)		No Head Brace	Longitudinal Transverse	-103,000 -108,000
Transition Plate Tank Weld	Pure Torsion Full Tank	No Head Brace	Longitudinal Circumferential	-11,400 -11,900
Transition Plate (End of Weld)	Offset Vertical Full Tank	Head Brace	Longitudinal Transverse	44,600 / -60,000 21,800 / -38,500
Transition Plate (End of Weld)		No Head Brace	Longitudinal Transverse	55,000 / -171,000 75,899 / -107,000
Tank Shell			Longitudinal Transverse	45,000 / -71,200 31,300 / -63,100
Z Section Lug Area			Longitudinal Transverse	89,500 / -70,000 60,900 / -74,200
Z-Section Transition Plate Weld			Longitudinal Maximum Principal	20,000 / -53,000 68,400

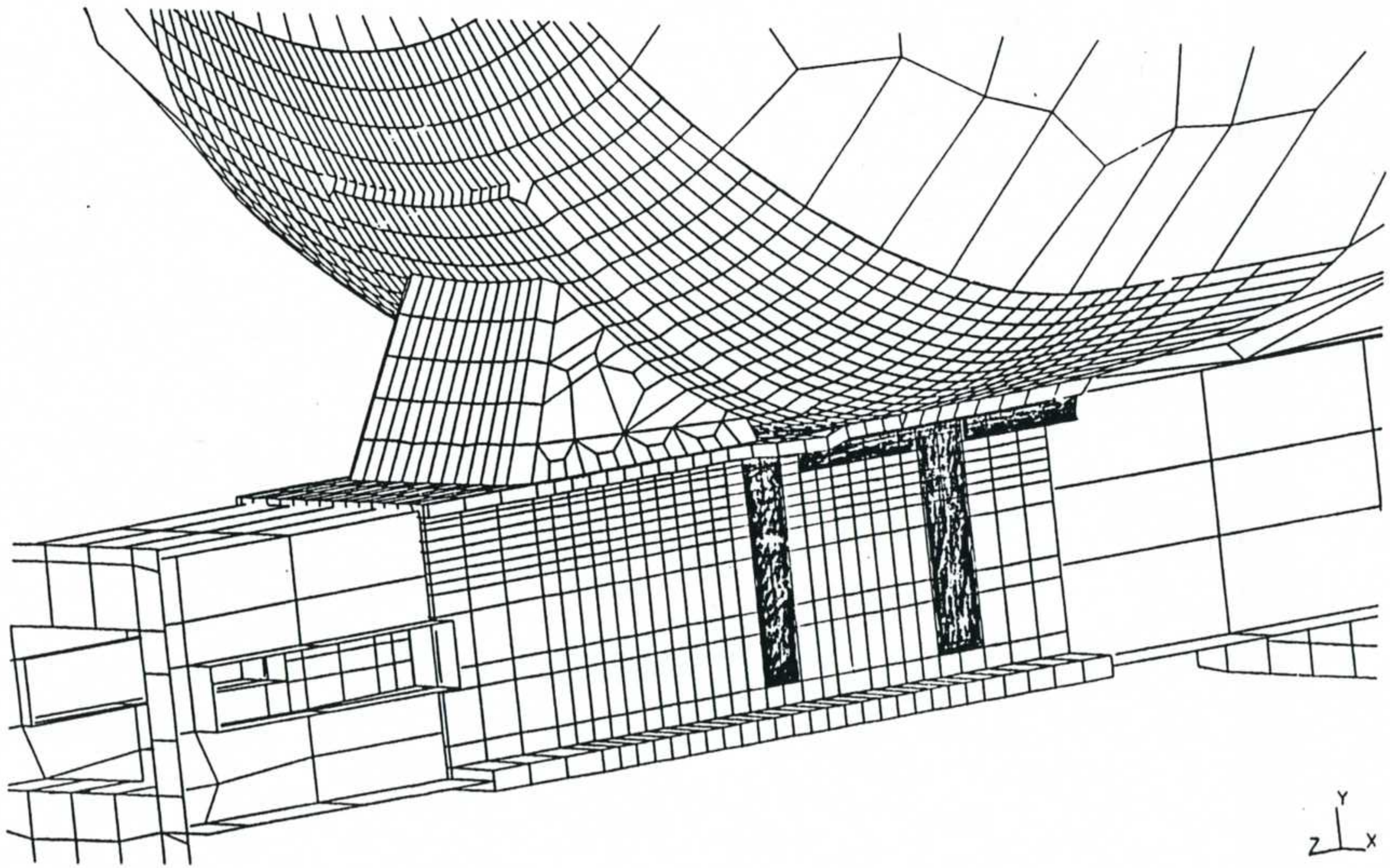

FIGURE 16. AAR DESIGNATED CRITICAL AREAS

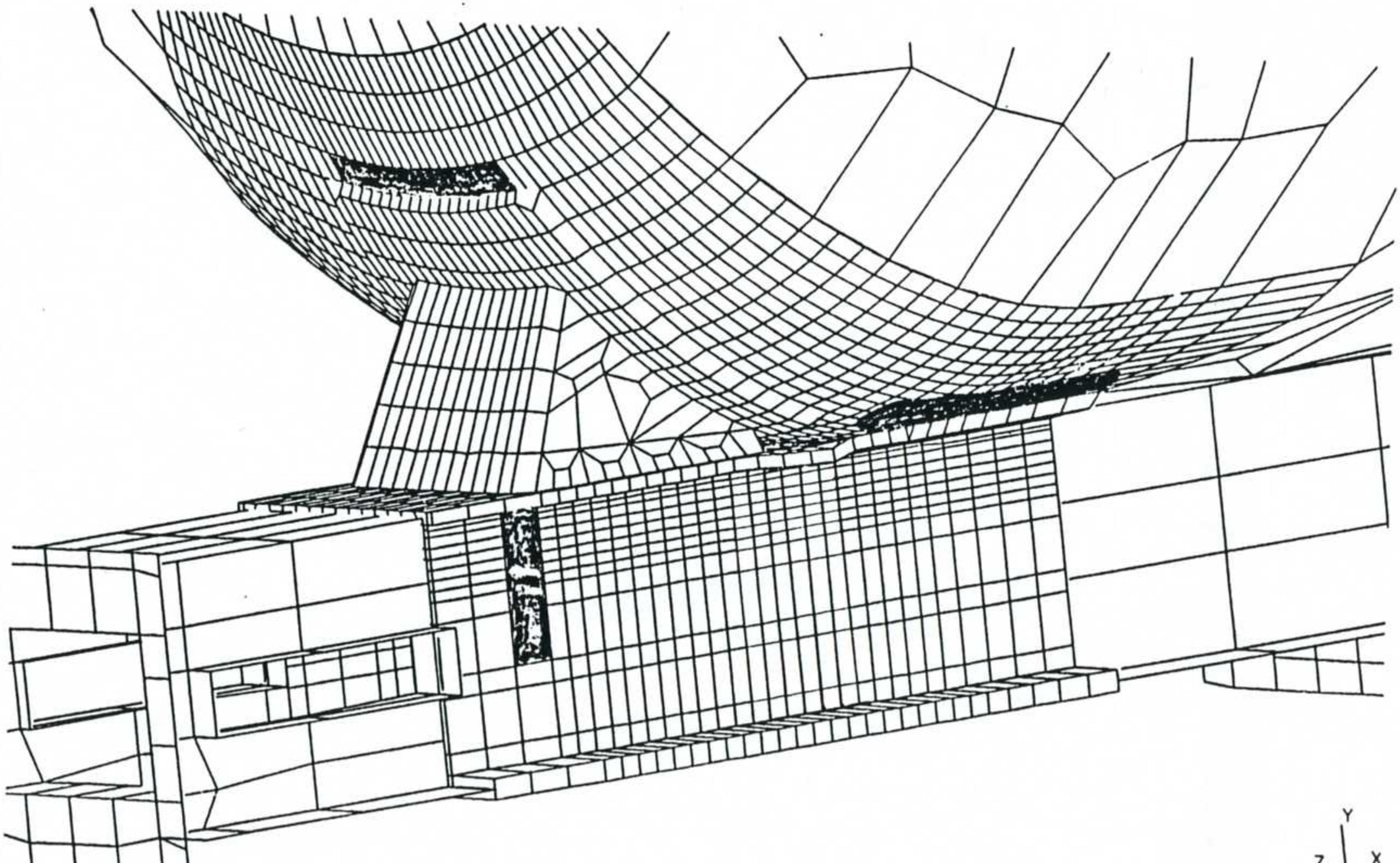

FIGURE 17. ADDITIONAL AREAS OF OBSERVED CRACKING

area, especially if large coupler draft loads were experienced with regularity. In this case, cracking across the Z-section (vertically) would be expected.

If fatigue cracks were already present in a tank car that was subjected to an offset vertical loading, further damage could be incurred, especially in the Z-section lug area and the transition plate. If significant cracks were present in the tank shell when a large offset vertical load was applied, further damage could also result, especially if there was no head brace installed. However, further damage from an offset vertical loading could be incurred in a cracked transition plate of an NATX tank car, even if a head brace were installed.

3.2 Trinity Car Class TK-S, ATSF 98600-94749

After the NATX tank car analysis was completed, a similar study of a Trinity car, class TK-S, was undertaken. The following paragraphs provide a summary of the findings from that analysis. The sites of greatest crack initiation potential are reviewed first, and then the locations of potentially dangerous fatigue cracking are identified.

3.2.1 Crack Initiation Potentials

A summary of the maximum Von Mises stresses for potentially critical stub sill locations in the Trinity Tank Car, Class TK-S, ATSF 98600-94749, is included in Table 7. As with the NATX car analysis, this table was constructed to allow simple comparisons between the maximum Von Mises stresses in various components as a function of tank condition. The substantial increase in maximum stress levels between the empty and full condition seen for the NATX car for the offset vertical loading case was also apparent in the Trinity car analysis. The maximum Von Mises stresses were also considerably higher in almost all cases for the Trinity tank car without the head brace installed than with it in place. There are a few minor exceptions such as in the tank shell for the offset vertical loading and in the rear draft lug area for the compression buff loading, where the introduction of a head brace actually increased stresses slightly.

Of the four load cases considered, the offset vertical loading produced the highest stresses at most locations in the stub sill/tank car interface area (as seen earlier with the NATX tank car). The

Table 7. Summary of Maximum Von Mises Stresses for Potentially Critical Stub Sill Locations, Trinity Car Class TK-S; ATSF 98600-94749

Potentially Critical Area	Load Case	Empty Tank		Full Tank	
		Head Brace	No Head Brace	Head Brace	No Head Brace
		Maximum Von Mises Stress, psi			
Z-Section Lug Area	Compression Buff			27070	27400
	Upward Vertical			11200	20000
	Pure Torsion			3700	7210
	Offset Vertical	5250	7500	20800	51940
Head Pad Radius	Compression Buff			7000	9900
	Upward Vertical			11000	27200
	Pure Torsion			2700	6760
	Offset Vertical	3400	5170	14400	29500
Z Section	Compression Buff			--	--
	Upward Vertical			19500	--
	Pure Torsion			6550	--
	Offset Vertical	--	9080	37150	--
Tank Shell	Compression Buff			5330	8700
	Upward Vertical			19060	23000
	Pure Torsion			5140	7530
	Offset Vertical	4900	16050	23630	19300

Table 7. (Cont.)

Potentially Critical Area	Load Case	Empty Tank		Full Tank	
		Head Brace	No Head Brace	Head Brace	No Head Brace
		Maximum Von Mises Stress, psi			
Z Section- Head Pad Weld	Compression Buff			4420	10100
	Upward Vertical			10000	25850
	Pure Torsion			4410	7210
	Offset Vertical	4000	7080	20800	35800
Z Section Weld	Compression Buff			4700	7000
	Upward Vertical			9000	17000
	Pure Torsion			4410	7210
	Offset Vertical	4000	6000	20800	35800
Head Brace Pad	Compression Buff			3100	--
	Upward Vertical			22700	--
	Pure Torsion			4000	--
	Offset Vertical	7700	--	31750	--
Head Pad	Compression Buff			8500	21210
	Upward Vertical			16000	58200
	Pure Torsion			5900	19800
	Offset Vertical	5600	11400	24820	86500
Rear Draft Lug	Compression Buff			36300	35900

potentially critical stub sill locations are illustrated in Appendix A, where color plots of the Von Mises stress contours are shown for each high stress location and loading combination.

The relative likelihood of fatigue crack initiation at each of these sites was again correlated with the magnitude of the Von Mises (or octahedral shear) stresses reported in Table 7. As with the NATX car, those locations showing Von Mises stresses in excess of the cyclic yield strength for these materials could be expected to initiate fatigue cracks after relatively few of these high loadings (hundreds to thousands of cycles). Locations showing lower Von Mises stresses may also eventually develop fatigue cracks, but the likelihood of their occurrence would depend on the nature and severity of the actual service spectrum.

The highest computed Von Mises stresses for the Trinity car for each type of loading are summarized in Table 8. Whether the tank was full or empty and whether a head brace was included or not is also identified. The computed Von Mises stress values are ranked separately for each loading condition, because the criticality of these sites in terms of fatigue crack initiation depends directly on the relative frequency of occurrence of these different types of loading. As stated earlier in the NATX tank car discussion, the first two loading conditions are commonly withstood by tank cars in normal service (at varying severity levels), while the last two loading conditions are not. However, the concern with the offset vertical loading is not so much the introduction of fatigue cracks, as it is the possibility of substantially and permanently deforming the tank car, especially a full tank car without head braces.

3.2.2 Potentially Dangerous Cracks

The sites of potentially dangerous cracks in the Trinity car were identified by examining the locations where the highest Von Mises stresses were identified (as in Table 8), comparing these locations with sites (and planes) where cracks have been most frequently observed in the field, and then assessing the potential for Mode I crack growth in these potentially critical cracking planes. In order to do this it was necessary (as done earlier for the NATX car) to identify the principal stress components at each of the sites identified in Appendix A. A variety of other cases showing relatively high stress levels orthogonal to the commonly observed cracking planes were also examined. These results are compiled in Table 9 and are shown in Appendix B. Where two stress components are shown for the same location and stress direction, they represent values at two different potentially

Table 8. Summary of Highest Stress Sites in the Trinity Car for each Load Case

Load Case	Highest Von Mises Stresses, ksi	Potentially Critical Area	Condition
Compression Buff	36	Rear Draft Lug	Full, Head Brace
	36	Rear Draft Lug	Full, No Head Brace
	27	Z-Section Lug Area	Full, No Head Brace
	27	Z-Section Lug Area	Full, Head Brace
	21	Head Pad	Full, No Head Brace
Upward Vertical	58	Head Pad	Full, No Head Brace
	27	Head Pad Radius	Full, No Head Brace
	26	Z-Section Head Pad Weld	Full, No Head Brace
	23	Tank Shell	Full, No Head Brace
	23	Head Brace Pad	Full, Head Brace
Pure Torsion	20	Head Pad	Full, No Head Brace
	8	Tank Shell	Full, No Head Brace
Offset Vertical*	45	Head Pad	Full, No Head Brace
	27	Z-Section Lug Area	Full, No Head Brace
	19	Z-Section	Full, Head Brace
	19	Z-Section Head Pad Weld and Z-Section Weld	Full, No Head Brace
	17	Head Brace Pad	Full, Head Brace
	16	Head Pad Radius	Full, No Head Brace
	13	Head Pad	Full, Head Brace

*Stress values for this case have been modified from original values - see Executive Summary.

critical sites within the component.

For the Trinity car it was assumed that the same potentially critical sites would apply as previously identified for the NATX car. (These areas were shown earlier as darkened regions on Figures 16 and 17.)

Based on this analysis, full Trinity tank cars without head braces show the greatest potential for dangerous service cracks in the Z section lug area. Longitudinal coupler loads would be the primary contributor. Cracking across the lug appears most likely (if buff and draft loads of approximately equal magnitude are experienced). However, large buff loads could also contribute to the growth of longitudinally oriented cracks in the Z section lug area.

Full Trinity tank cars with head braces installed are also susceptible to the development of dangerous service cracks. The analysis suggests that the most likely site remains the Z-section lug area. Assuming that the stresses due to a draft load are opposite in sign to the stresses from the compression buff load, cracking in the draft lug itself could occur if large coupler draft loads were experienced with regularity.

If fatigue cracks were already present in a tank car that was subjected to an offset vertical loading, further damage could be incurred in the Z-section lug area and the head pad. If significant cracks were present in the tank shell when a large offset vertical load was applied, further damage could also result. For the Trinity car, the presence or absence of a head brace has little impact on the likelihood of further tank shell cracking due to an offset vertical loading.

4.0 EVALUATION OF STUB SILL INSPECTION PROCEDURE

The inspection procedure, also known as the "acoustic emissions" test, is done by attaching a rigid 36" bar to the sill at the coupler end and lifting the end of the bar until one of the car's wheels lifts off the track a specified height. (The force required to lift the car during the inspection procedure has not been measured.) During this jacking operation, the inspector listens for acoustic emissions to isolate cracking locations. This loading was called the "Offset Vertical" load case in this study. (See Figure 12 for an illustration of this load case).

The maximum computed stresses at the stub sill/tank car interface were quite high for the offset vertical load case applied to a full tank (for both the NATX and Trinity Cars), particularly when a head brace was not included in the model. Appendix C shows the Von Mises and Maximum principal stress contours from various views for both the NATX and the Trinity tank cars under the Offset Vertical (Acoustic Emissions Test) loading. These stress contours are shown for the full tank car condition, with and without head braces.

Table 9. Summary of Orthogonal Stress Components in the Trinity Car at Potentially Critical Sites Identified in Appendix A

Location(s)	Loading Conditions	Head Brace Installed?	Orthogonal Stress Components	Approx. Maximum Stress, psi
Z-Section Lug Area (Lug Included)	Compression Buff Full Tank	Head Brace	Longitudinal Vertical	-23,200 -10,800
Z-Section Lug Area (Lug Not Included)		Head Brace	Longitudinal Vertical	-24,000 -10,000
Rear Draft Lug		Head Brace	Longitudinal Vertical	13,100 / -42,000 12,500 / -13,300
Z-Section Lug Area (Lug Not Included)		No Head Brace	Longitudinal Vertical	-34,700 -11,800
Head Brace Pad	Upward Vertical Full Tank	Head Brace	Longitudinal Transverse	-25,600 -24,200
Head Pad		No Head Brace	Longitudinal Transverse	32,900 / -61,900 34,800 / -59,900
Head Pad	Pure Torsion Full Tank	No Head Brace	Longitudinal Transverse	-19,900 -19,900
Z-Section Lug Area	Offset Vertical Full Tank	Head Brace	Longitudinal Vertical	34,200 / -27,900 20,900 / -21,000
		No Head Brace	Longitudinal Transverse	51,900 / -46,700 21,200 / -30,000
Head Pad		Head Brace	Longitudinal Transverse	-38,400 21,800 / -31,200
		No Head Brace	Longitudinal Transverse	43,900 / -91,800 60,800 / -92,400
Tank Shell		Head Brace	Longitudinal Transverse	14,500 / -21,000 -18,400
		No Head Brace	Longitudinal Transverse	20,900 / -26,500 19,300 / -21,700

If significant cracks were present in any of the regions exposed to these high stresses, the acoustic emission procedure would likely be sensitive to them. This would be especially true if the maximum principal stresses in these regions tended to open up these cracks. Because the regions of highest stress resulting from the offset vertical loading most closely parallel the regions of maximum stress resulting from the upward vertical loading, it appears likely that the inspection procedure would be more sensitive to cracks caused by upward vertical service loadings than cracks caused by compression buff service loadings.

There is some risk of damage to either of these tank cars from the inspection procedure, especially if the procedure is performed on cars with no head brace and a full tank. For this condition the local stresses are likely to be so high that significant, permanent deformation (or even failure) of the tank car could occur. The likelihood of damage would be reduced if the load could be applied incrementally, while listening for acoustic emissions at each load step. If significant acoustic emissions are heard, a careful inspection of the tank car should be made before increasing the load further.

5.0 CORRELATION OF ANALYTICAL AND EXPERIMENTAL RESULTS

Two of the Trinity Tank car test cases run at TTC were found to be equivalent to two of the finite element analysis cases. The "Longitudinal Coupler Force" test was equivalent to the "Compression Buff Load" analysis case, and the "Vertical Coupler Force" test was equivalent to the "Upward Vertical" analysis case. Both were performed with a full tank on a tank car without a head brace.

The strain gage data came from several sets of strain gages that were placed near the termination of the sill-to-tank weld near the tank-head on the end of the tank car with no head brace, as shown in Figures 18 and 19. Some of the strain gage locations were duplicated symmetrically left to right. This is evident in Figure 19 at those sites showing two gage ID's with the suffixes "L" or "R". Figure 18 shows the general area on the tank car where these strain gages were located. Figure 19 is a close-up of this area showing the strain gage numbers and their orientations. Note that this figure shows only the orthogonal gages referenced in this comparison.

Since there were only stress results available for the Compression Buff load finite element analysis, comparisons with test data were made in terms of stress for this load case. For the Upward

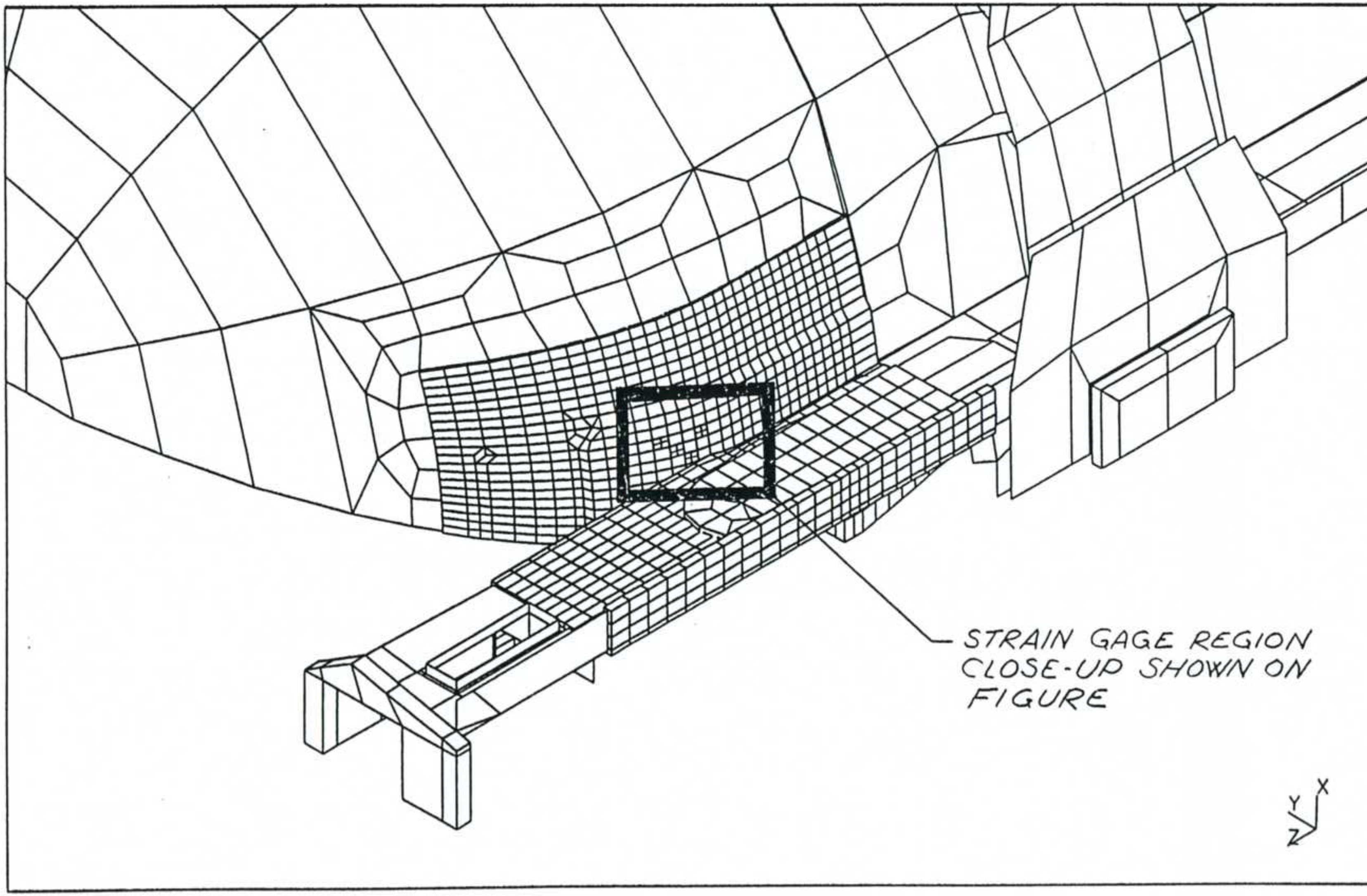

FIGURE 18. GENERAL VIEW OF STRAIN GAGED AREA ADJACENT TO THE STUB SILL ON THE TRINITY CAR

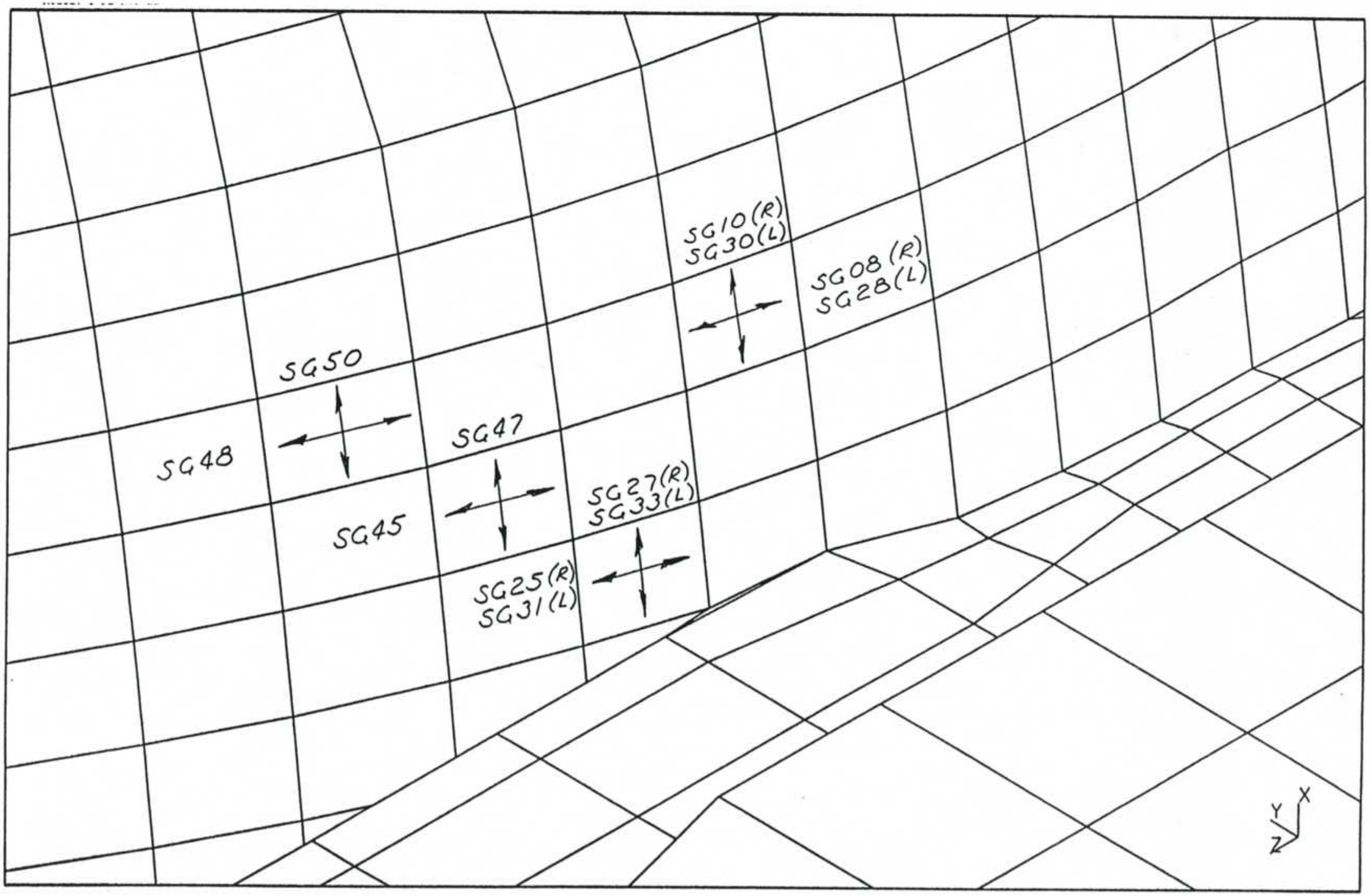

FIGURE 19. CLOSEUP VIEW OF STRAIN GAGED AREA ON THE TRINITY CAR

Vertical load case, comparisons were made wherever possible in terms of both stress and strain.

Data from the laterally and longitudinally oriented strain gages were multiplied by Young's modulus (30,000,000 psi) to convert them to stress values, and then compared with the finite element stress results in the lateral and longitudinal directions relative to the model's local "elemental" coordinate system. Maximum and minimum principal stresses were calculated from the strain data and from the finite element analysis results to provide an additional comparison.

The load magnitudes used in the tests were not exactly the same as the loads used in the corresponding finite element analysis load cases. The maximum "Longitudinal Coupler Force" (LCF) load used in the test was 324,500 lbs. The "Compression Buff Load" applied in the corresponding finite element analysis case was 350,000 lbs. Finite element analysis stress results were scaled to provide a direct comparison with test results. For example, the stress results from the compression buff load case finite element analysis would have to be multiplied by 0.926 before comparing them with the stresses calculated from the test results.

The maximum "Vertical Coupler Force" (VCF) used in the test was 20,100 lbs applied where the car couplers meet - 15.75 inches away from the striker plate. The "Upward Vertical" load in the finite element analysis case was 50,000 lbs applied at the striker plate. This means that the loading used in the finite element analysis was substantially different from the loading used in the test. When compared directly, one is a force, and one is a force plus a moment, so the results could not be scaled exactly for comparison. However, the area of comparison (strain gaged area) is relatively far from the load application point, so the results could be approximately scaled by converting the loads to moments about the truck center line and scaling to their ratio. Figure 20 shows a simple diagram of the equivalence calculations. This method yielded a scale factor of about 2.

To ensure an accurate comparison, a new "Upward Vertical" finite element analysis case was run using the same load and moment arm as in the test. Both stresses and strains were recovered in this new analysis and compared with the test results.

The orthogonal strains were compared at four locations. The finite element analysis strain results predicted higher strains than those found experimentally in the areas of highest stress (SC 30-32). The comparison was closer in other areas. In general, the strains predicted by the finite element analysis were always the same sign as the strains from the test results, and their magnitudes were in the same range.

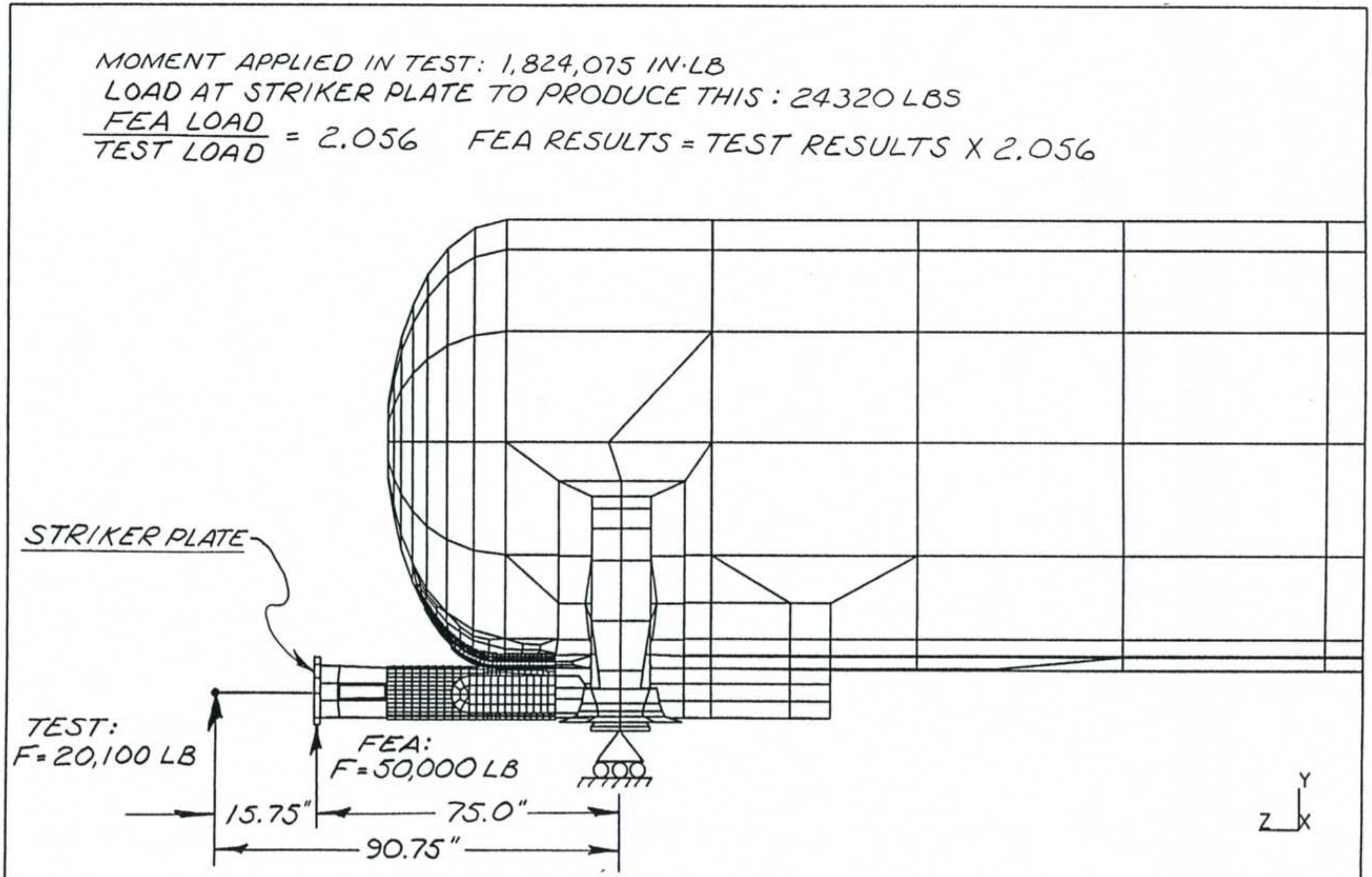

FIGURE 20. ILLUSTRATION OF EQUIVALENT UPWARD VERTICAL MOMENTS APPLIED IN THE FIELD AND IN THE ANALYSIS

Table 10a shows finite element predicted strains compared with measured strains for the vertical coupler force case. Figures 21 and 22 provide color contour plots of the finite element analysis strains in the longitudinal and circumferential directions.

The stress/strain gradients were fairly high in this area relative to the element sizes. This need for interpretation of the contour plots led to some uncertainty in the comparison with test results. The stress value at a specific location was estimated by interpolation within the contour lines.

There were some discrepancies side-to-side in some of the experimental strain readings from symmetric load cases. The strain gages were probably not placed exactly symmetrically from one side to the other. The high strain gradients in this area, especially near the tank/sill intersection, may also have contributed to the differences in side-to-side strain readings. Also, conversations with David Cackovic at TTC revealed that some of the strain-gaged cars had cracks or developed cracks during some of the tests[15].

Table 10. Comparison of TTC Strain Gage Results with Battelle Finite Element Analysis Results

(a) Strain results comparison - Vertical Coupler Force/Upward Vertical Load

Strain Components	Strain Gage No.	Test (μ Strain)	FEA (μ Strain)
ϵ_{long}	25/31	-391 to -439	-482 to -750
	48	-98	-135 to -482
	48	-50	0 to -135
	8/28	-180 to -232	-205 to -344
ϵ_{circ}	27/33	-227 to -346	-400 to -700
	47	-216	-100 to -360
	50	-140	0 to -100
	10/30	-52	-17 to -187

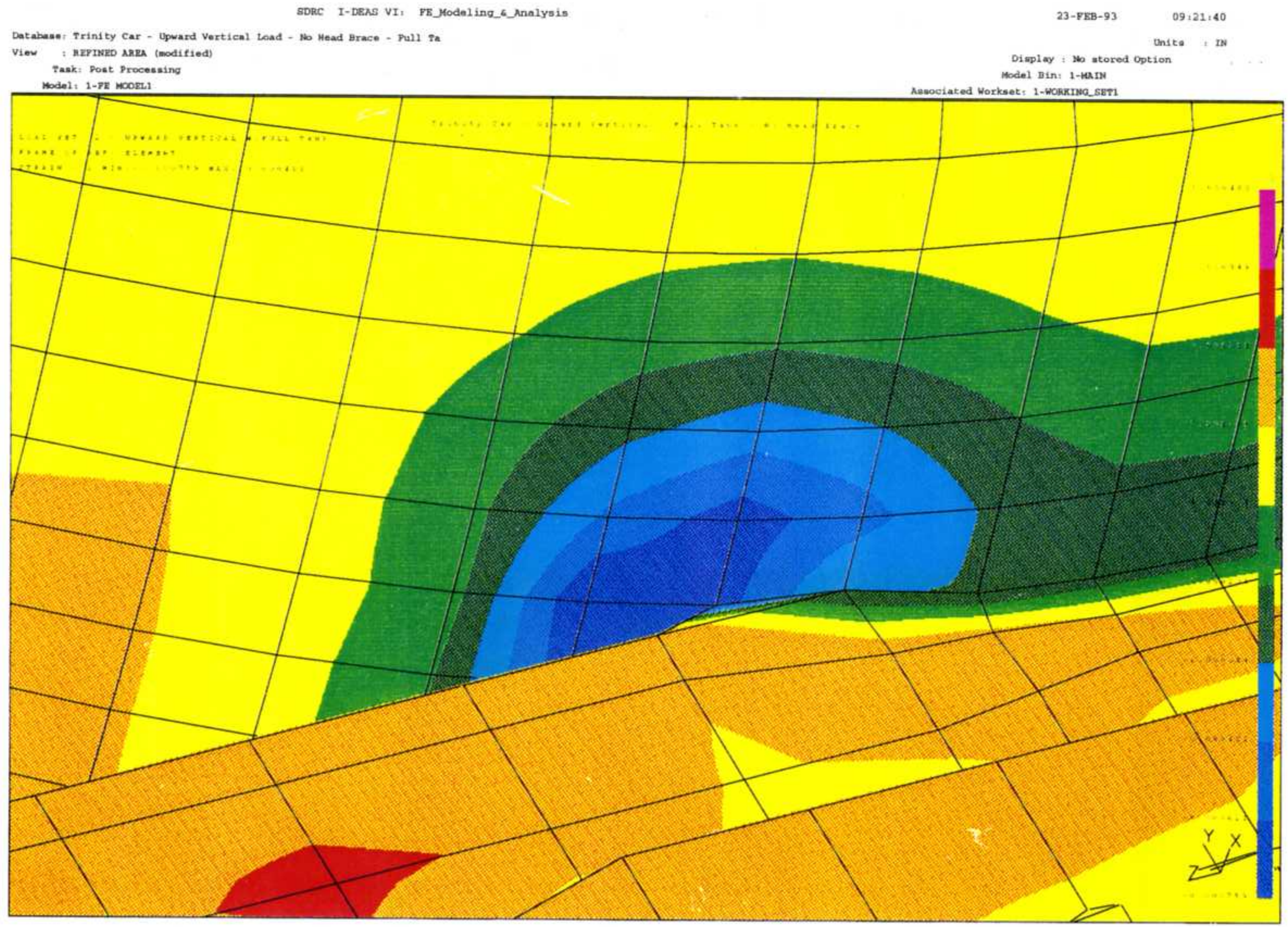

FIGURE 21. LONGITUDINAL STRAIN CONTOURS IN THE STRAIN GAGED AREA FOR THE UPWARD VERTICAL LOADING CASE; Maximum Strain = 0.000488, Minimum Strain = -0.000759

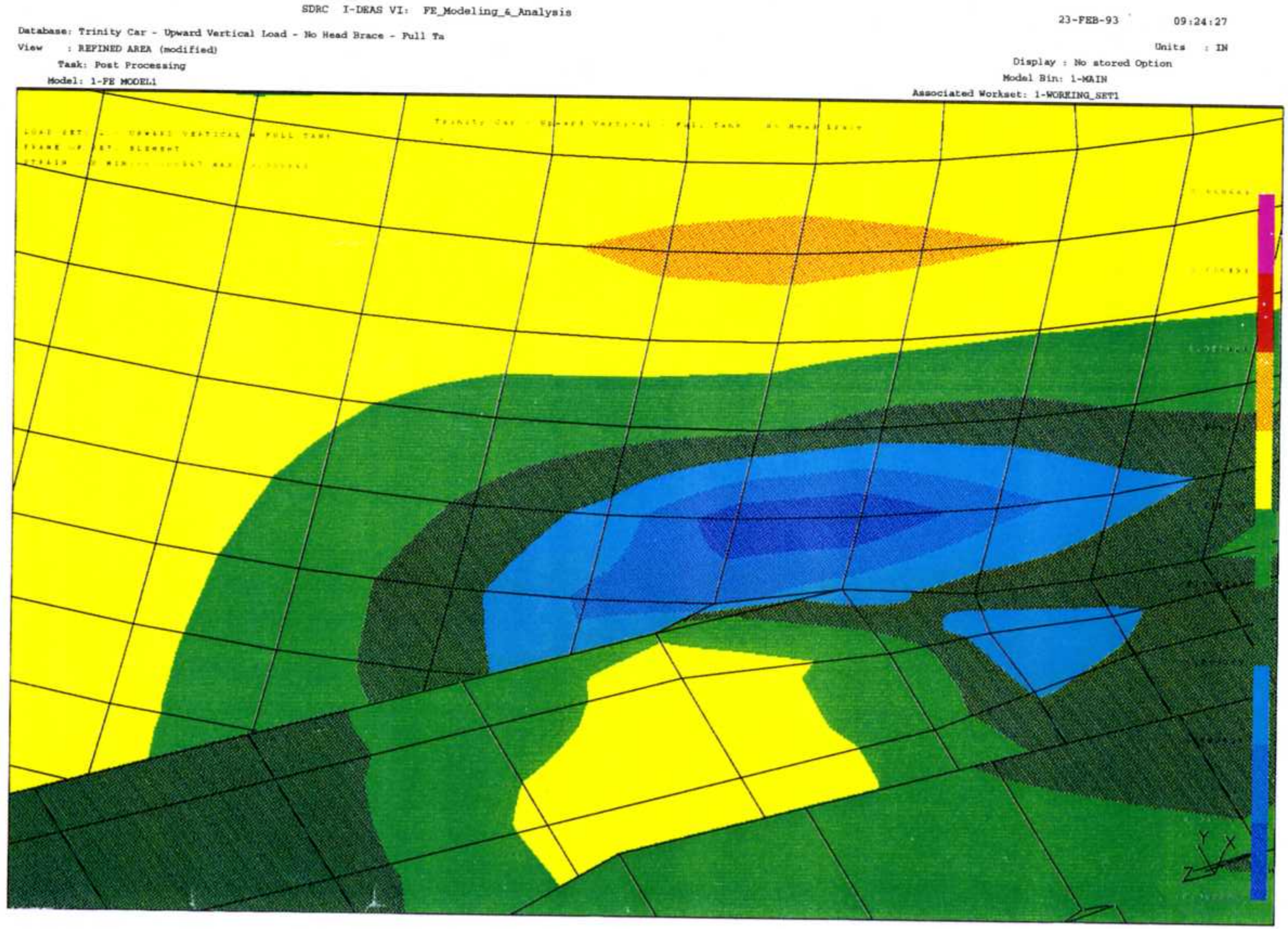

FIGURE 22. CIRCUMFERENTIAL STRAIN CONTOURS IN THE STRAIN GAGED AREA FOR THE UPWARD VERTICAL LOADING CASE; Maximum Strain = 0.000663, Minimum Strain = -0.000867

Figures 23 through 30 include stress and strain contour plots from the finite element analysis for the strain gaged area under comparison. The stress values used for the comparison with test data were estimated near the center of the element located closest to the corresponding strain gage set. Each contour color band represents a variation in stress of at least 4,000 psi, and occasionally a variation as high as 10,000 psi.

Tables 10b and 10c show the comparison of TTC's strain gage data (converted to stress) with Battelle's finite element stress analysis results for the Vertical Coupler Force and Longitudinal Coupler Force load cases. Figures 23 and 24 are color contour plots of the finite element analysis stress results in the longitudinal and circumferential directions for the Upward Vertical load case. Figures 25 and 26 are color contour plots of the maximum and minimum principal stresses for the Upward Vertical load case. Figures 27 and 28 are color contour plots of the finite element analysis stress results in the longitudinal and circumferential directions for the Compression Buff load case. Figures 29 and 30 are color contour plots of the maximum and minimum principal stresses for the Compression Buff load case.

The experimental and analytical results agree fairly well in most locations considering all the uncertainties inherent in this kind of comparison. The finite-element-calculated stress values in the table can be interpreted within a tolerance of about 5 ksi. In general, the comparison of "Vertical Coupler Force" to "Upward Vertical Load" and "Longitudinal Coupler Force" to "Compression Buff Load" are within expected tolerances.

This level of agreement says that this model can be used to predict nominal stress levels in the tank car structure. This model does not precisely account for the effect of highly local stress concentrations such as in the vicinity of welds, bolts, and valves, since local geometric variations and design anomolies substantially affect the severity of local stresses. However, this model can be used to make meaningful qualitative comparisons between different design features and can also be used to help select strain gage locations for other detailed experimental studies.

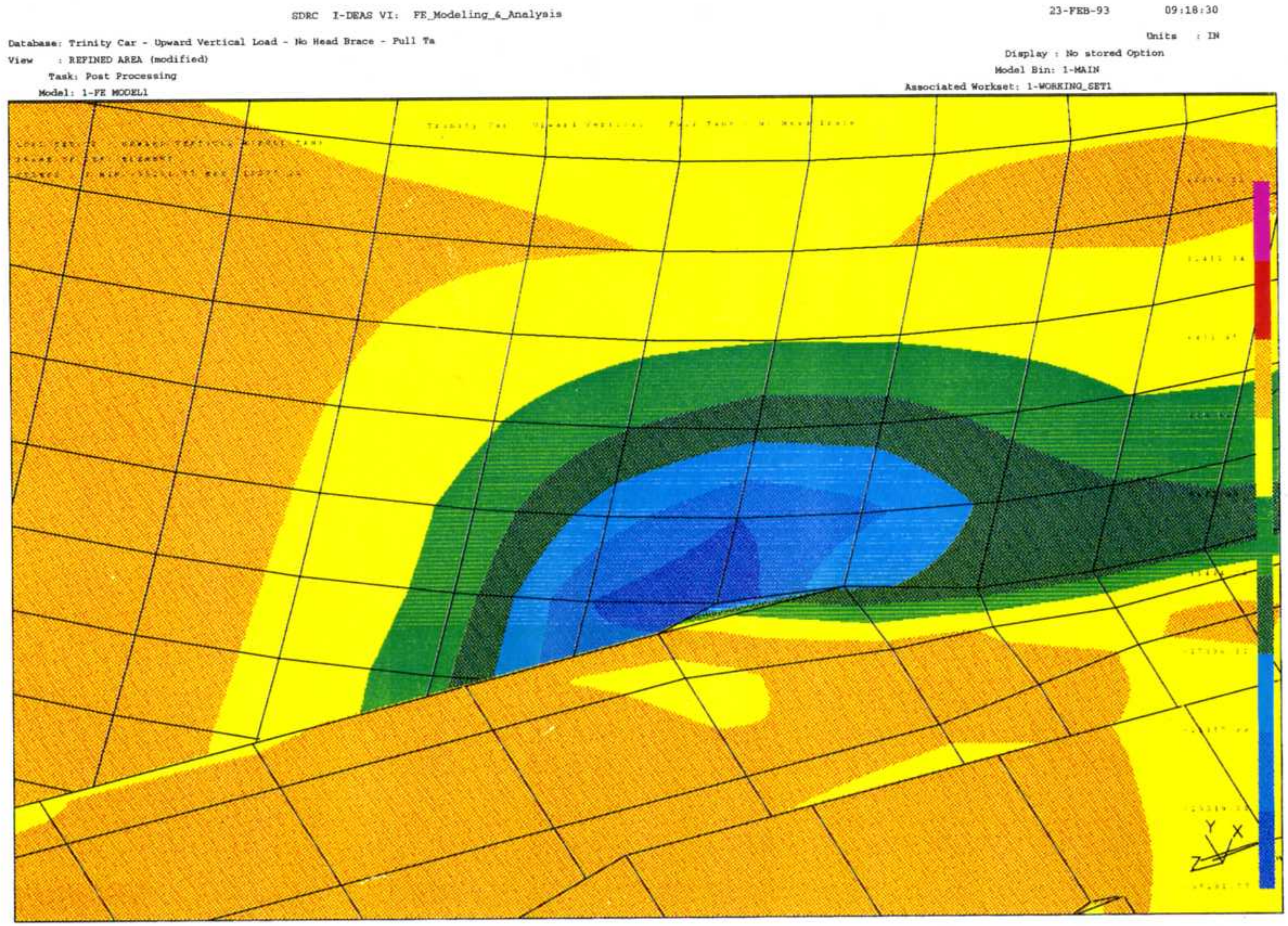

FIGURE 23. LONGITUDINAL STRESS CONTOURS IN THE STRAIN GAGED AREA FOR THE UPWARD VERTICAL LOADING CASE; Maximum Stress = 18.4 ksi, Minimum Stress = -35.3 ksi

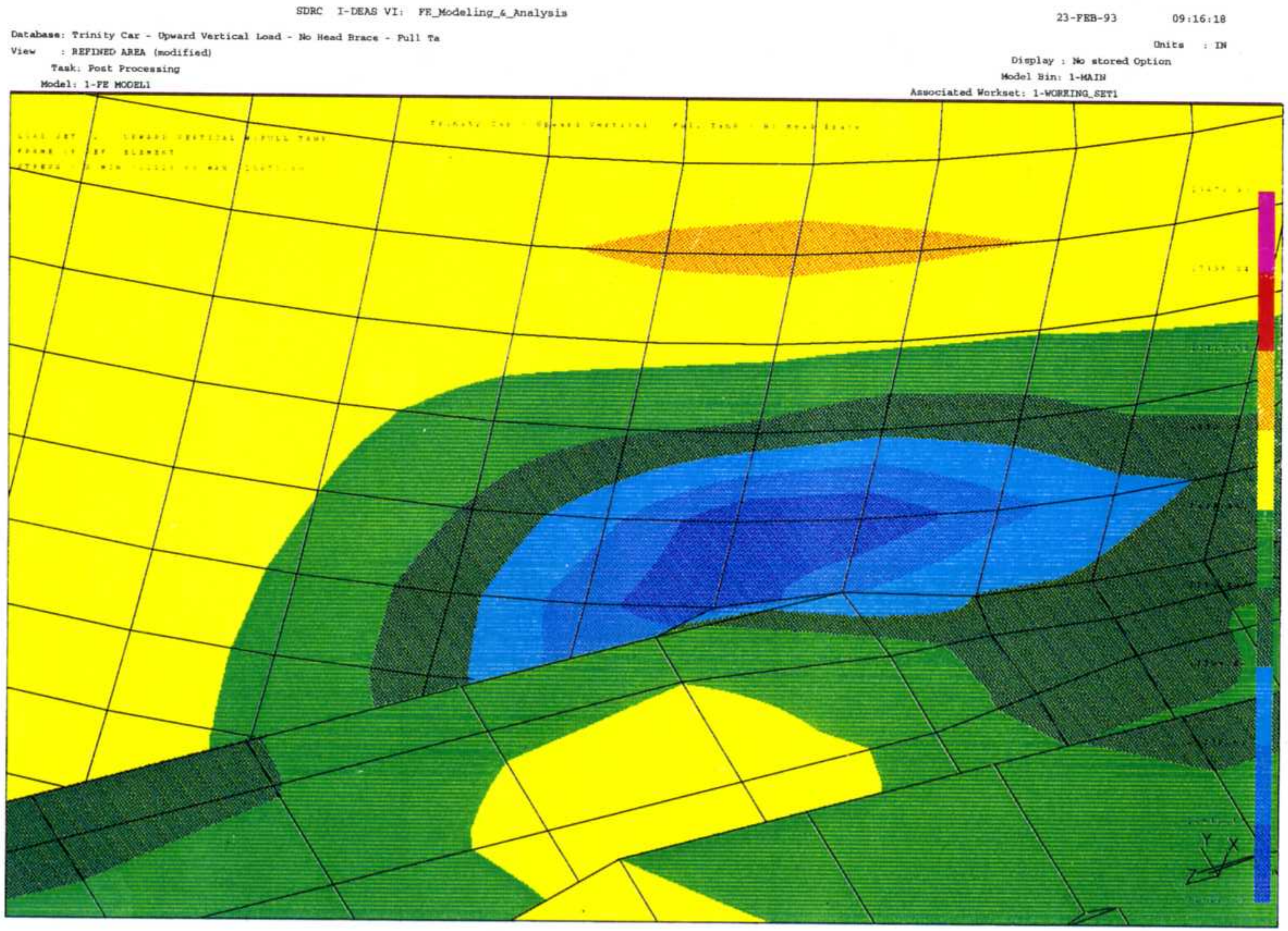

FIGURE 24. CIRCUMFERENTIAL STRESS CONTOURS IN THE STRAIN GAGED AREA FOR THE UPWARD VERTICAL LOADING CASE; Maximum Stress = 23.7 ksi, Minimum Stress = -32.8 ksi

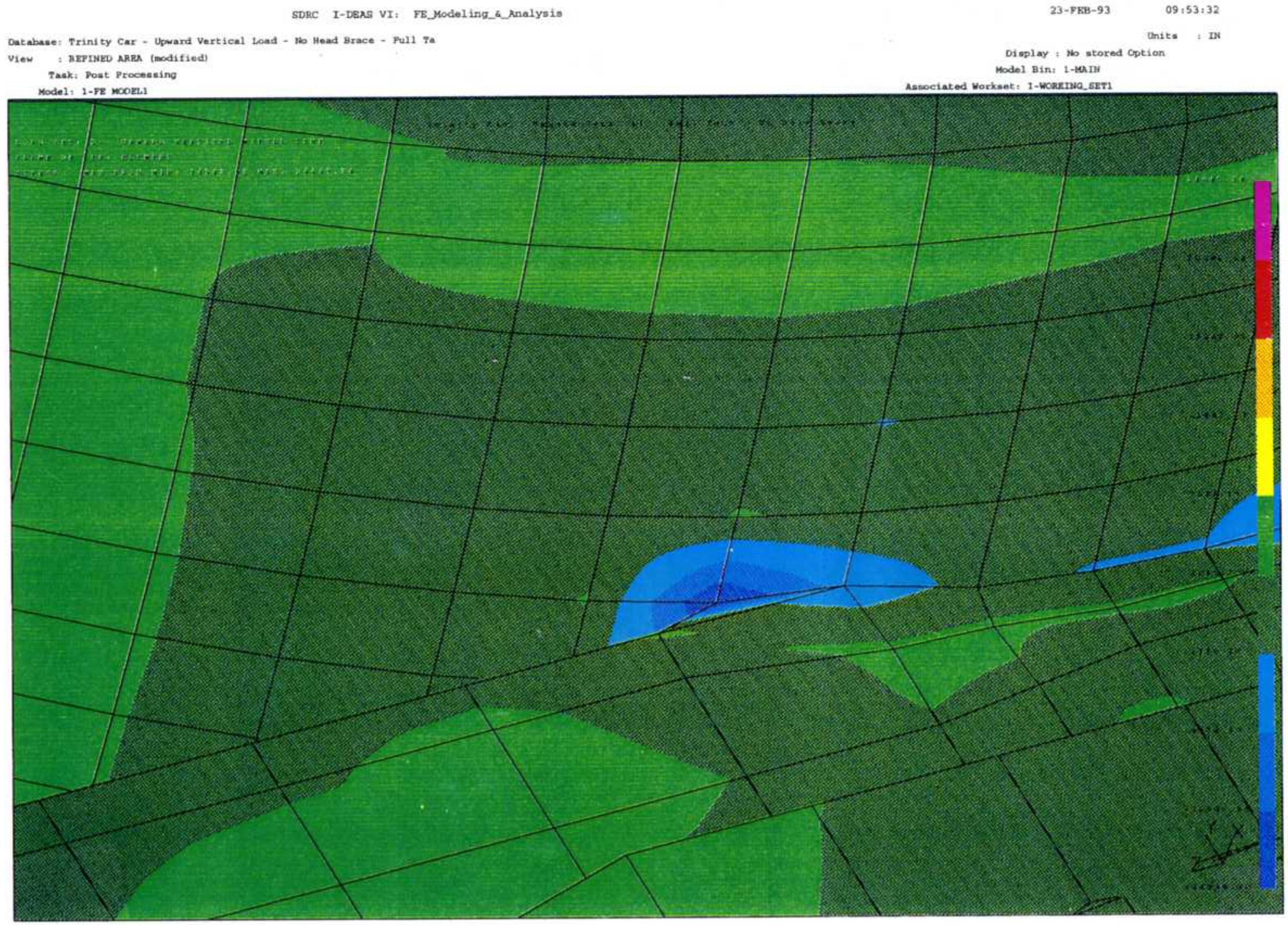

FIGURE 25. MAXIMUM PRINCIPAL STRESS CONTOURS IN THE STRAIN GAGED AREA FOR THE UPWARD VERTICAL LOADING CASE; Maximum Stress = 24.6 ksi, Minimum Stress = -14.9 ksi

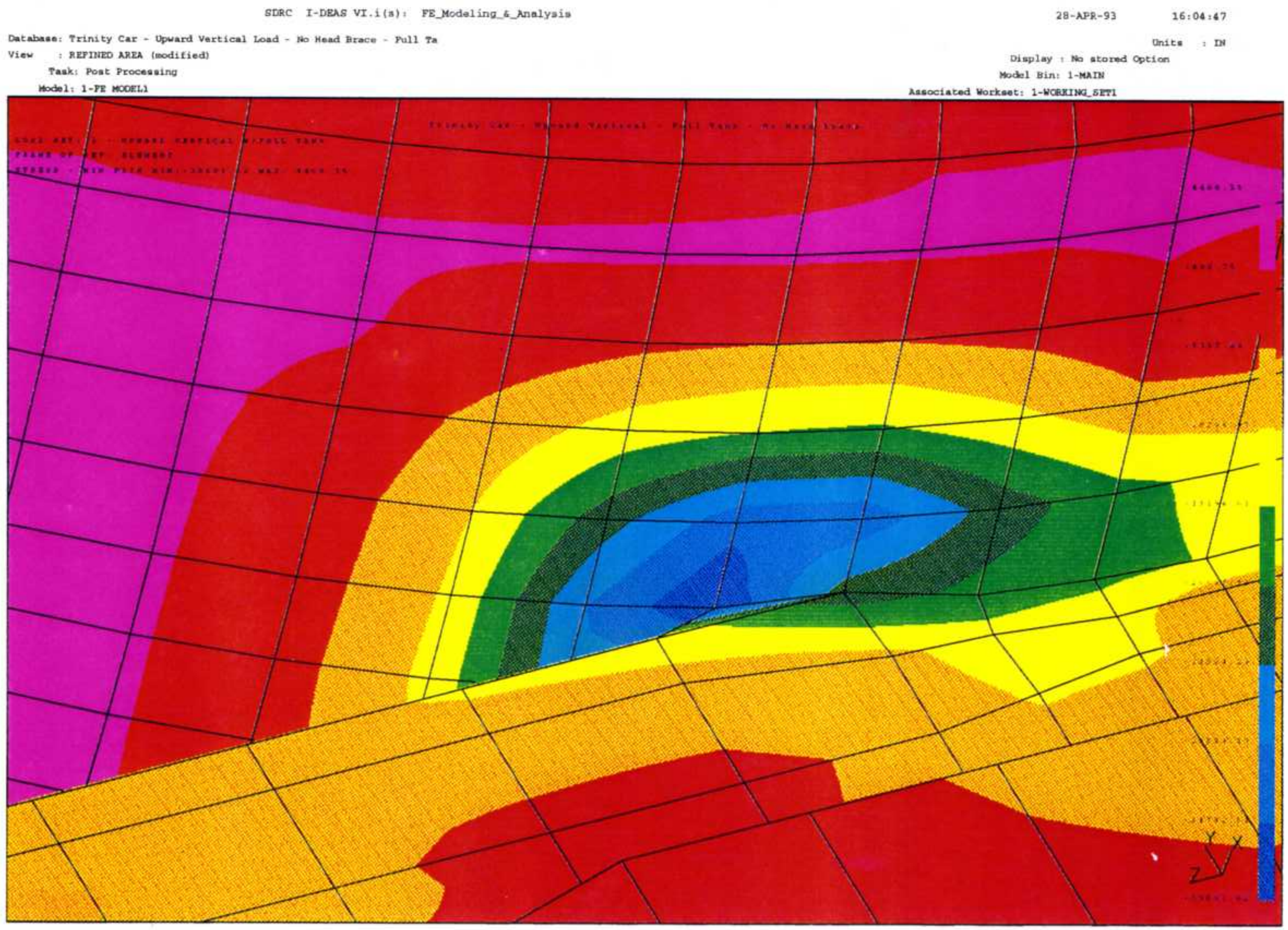

FIGURE 26. MINIMUM PRINCIPAL STRESS CONTOURS IN THE STRAIN GAGED AREA FOR THE UPWARD VERTICAL LOADING CASE; Maximum Stress = 4.4 ksi, Minimum Stress = -39.7 ksi

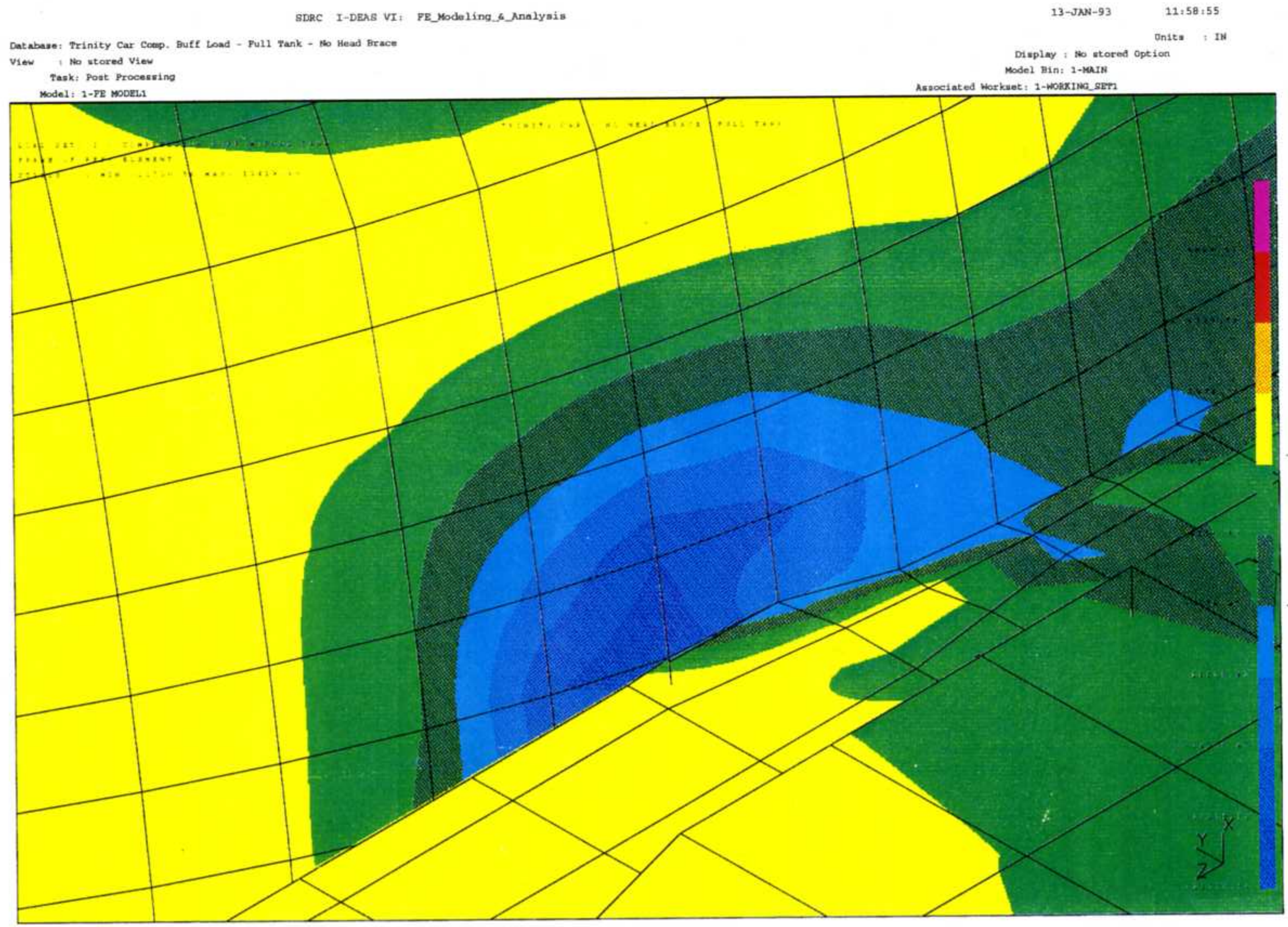

FIGURE 27. LONGITUDINAL STRESS CONTOURS IN THE STRAIN GAGED AREA FOR THE COMPRESSION BUFF LOADING CASE; Maximum Stress = 13.4 ksi, Minimum Stress = -21.7 ksi

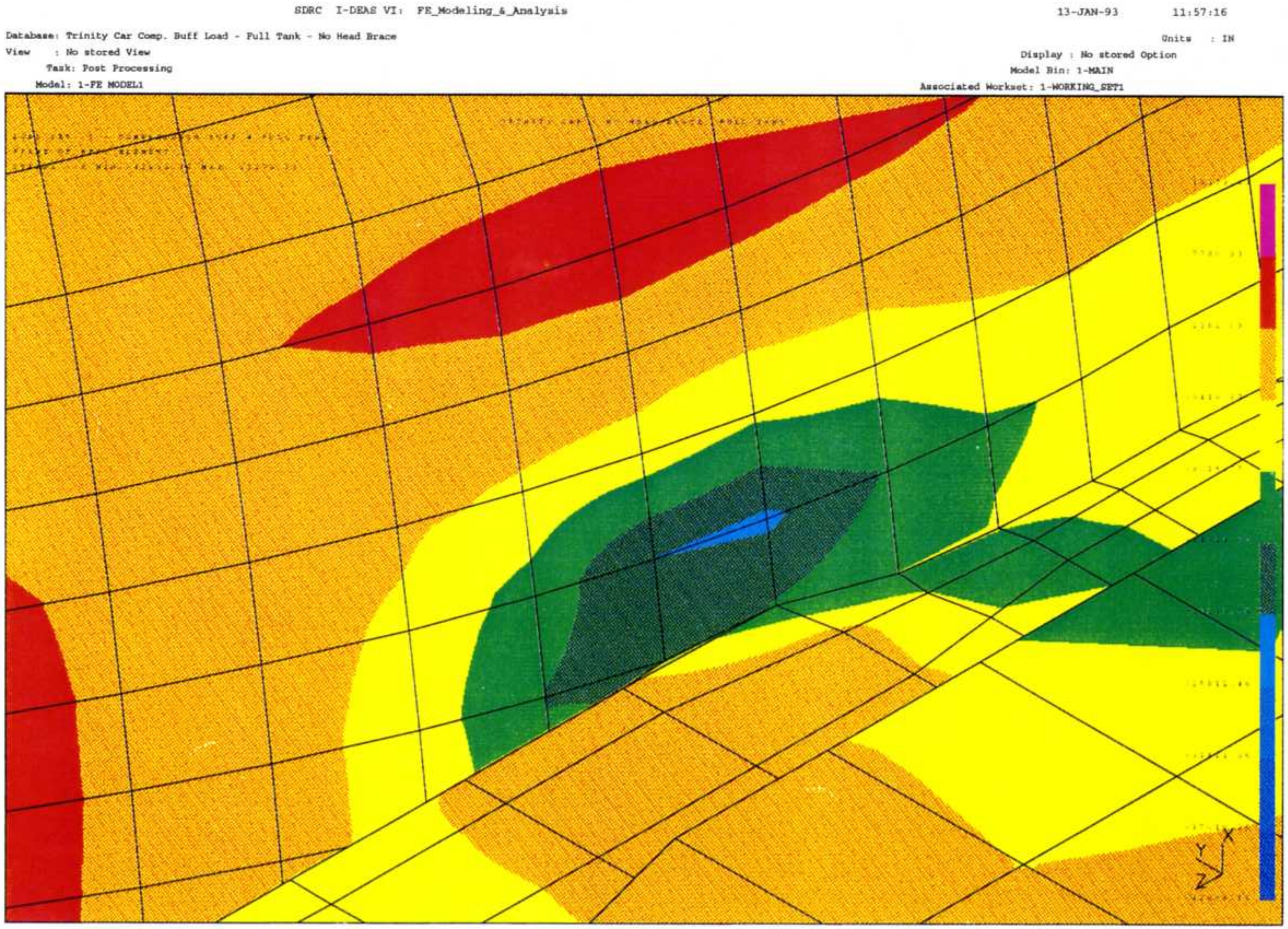

FIGURE 28. CIRCUMFERENTIAL STRESS CONTOURS IN THE STRAIN GAGED AREA FOR THE COMPRESSION BUFF LOADING CASE; Maximum Stress = 13.4 ksi, Minimum Stress = -42.6 ksi

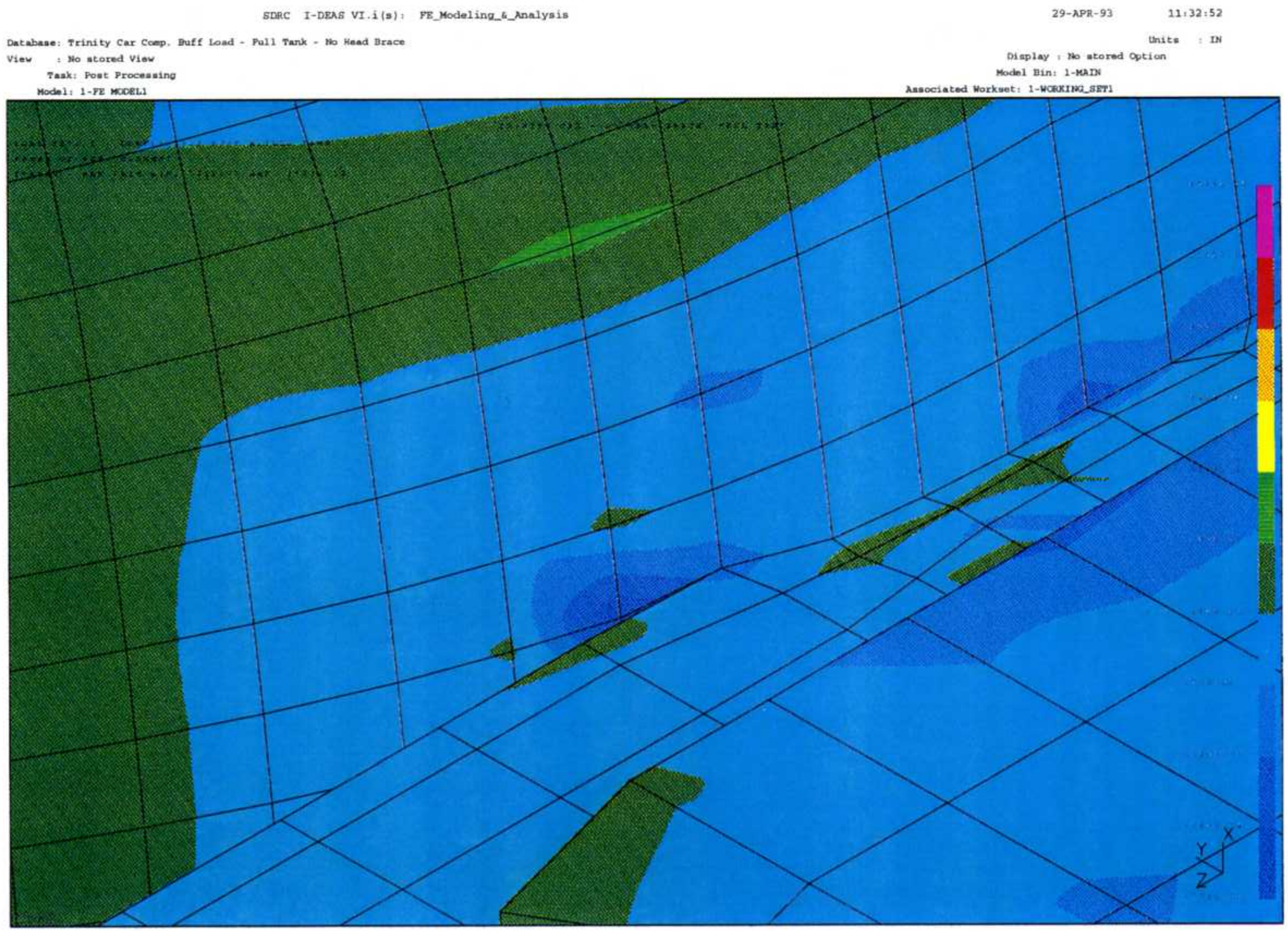

FIGURE 29. MAXIMUM PRINCIPAL STRESS CONTOURS IN THE STRAIN GAGED AREA FOR THE COMPRESSION BUFF LOADING CASE; Maximum Stress = 18.3 ksi, Minimum Stress = -7.7 ksi

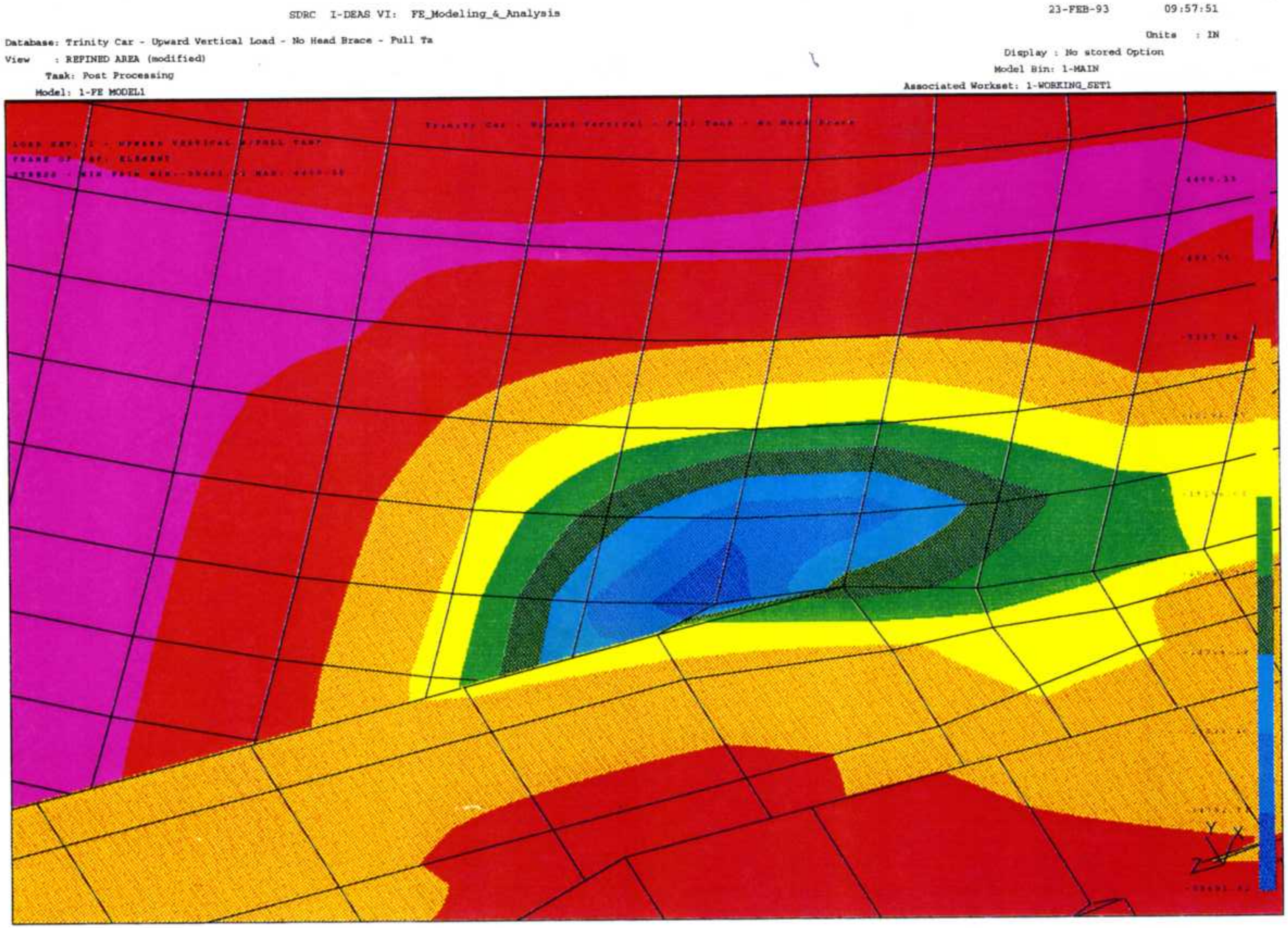

FIGURE 30. MINIMUM PRINCIPAL STRESS CONTOURS IN THE STRAIN GAGED AREA FOR THE COMPRESSION BUFF LOADING CASE; Maximum Stress = 4.4 ksi, Minimum Stress = -39.7 ksi

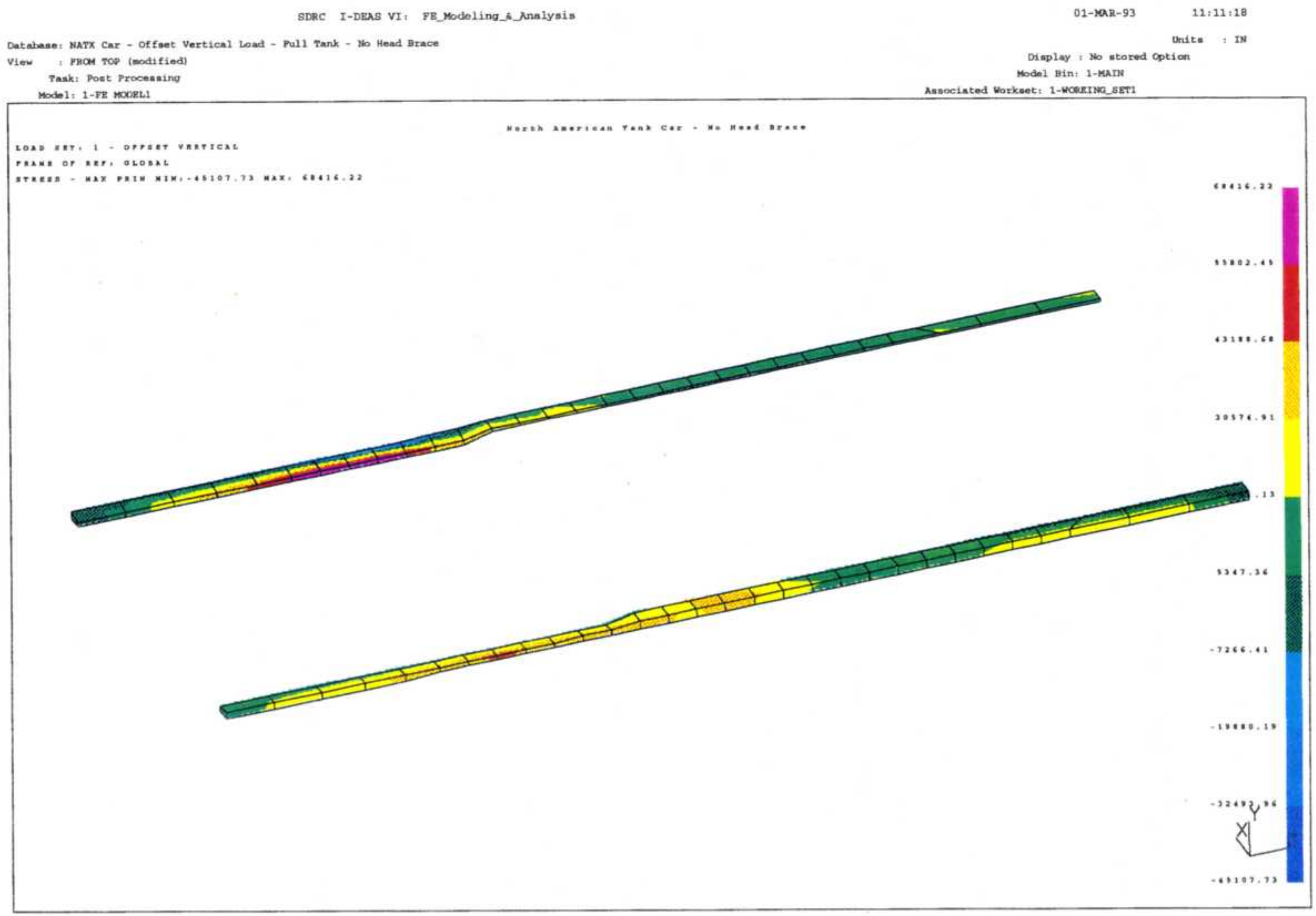

FIGURE B-28. NATX Z SECTION TO TRANSITION PLATE WELD, MAXIMUM PRINCIPAL STRESS, OFFSET VERTICAL, FULL TANK, NO HEAD BRACE; Maximum Stress = 68.4 ksi, Minimum Stress = -45.1 ksi

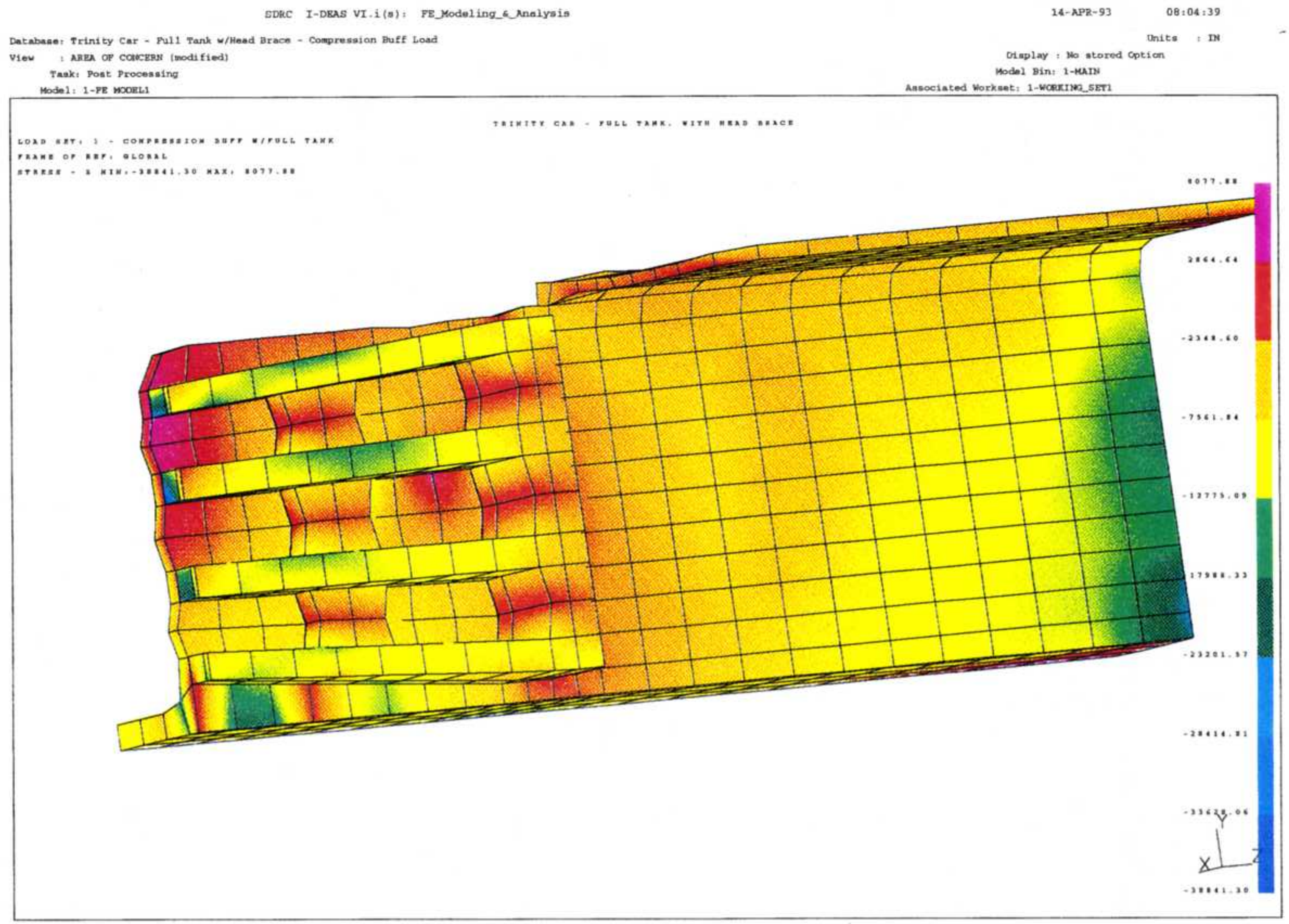

FIGURE B-29. TRINITY Z SECTION LUG AREA, LONGITUDINAL STRESS, COMPRESSION BUFF, FULL TANK, HEAD BRACE; Maximum Stress = 8.1 ksi, Minimum Stress = -38.8 ksi

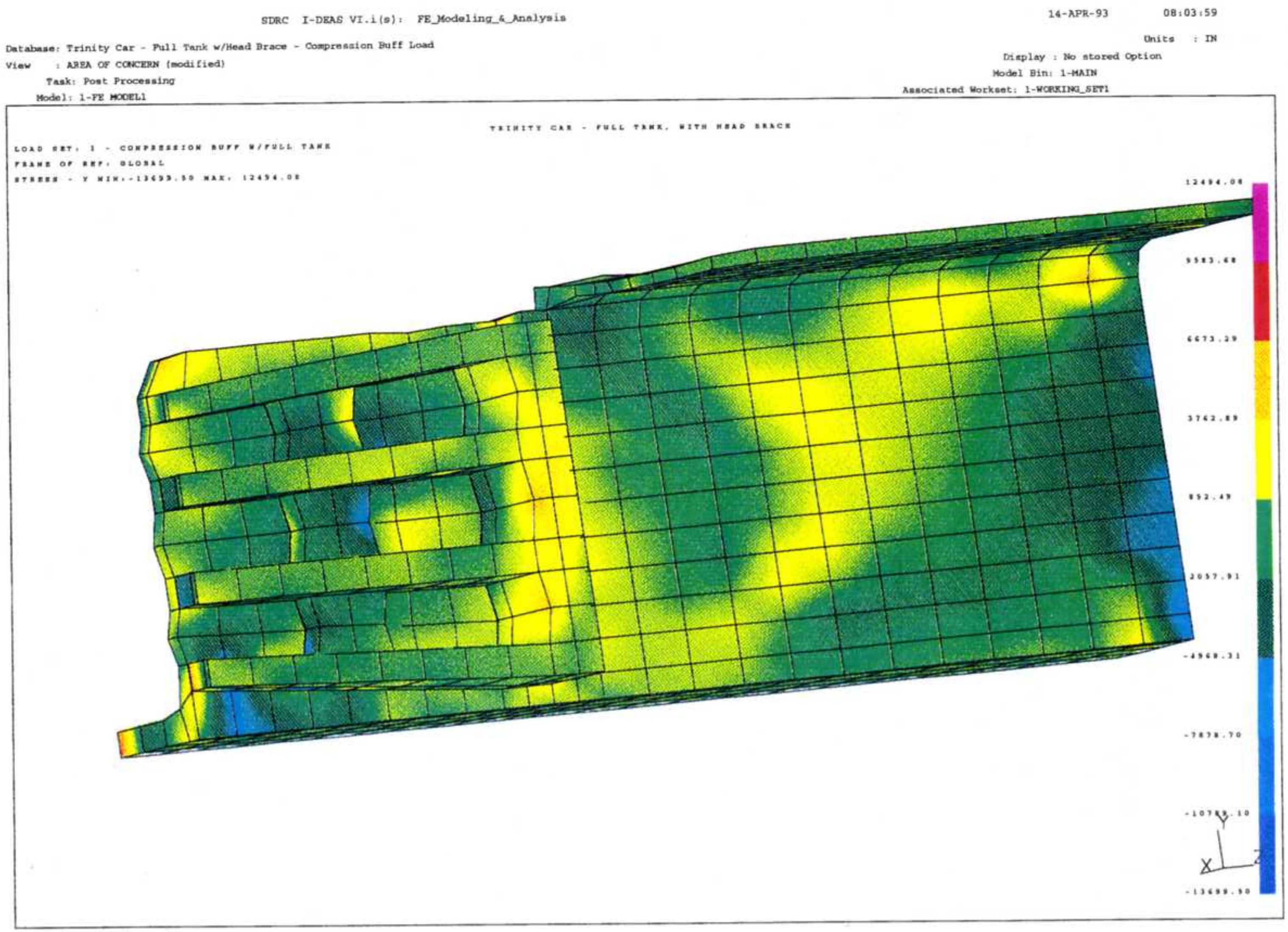

FIGURE B-30. TRINITY Z SECTION LUG AREA, VERTICAL STRESS, COMPRESSION BUFF LOAD, FULL TANK, WITH HEAD BRACE; Maximum Stress = 12.5 ksi, Minimum Stress = -13.7 ksi

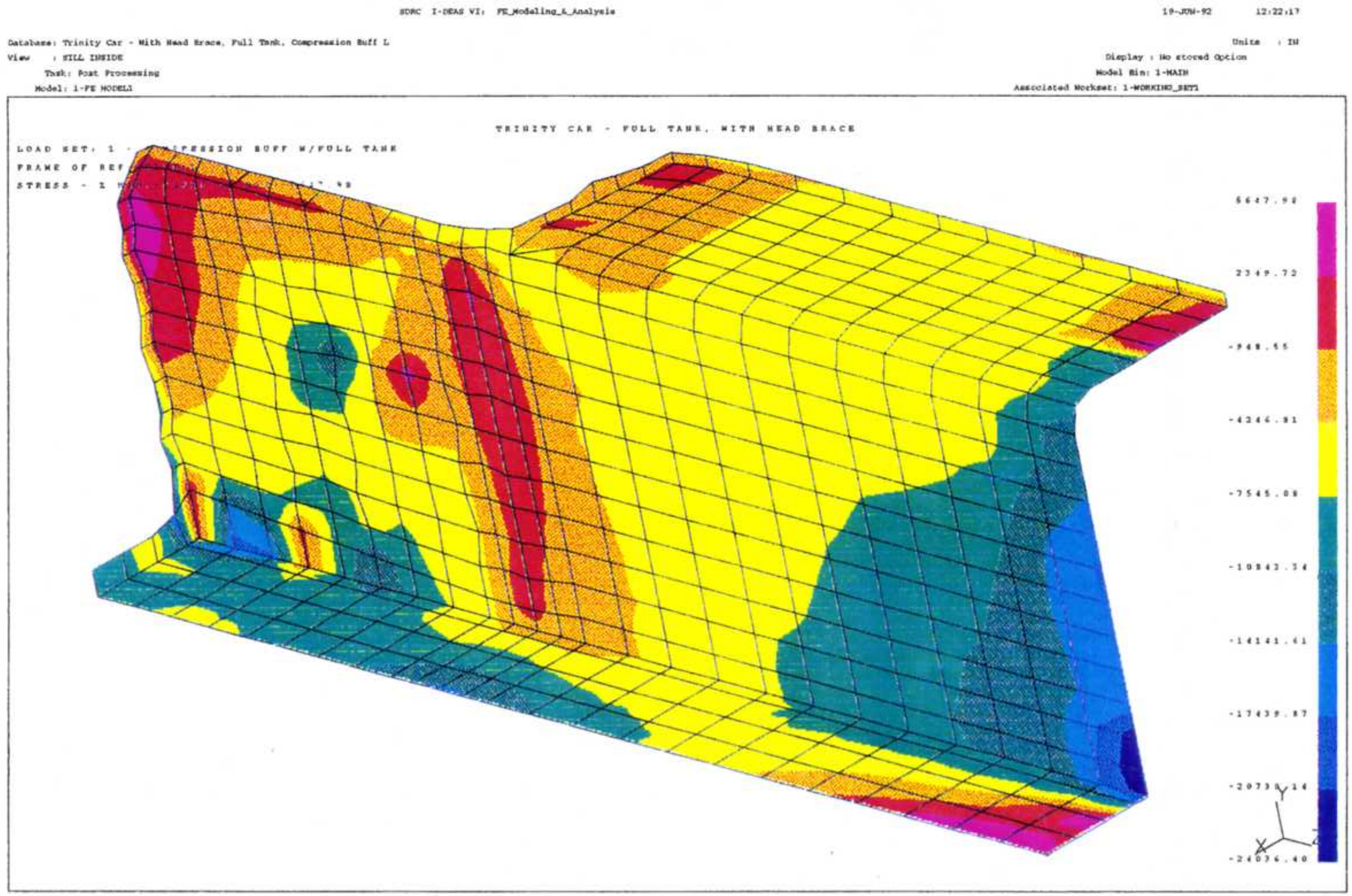

FIGURE B-31. TRINITY Z SECTION LUG AREA, LONGITUDINAL STRESS, COMPRESSION BUFF LOAD, FULL TANK, WITH HEAD BRACE (FIRST VIEW); Maximum Stress = 5.6 ksi, Minimum Stress = -24.0 ksi

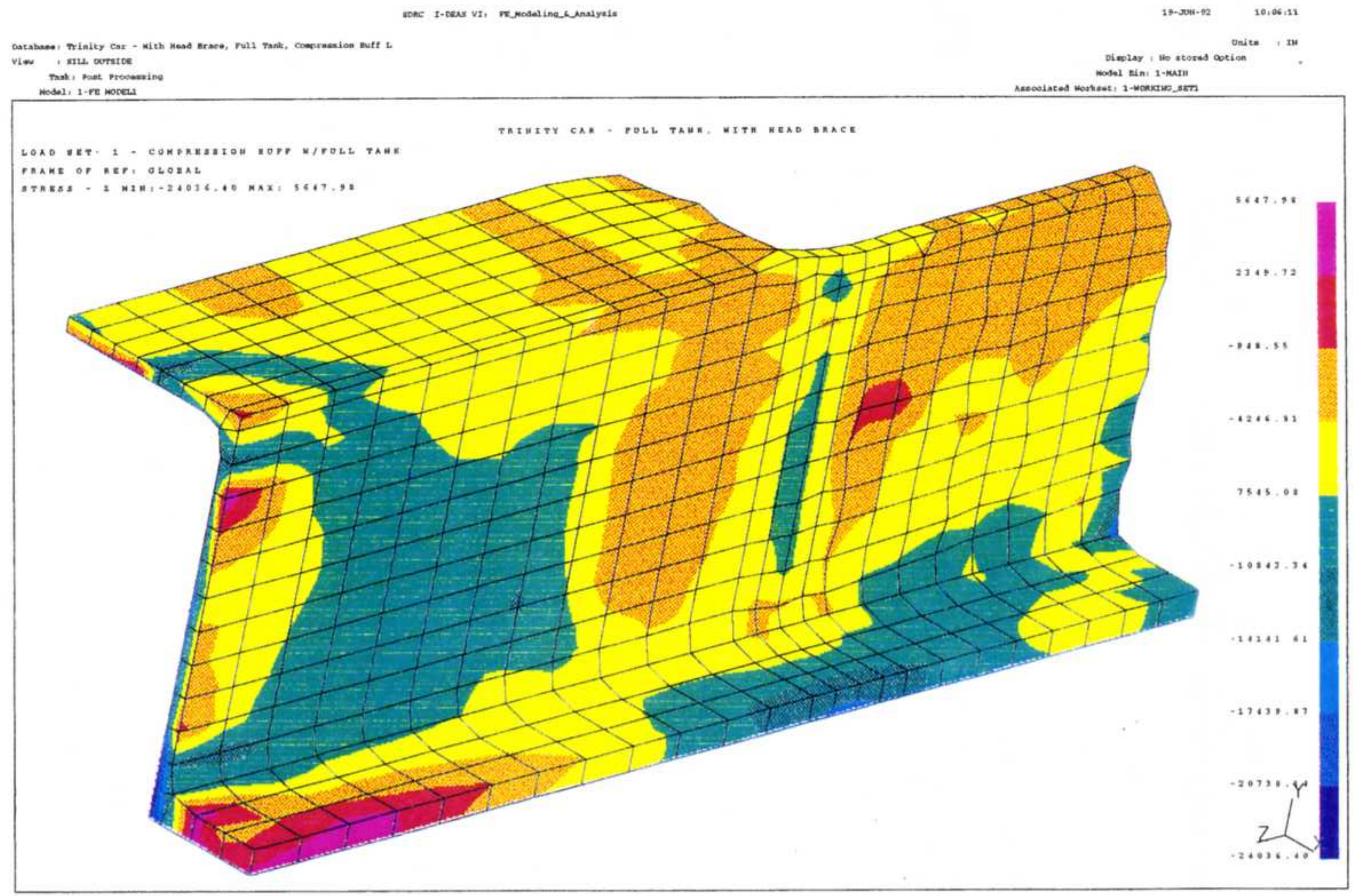

FIGURE B-32. TRINITY Z SECTION LUG AREA, LONGITUDINAL STRESS, COMPRESSION BUFF LOAD, FULL TANK, WITH HEAD BRACE (SECOND VIEW); Maximum Stress = 5.6 ksi, Minimum Stress = -24.0 ksi

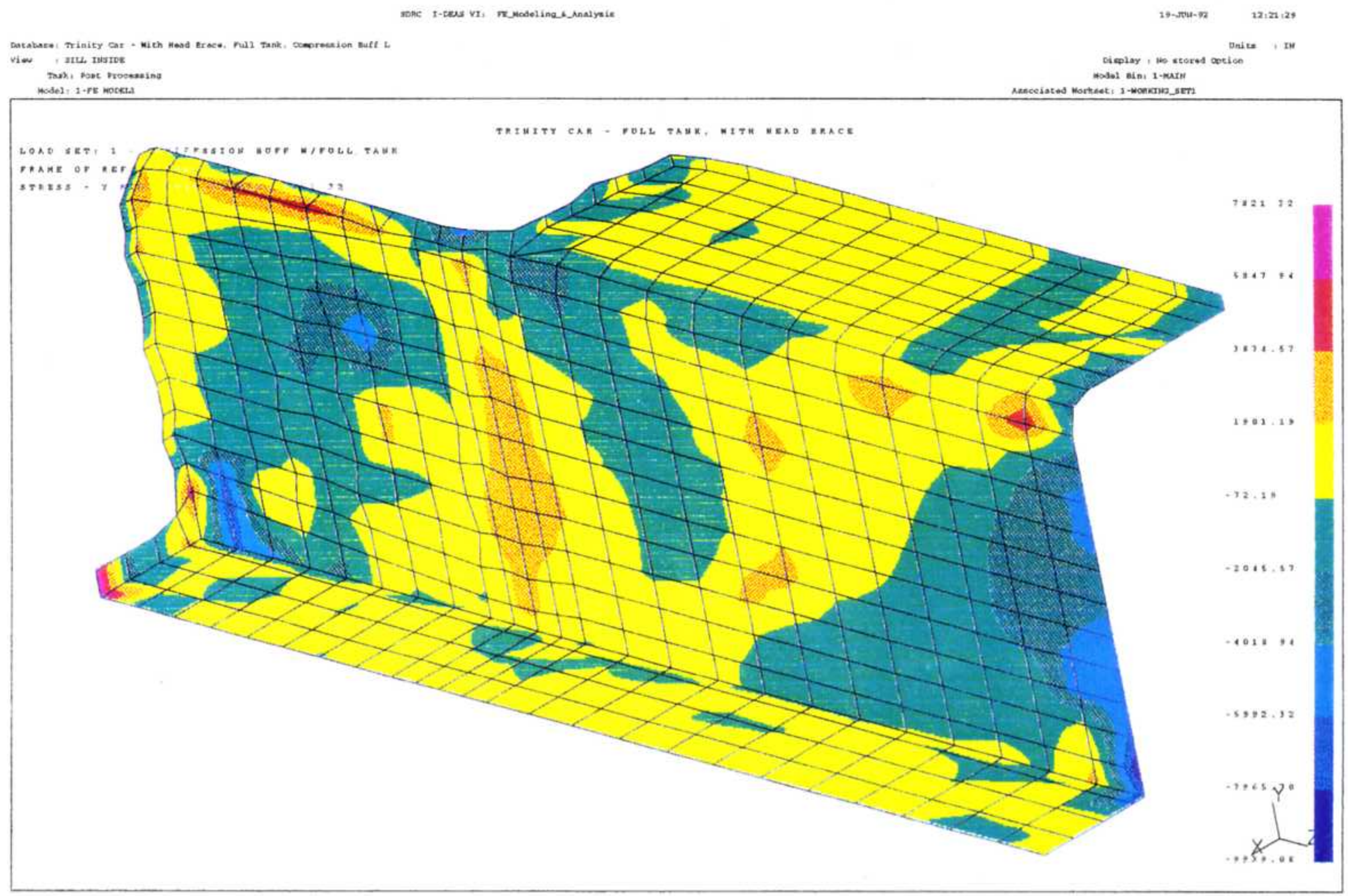

FIGURE B-33. TRINITY Z SECTION LUG AREA, VERTICAL STRESS, COMPRESSION BUFF LOAD, FULL TANK, WITH HEAD BRACE (FIRST VIEW); Maximum Stress = 7.8 ksi, Minimum Stress =-9.9 ksi

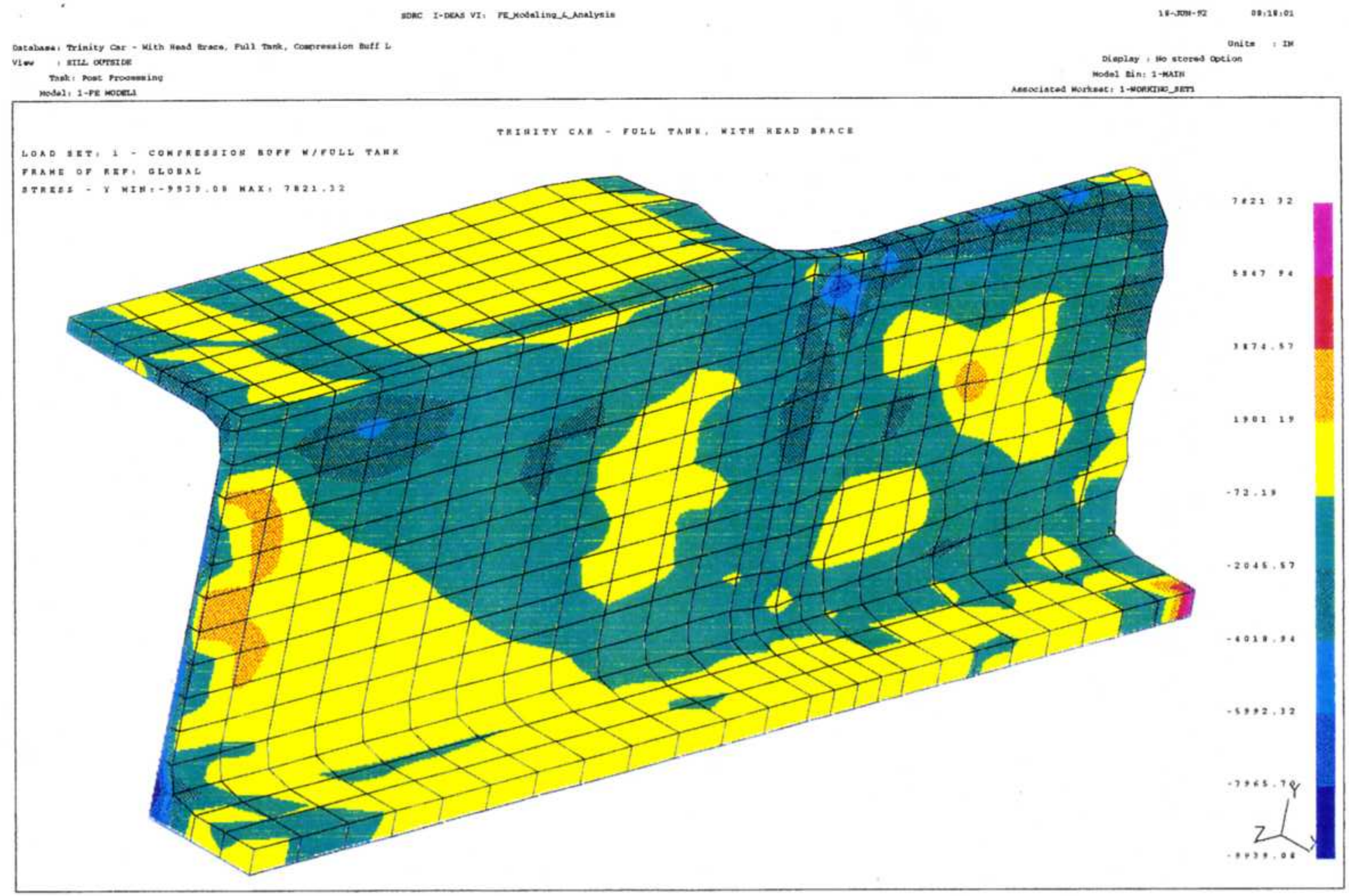

FIGURE B-34. TRINITY Z SECTION LUG AREA, VERTICAL STRESS, COMPRESSION BUFF LOAD, FULL TANK, WITH HEAD BRACE (SECOND VIEW); Maximum Stress = 7.8 ksi, Minimum Stress = -9.9 ksi

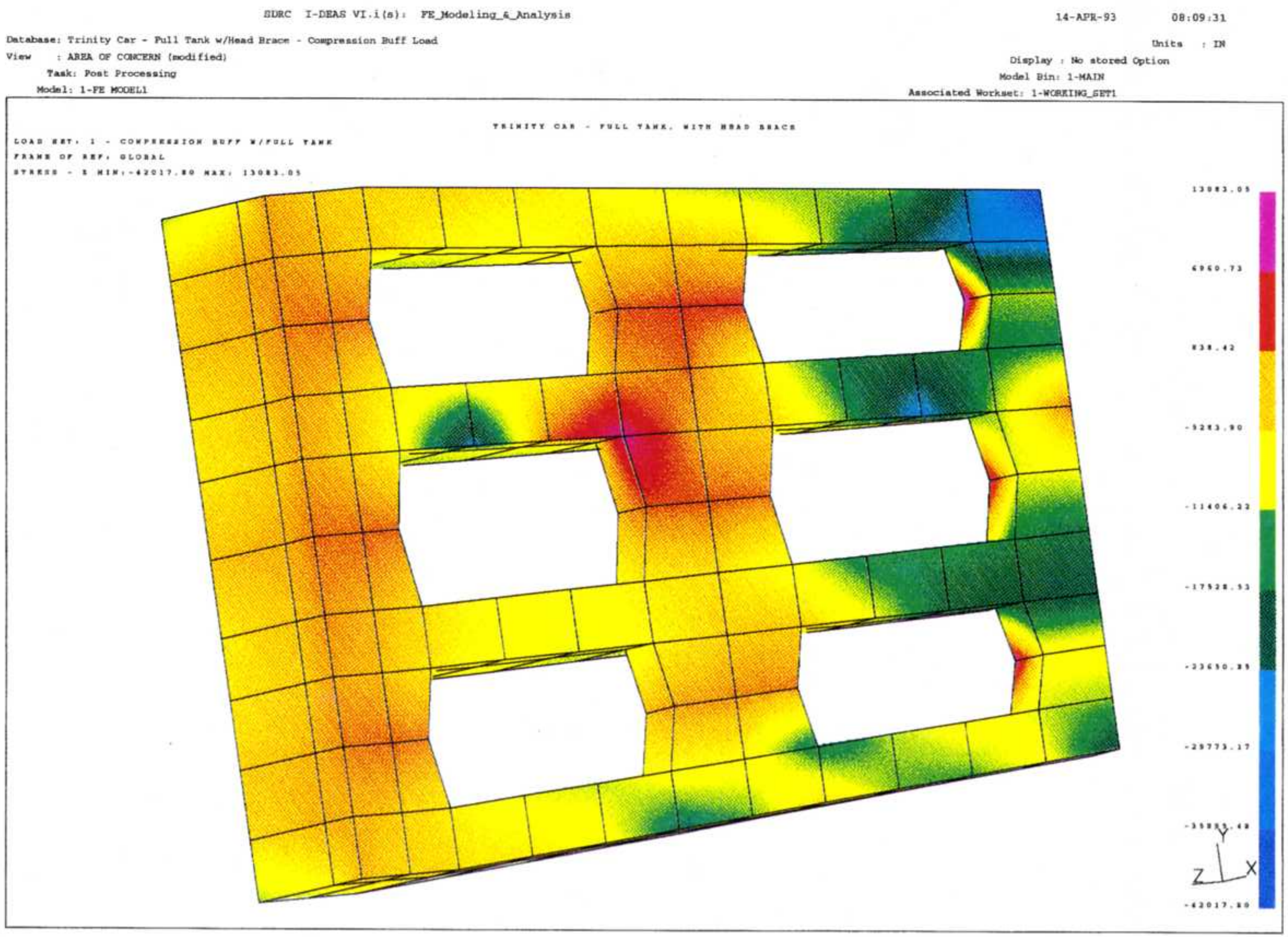

FIGURE B-35. TRINITY REAR LUG, LONGITUDINAL STRESS, COMPRESSION BUFF LOAD, FULL TANK, WITH HEAD BRACE; Maximum Stress = 13.1 ksi, Minimum Stress = -42.0 ksi

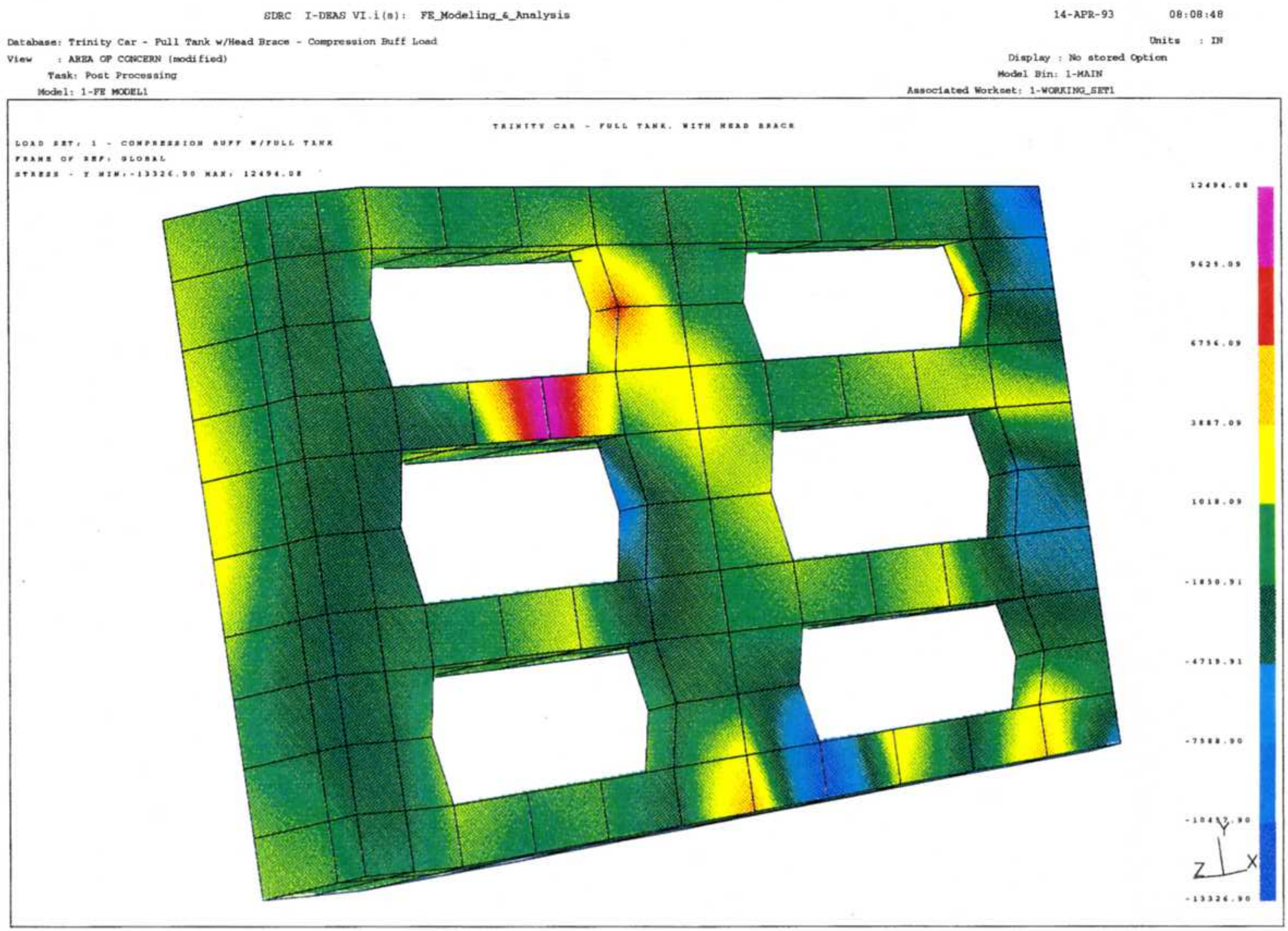

FIGURE B-36. TRINITY REAR LUG, VERTICAL STRESS, COMPRESSION BUFF LOAD, FULL TANK, WITH HEAD BRACE; Maximum Stress = 12.5 ksi, Minimum Stress = -13.3 ksi

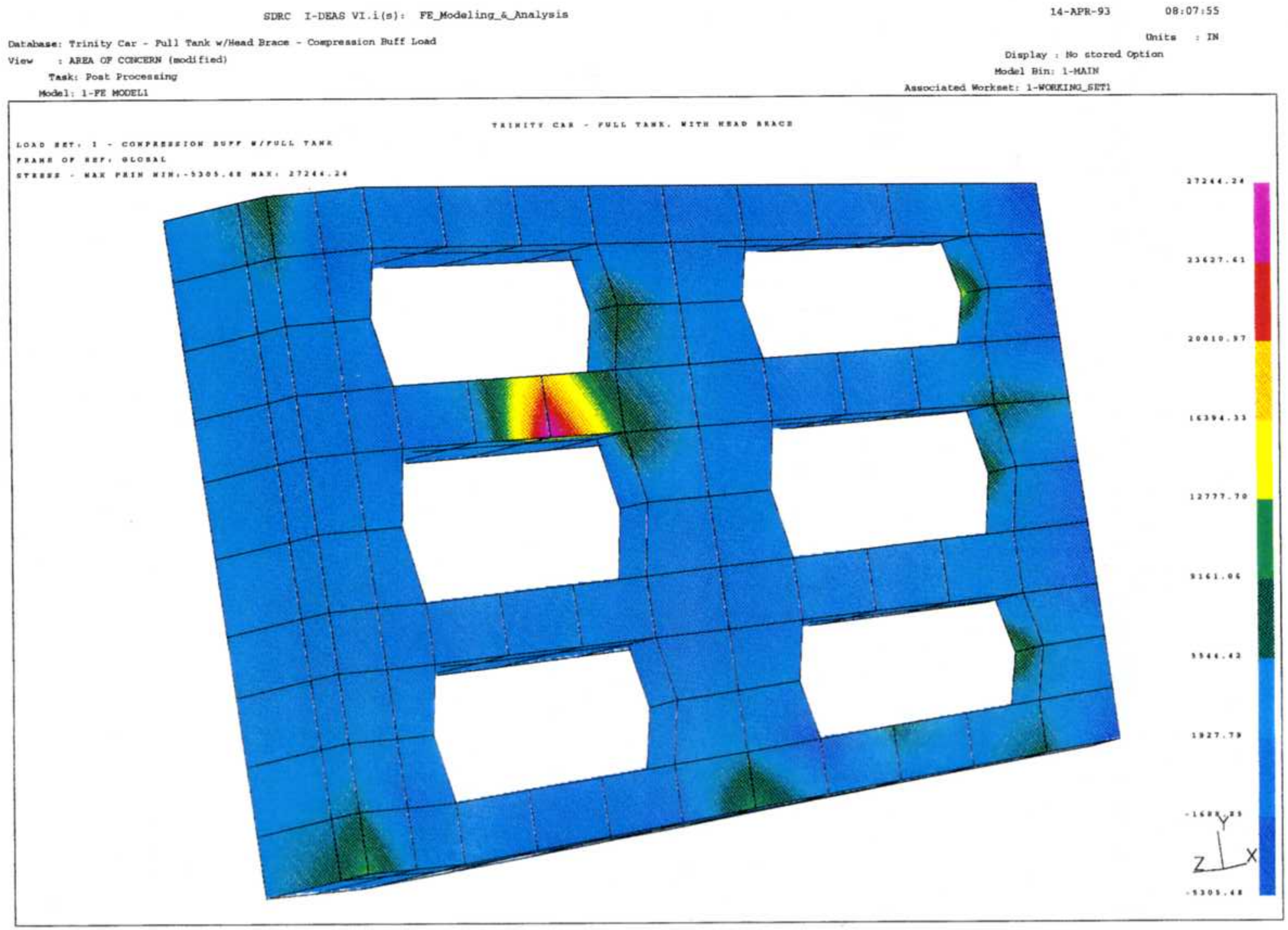

FIGURE B-37. TRINITY REAR DRAFT LUG, MAXIMUM PRINCIPAL STRESS, COMPRESSION BUFF LOAD, FULL TANK, WITH HEAD BRACE; Maximum Stress = 27.2 ksi, Minimum Stress = -5.3 ksi

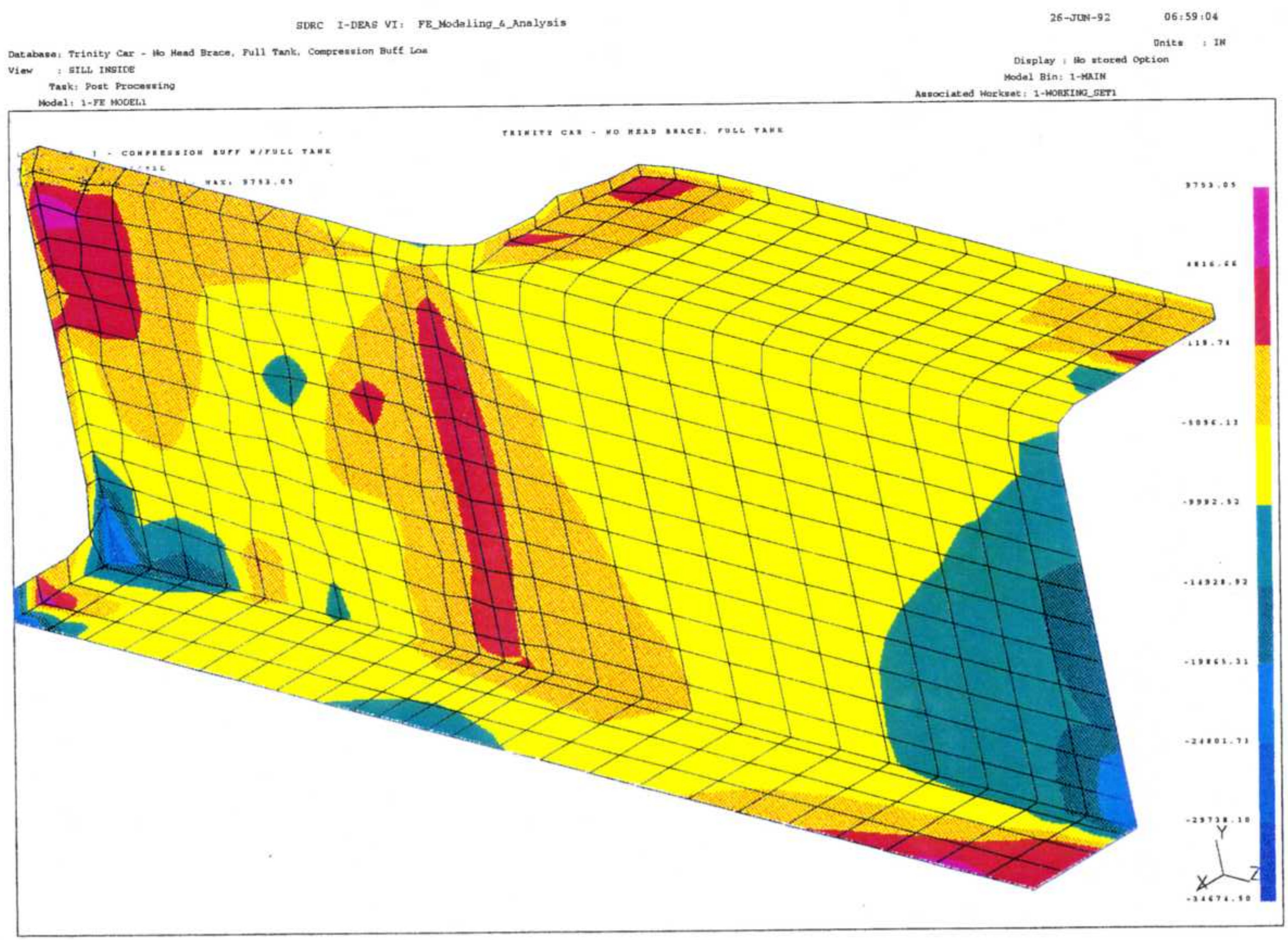

FIGURE B-38. TRINITY Z SECTION LUG AREA, LONGITUDINAL STRESS, COMPRESSION BUFF LOAD, FULL TANK, NO HEAD BRACE (FIRST VIEW); Maximum Stress = 9.8 ksi, Minimum Stress = -34.7 ksi

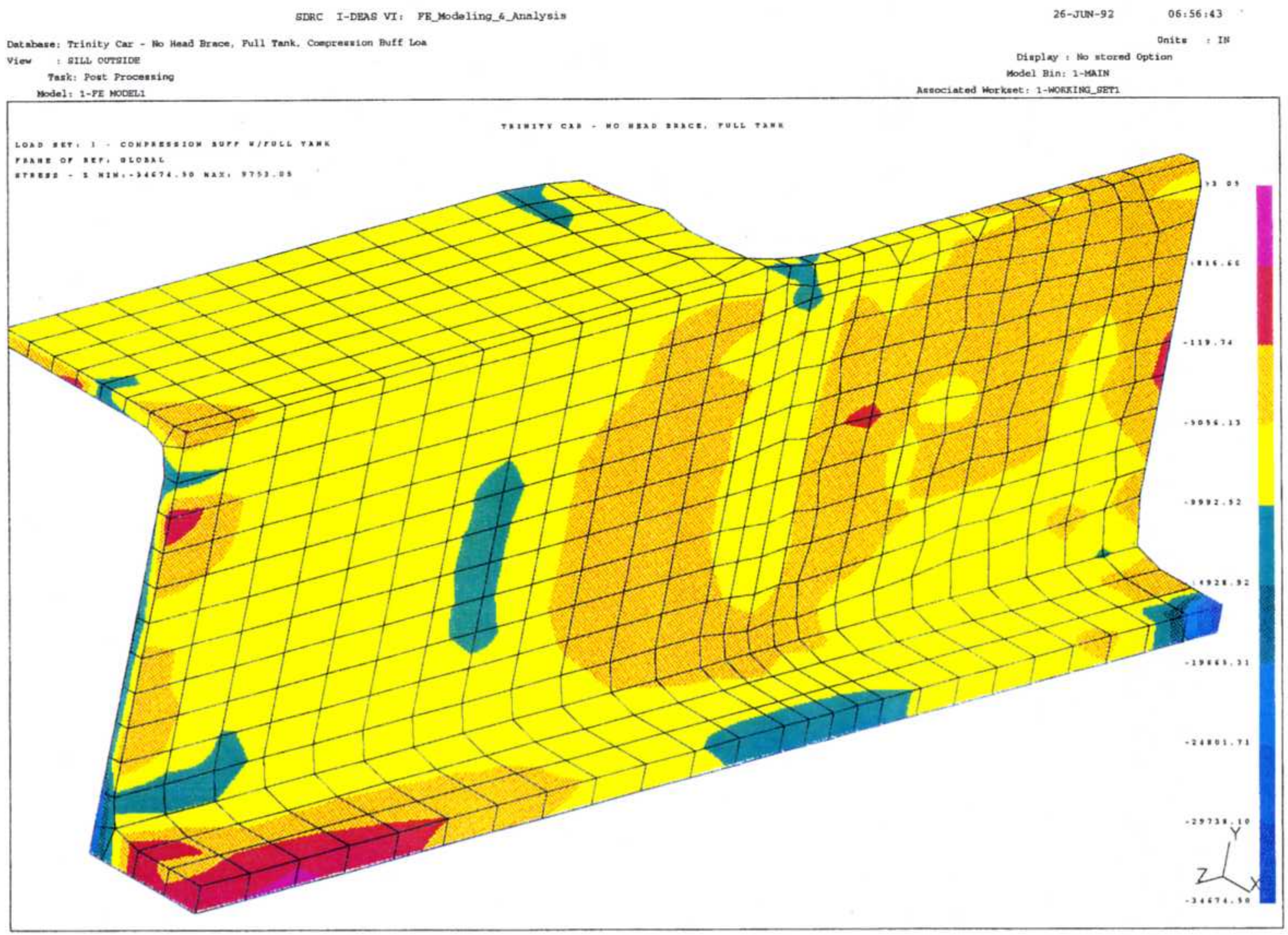

FIGURE B-39. TRINITY Z SECTION LUG AREA, LONGITUDINAL STRESS, COMPRESSION BUFF LOAD, FULL TANK, NO HEAD BRACE (SECOND VIEW); Maximum Stress = 9.8 ksi, Minimum Stress = -34.7 ksi

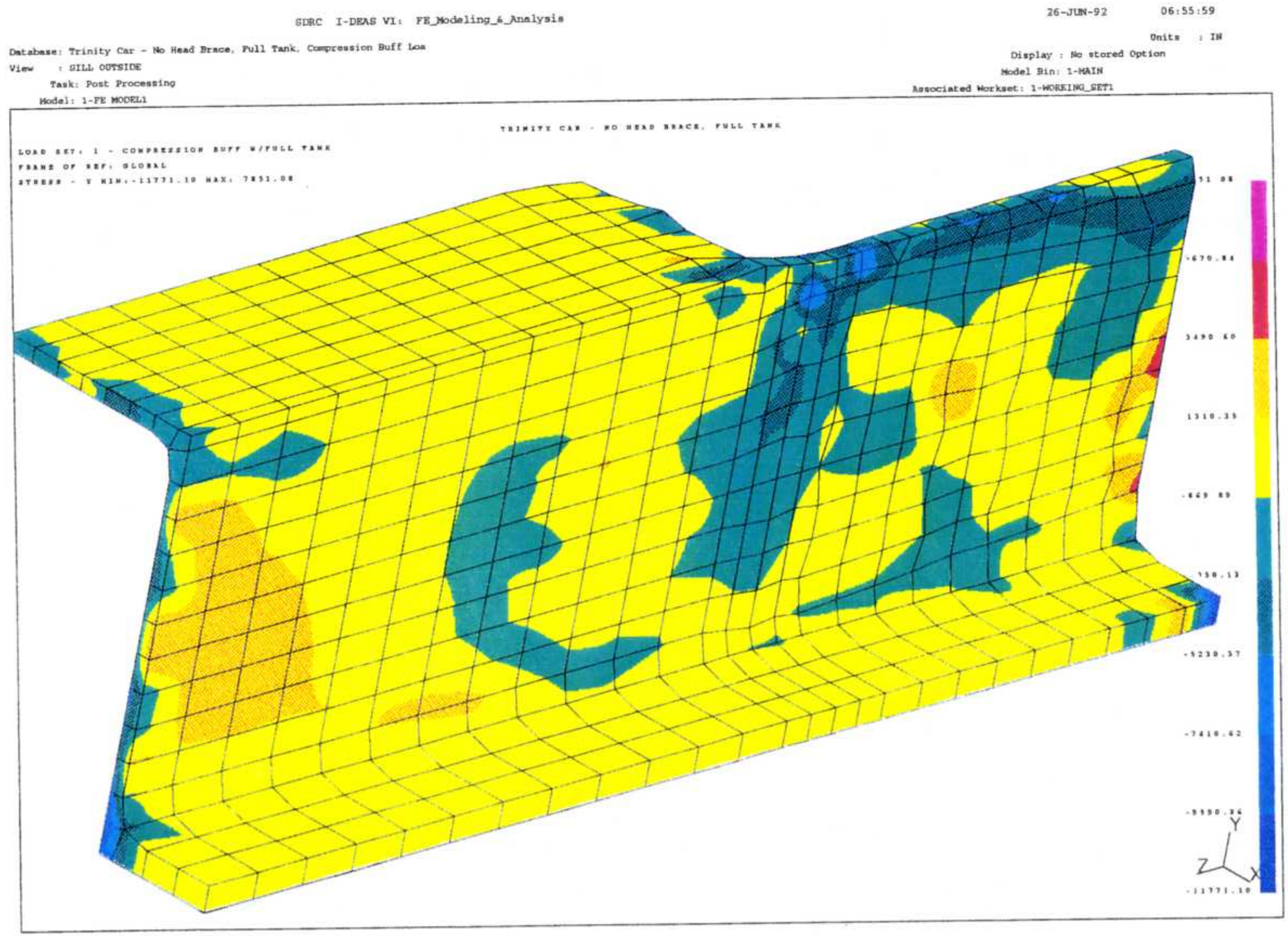

FIGURE B-41. TRINITY Z SECTION LUG AREA, VERTICAL STRESS, COMPRESSION BUFF LOAD, FULL TANK, NO HEAD BRACE (SECOND VIEW); Maximum Stress = 7.9 ksi, Minimum Stress = -11.8 ksi

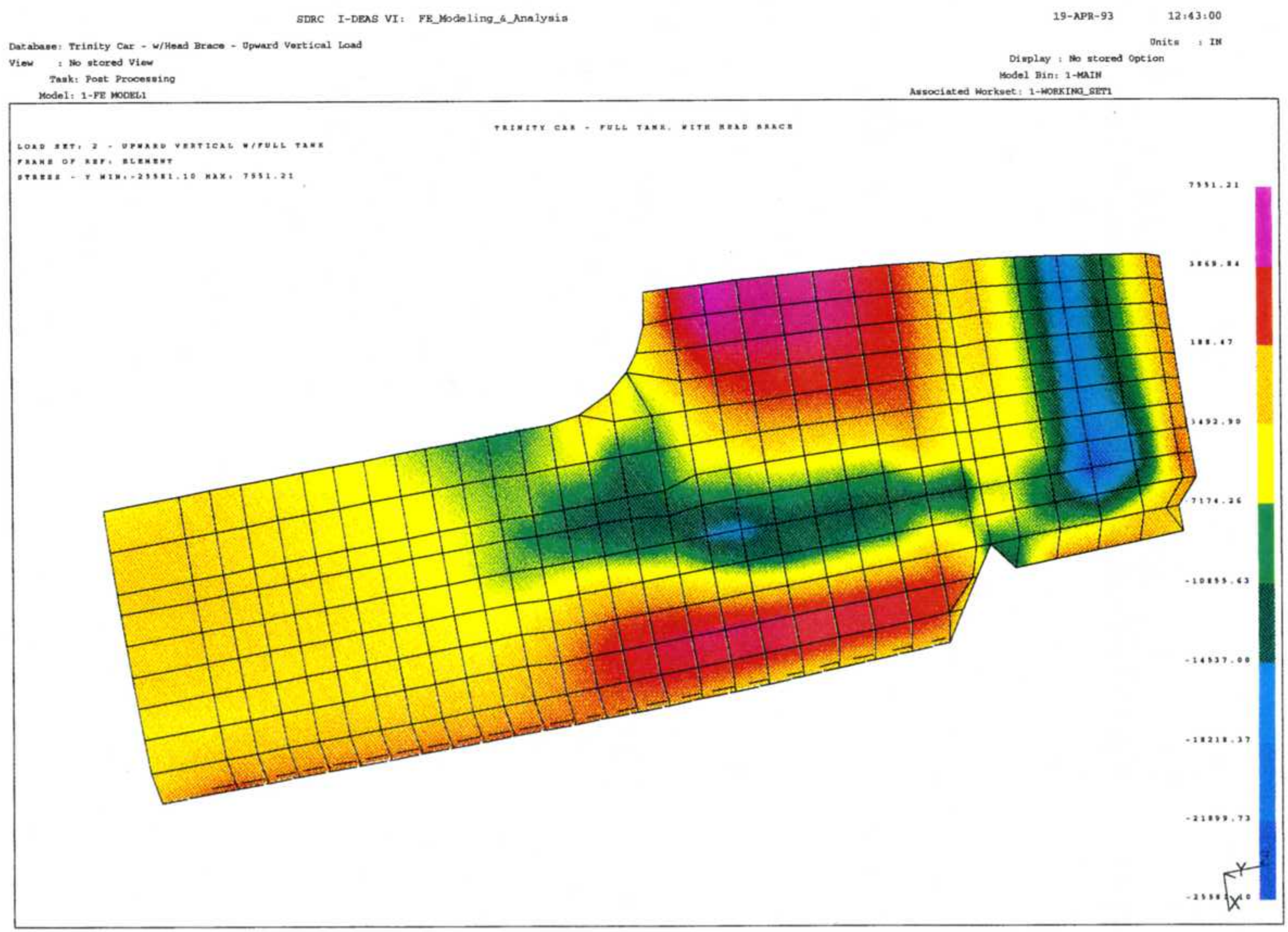

FIGURE B-42. TRINITY HEAD BRACE PAD, LONGITUDINAL STRESS, UPWARD VERTICAL LOAD, FULL TANK, WITH HEAD BRACE; Maximum Stress = 7.6 ksi, Minimum Stress = -25.6 ksi

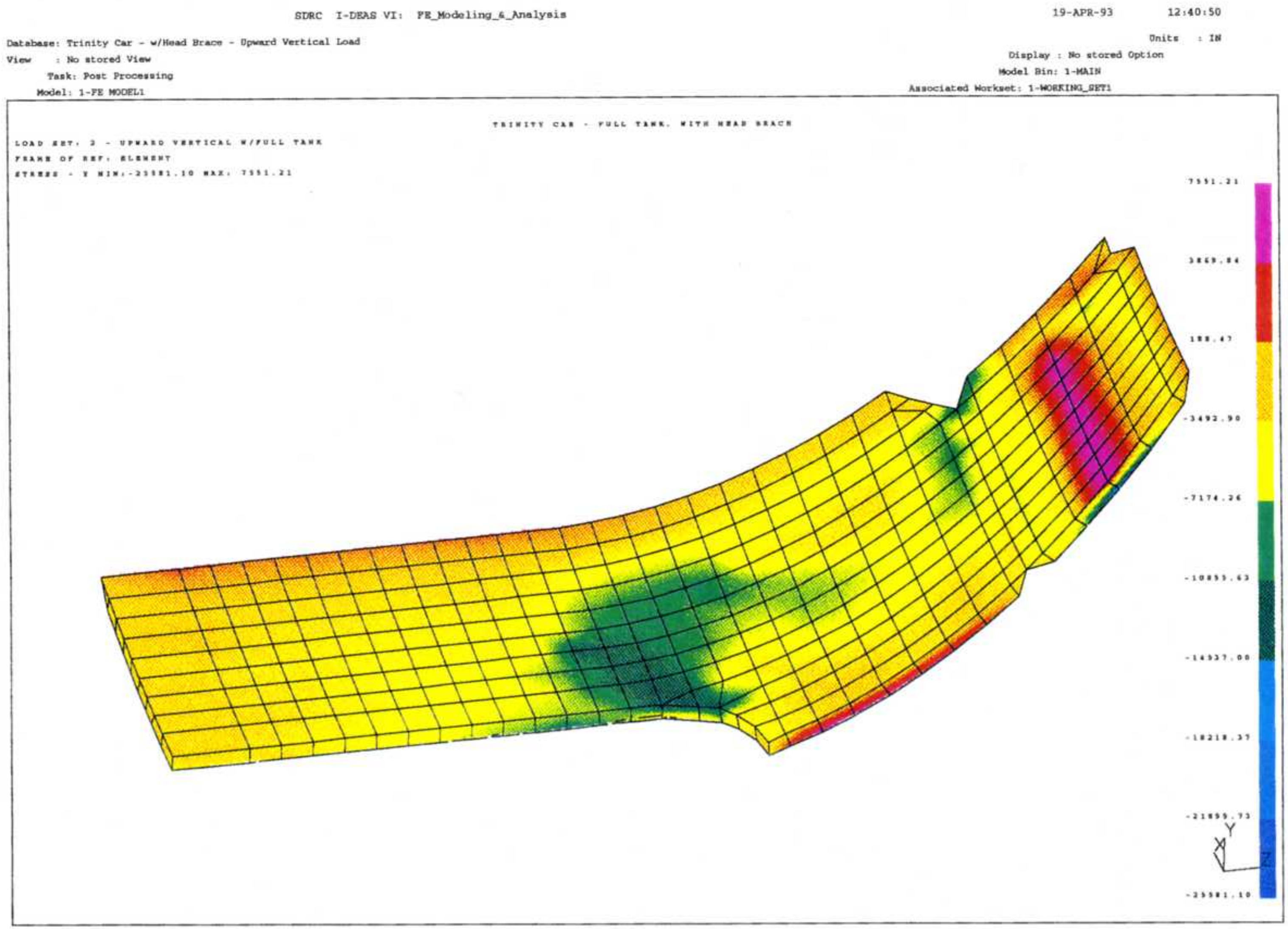

FIGURE B-43. TRINITY HEAD BRACE PAD, LONGITUDINAL STRESS, UPWARD VERTICAL LOAD, FULL TANK, WITH HEAD BRACE; Maximum Stress = 7.6 ksi, Minimum Stress = -25.6 ksi

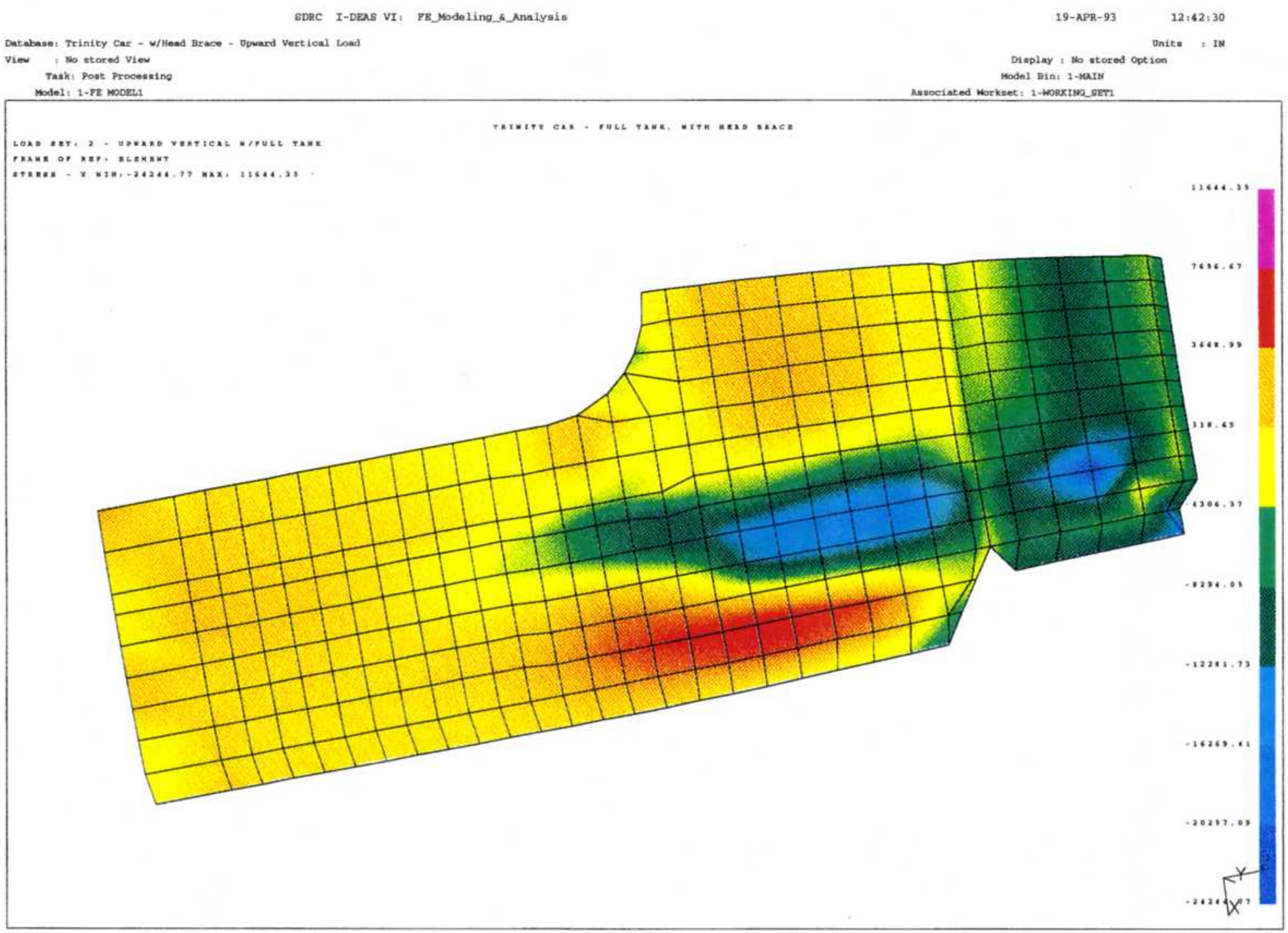

FIGURE B-44. TRINITY HEAD BRACE PAD, TRANSVERSE STRESS, UPWARD VERTICAL LOAD, FULL TANK, WITH HEAD BRACE; Maximum Stress = 11.6 ksi, Minimum Stress = -24.2 ksi

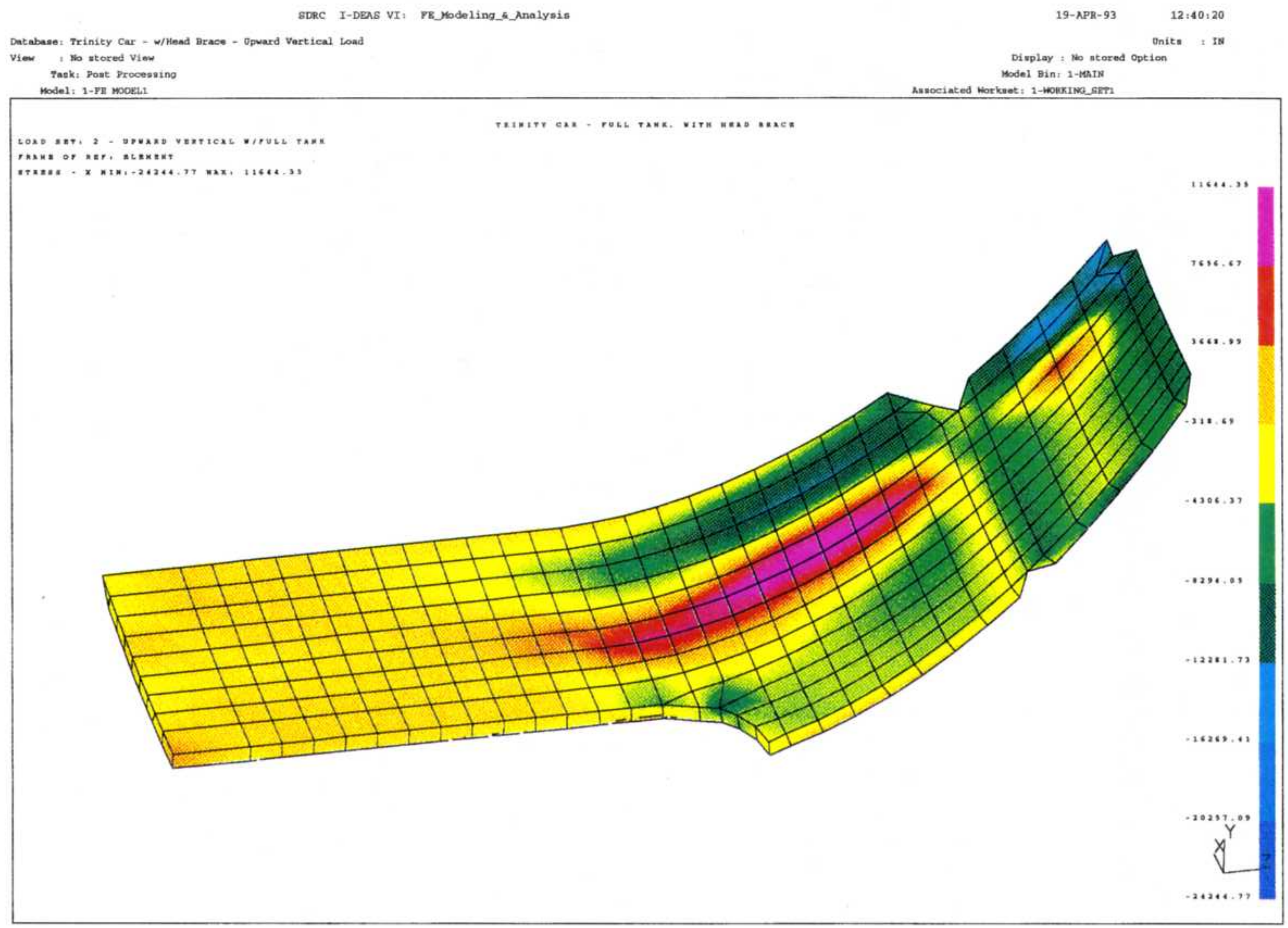

FIGURE B-45. TRINITY HEAD BRACE PAD, TRANSVERSE STRESS, UPWARD VERTICAL LOAD, FULL TANK, WITH HEAD BRACE; Maximum Stress = 11.6 ksi, Minimum Stress = -24.2 ksi

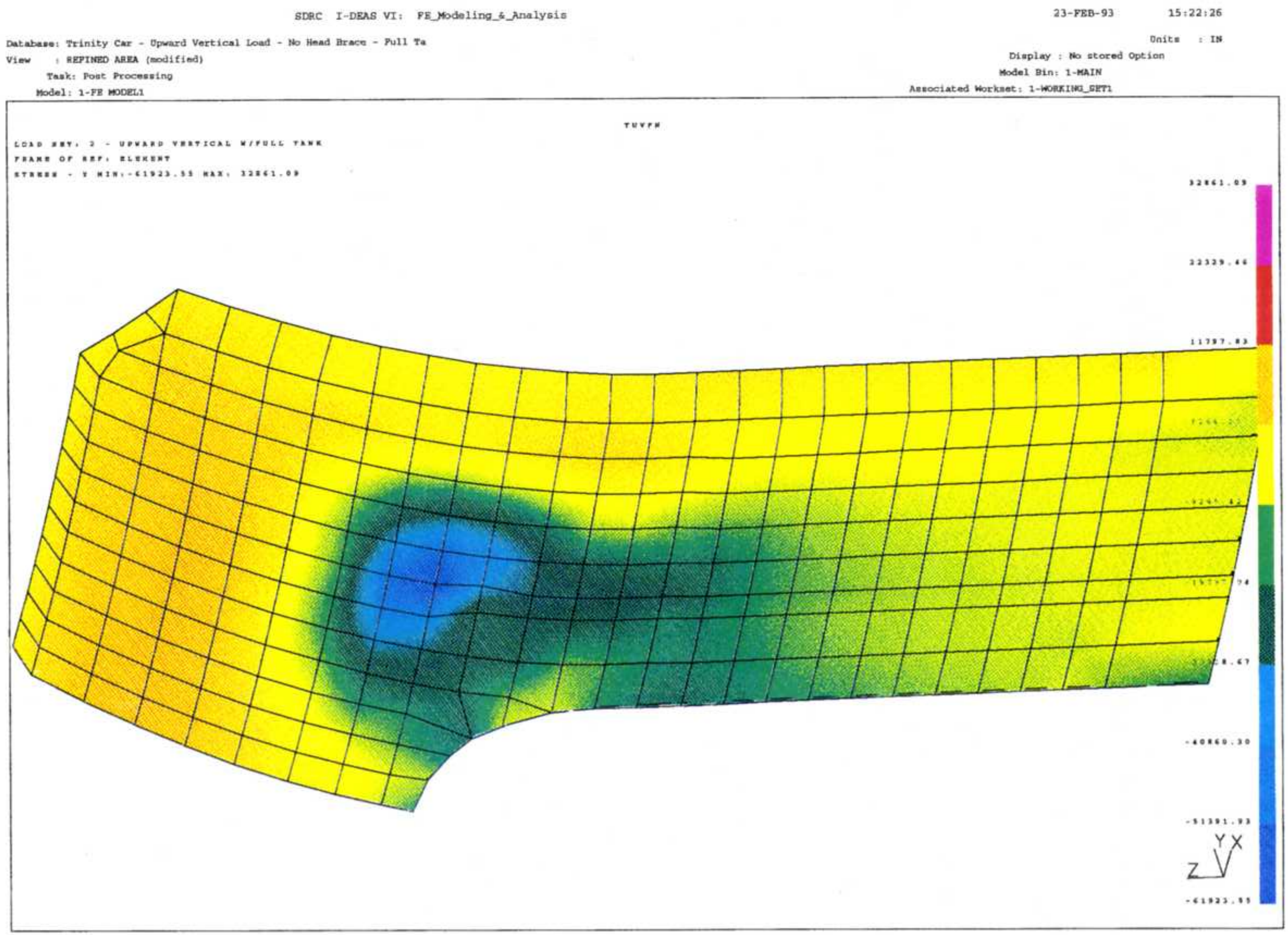

FIGURE B-46. TRINITY HEAD PAD, LONGITUDINAL STRESS, UPWARD VERTICAL LOAD, FULL TANK, NO HEAD BRACE; Maximum Stress = 32.9 ksi, Minimum Stress = -61.9 ksi

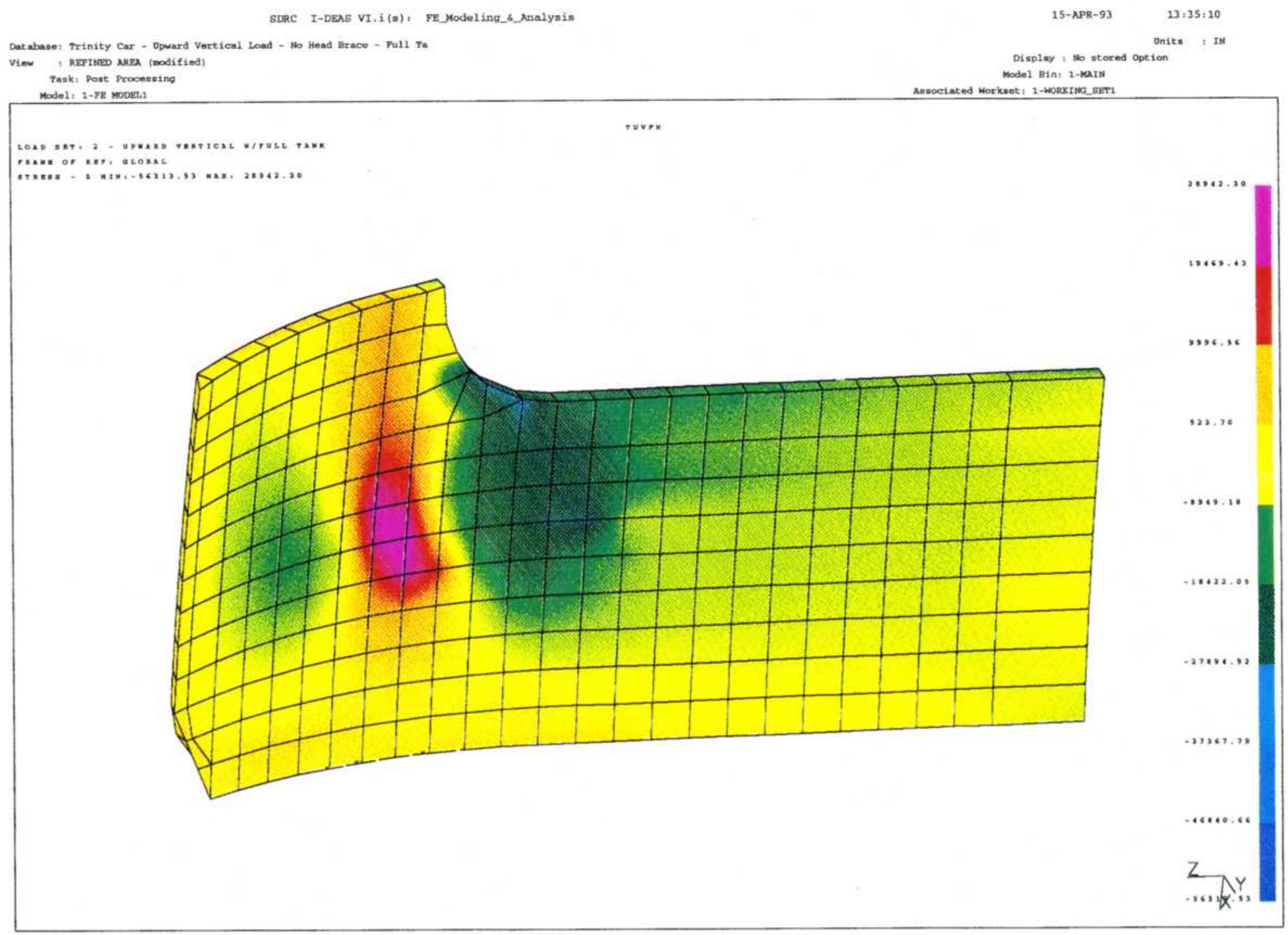

FIGURE B-47. TRINITY HEAD PAD, LONGITUDINAL STRESS, UPWARD VERTICAL LOAD, FULL TANK, NO HEAD BRACE; Maximum Stress = 28.9 ksi, Minimum Stress = -56.3 ksi

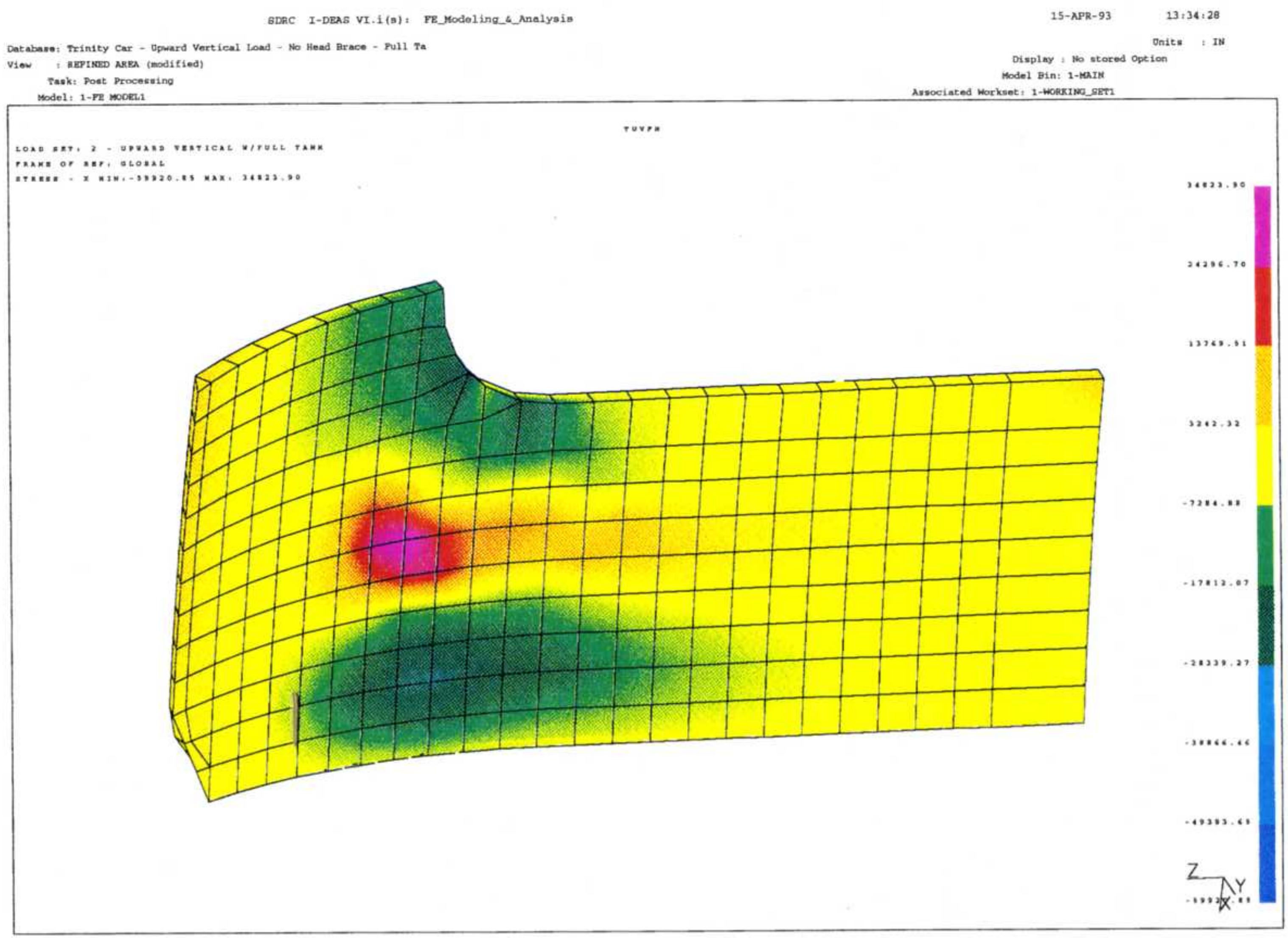

FIGURE B-48. TRINITY HEAD PAD, TRANSVERSE STRESS, UPWARD VERTICAL LOAD, FULL TANK, NO HEAD BRACE; Maximum Stress = 34.8 ksi, Minimum Stress = -59.9 ksi

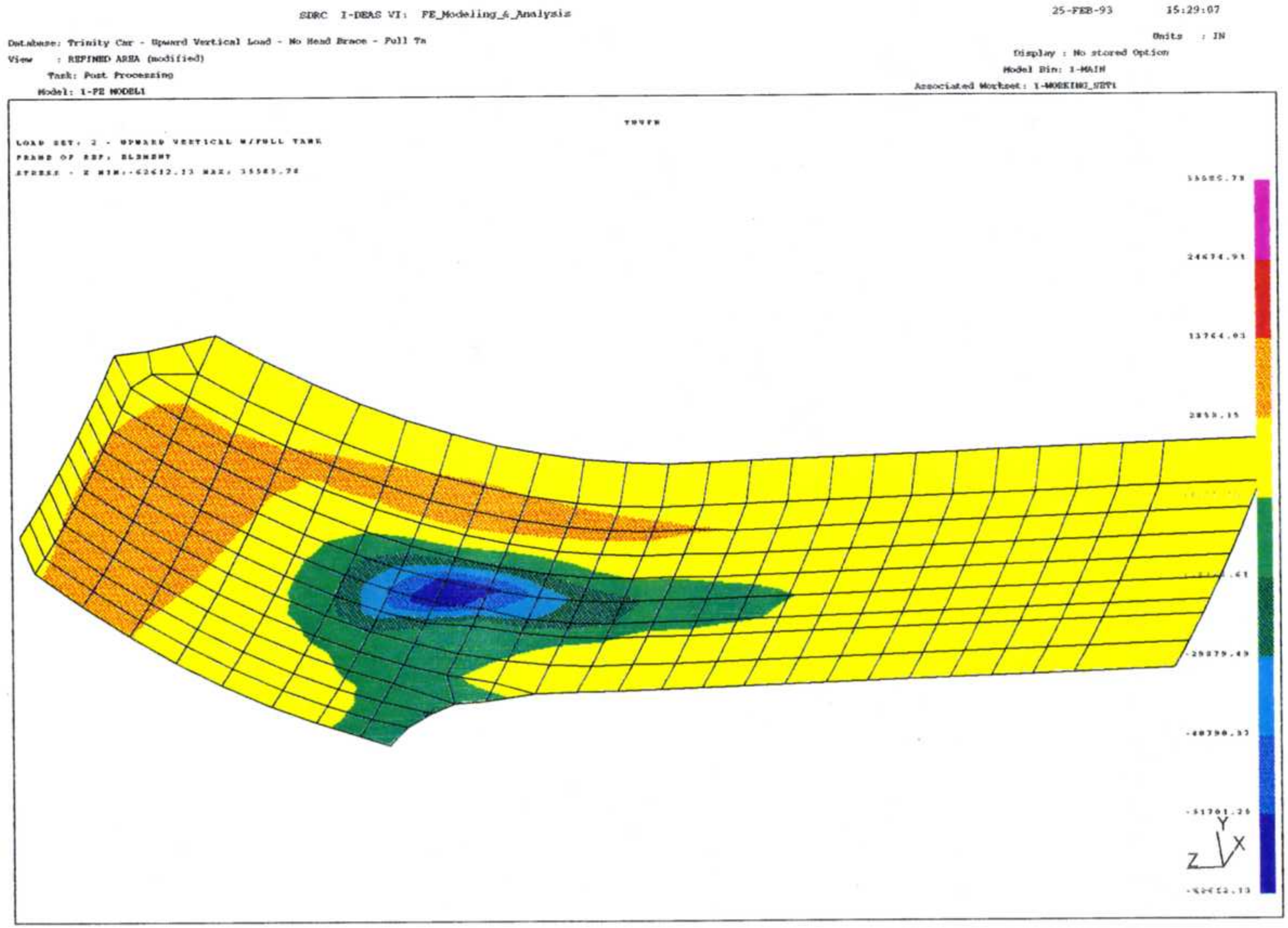

FIGURE B-49. TRINITY HEAD PAD, TRANSVERSE STRESS, UPWARD VERTICAL LOAD, FULL TANK, NO HEAD BRACE;
Maximum Stress = 34.8 ksi, Minimum Stress = -62.6 ksi

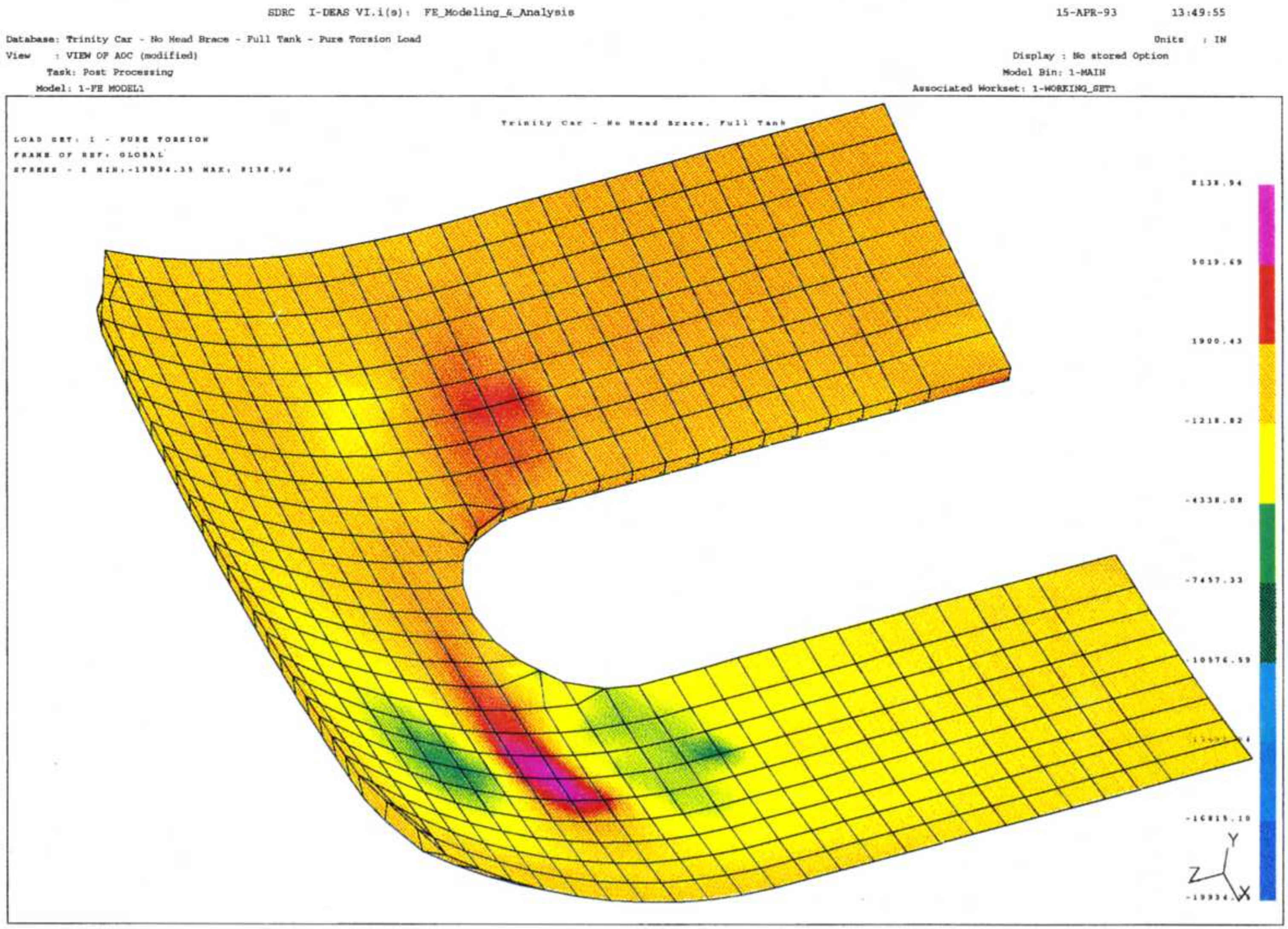

FIGURE B-50. TRINITY HEAD PAD, LONGITUDINAL STRESS, PURE TORSION LOAD, FULL TANK, NO HEAD BRACE; Maximum Stress = 8.1 ksi, Minimum Stress = -19.9 ksi

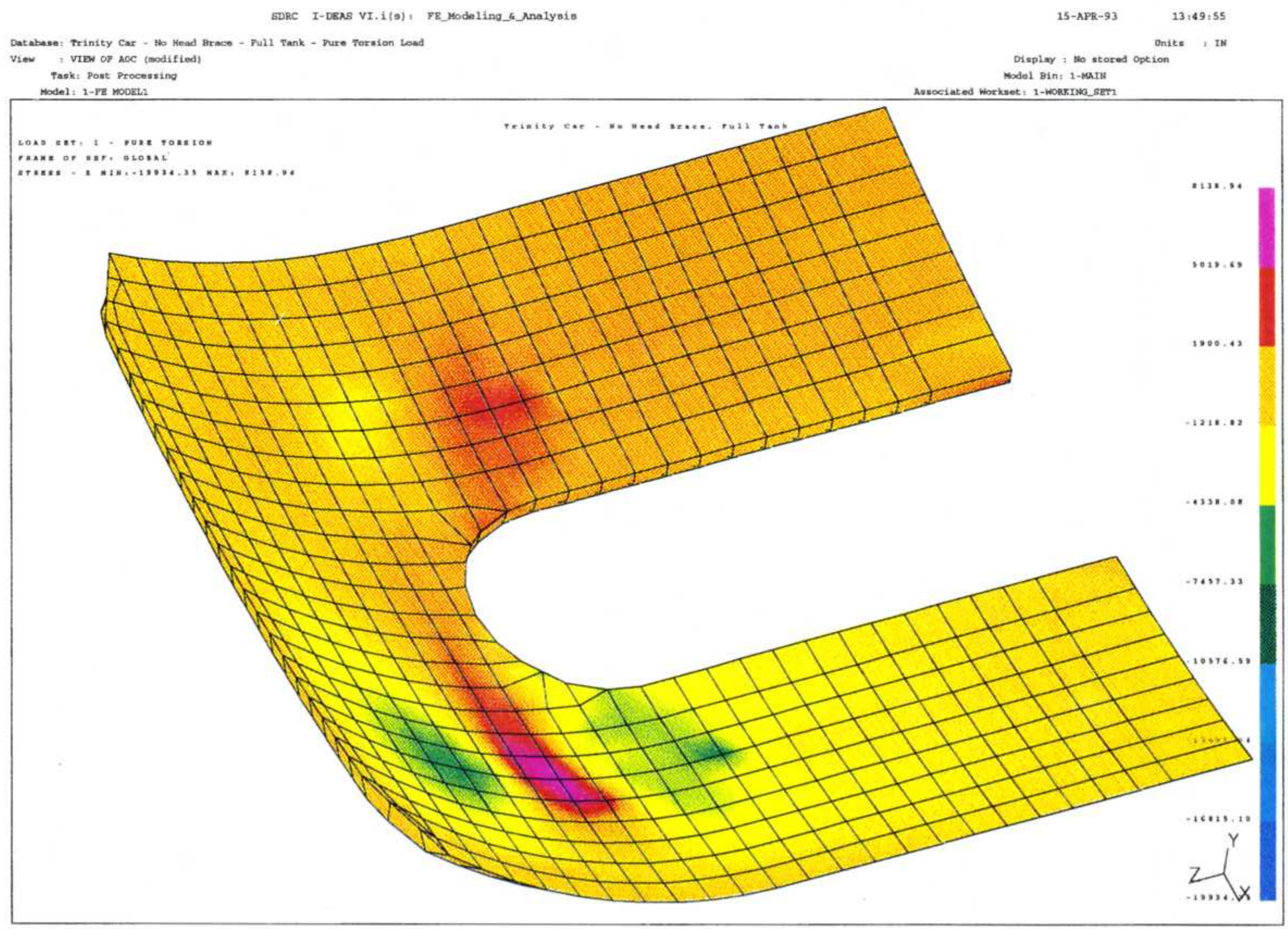

FIGURE B-50. TRINITY HEAD PAD, LONGITUDINAL STRESS, PURE TORSION LOAD, FULL TANK, NO HEAD BRACE; Maximum Stress = 8.1 ksi, Minimum Stress = -19.9 ksi

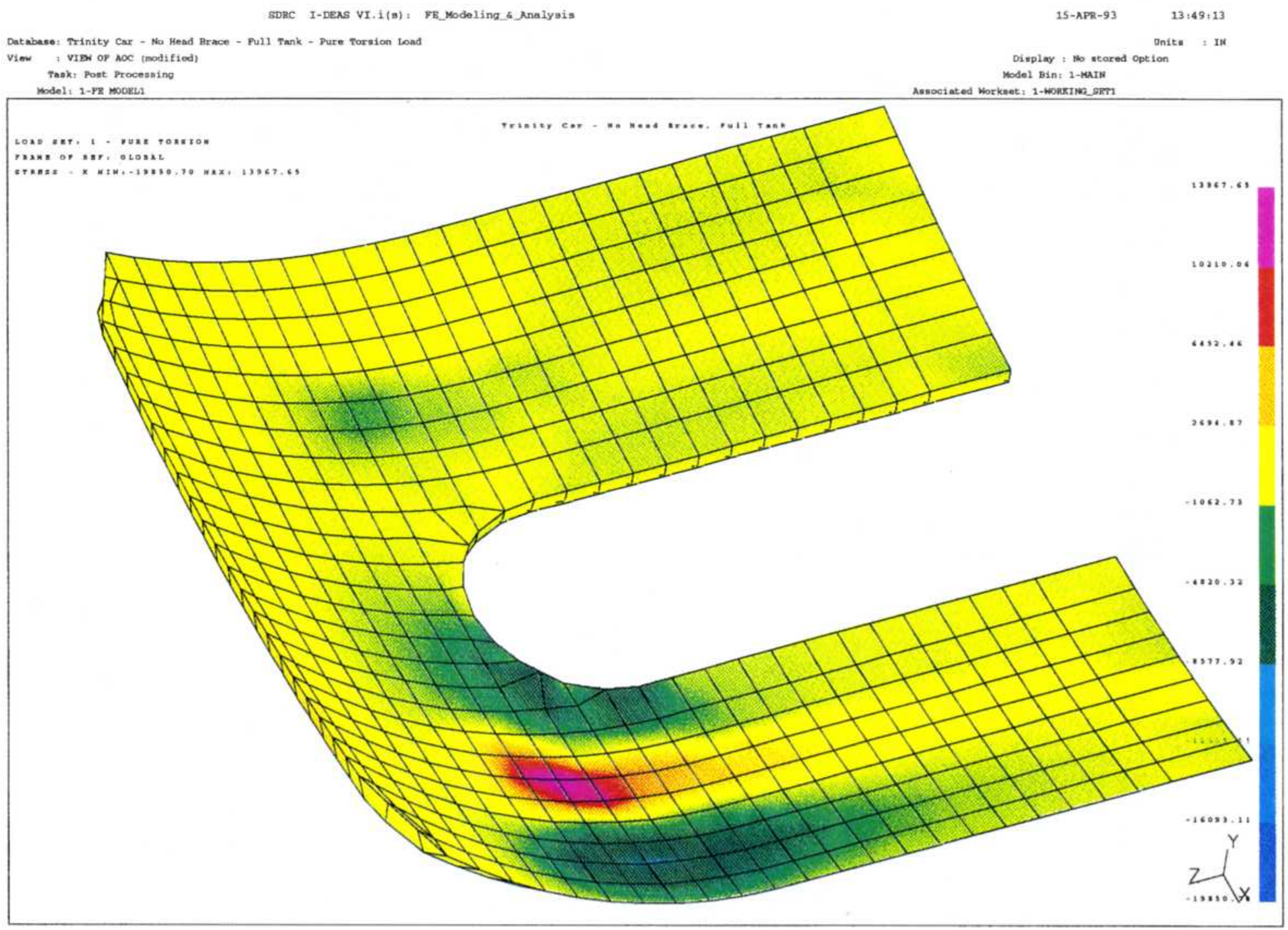

FIGURE B-51. TRINITY HEAD PAD, TRANSVERSE STRESS, PURE TORSION LOAD, FULL TANK, NO HEAD BRACE; Maximum Stress = 14.0 ksi, Minimum Stress = -19.9 ksi

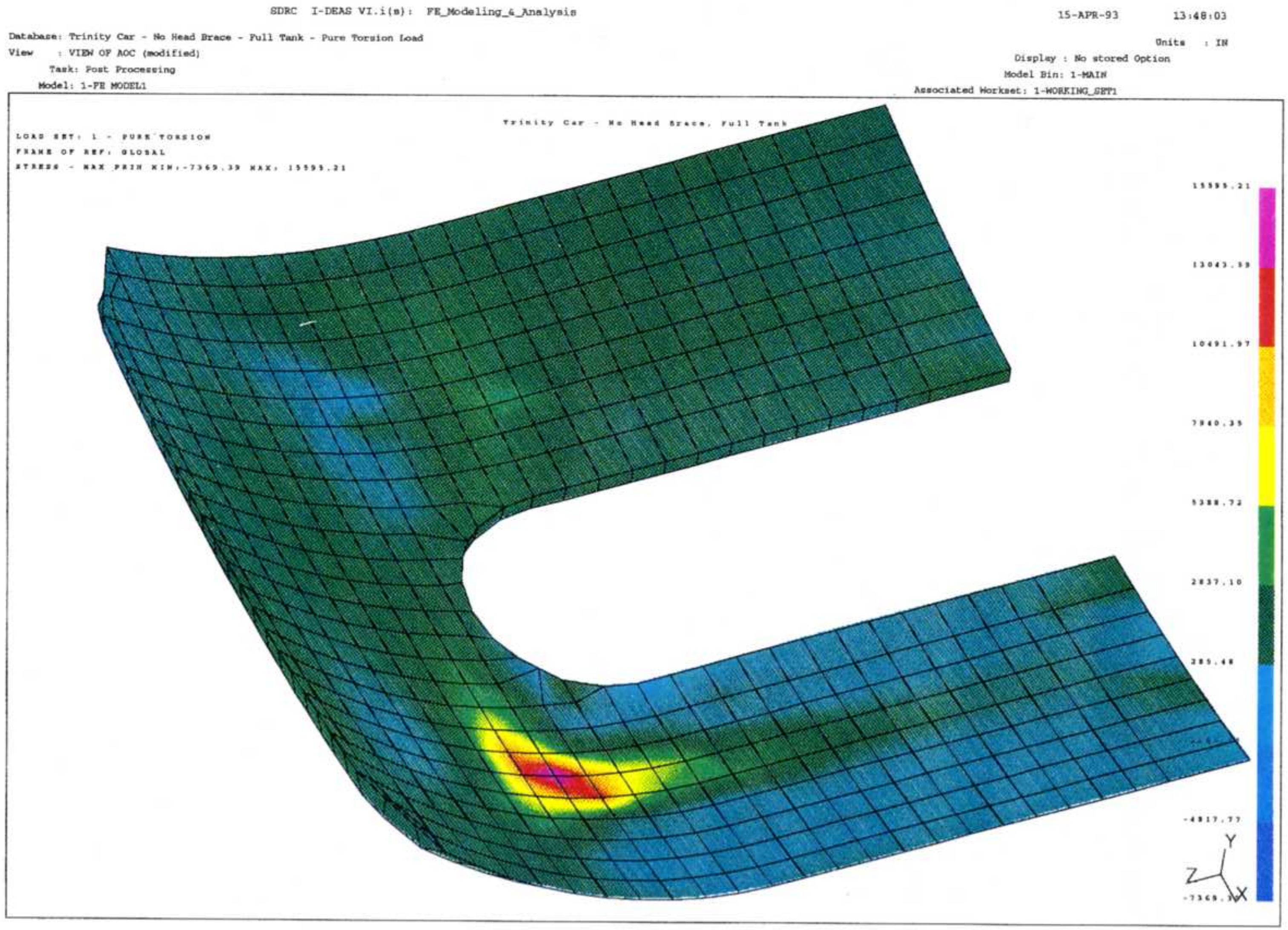

FIGURE B-52. TRINITY HEAD PAD, MAX PRINCIPAL STRESS, PURE TORSION LOAD, FULL TANK, NO HEAD BRACE; Maximum Stress = 15.6 ksi, Minimum Stress = -7.4 ksi

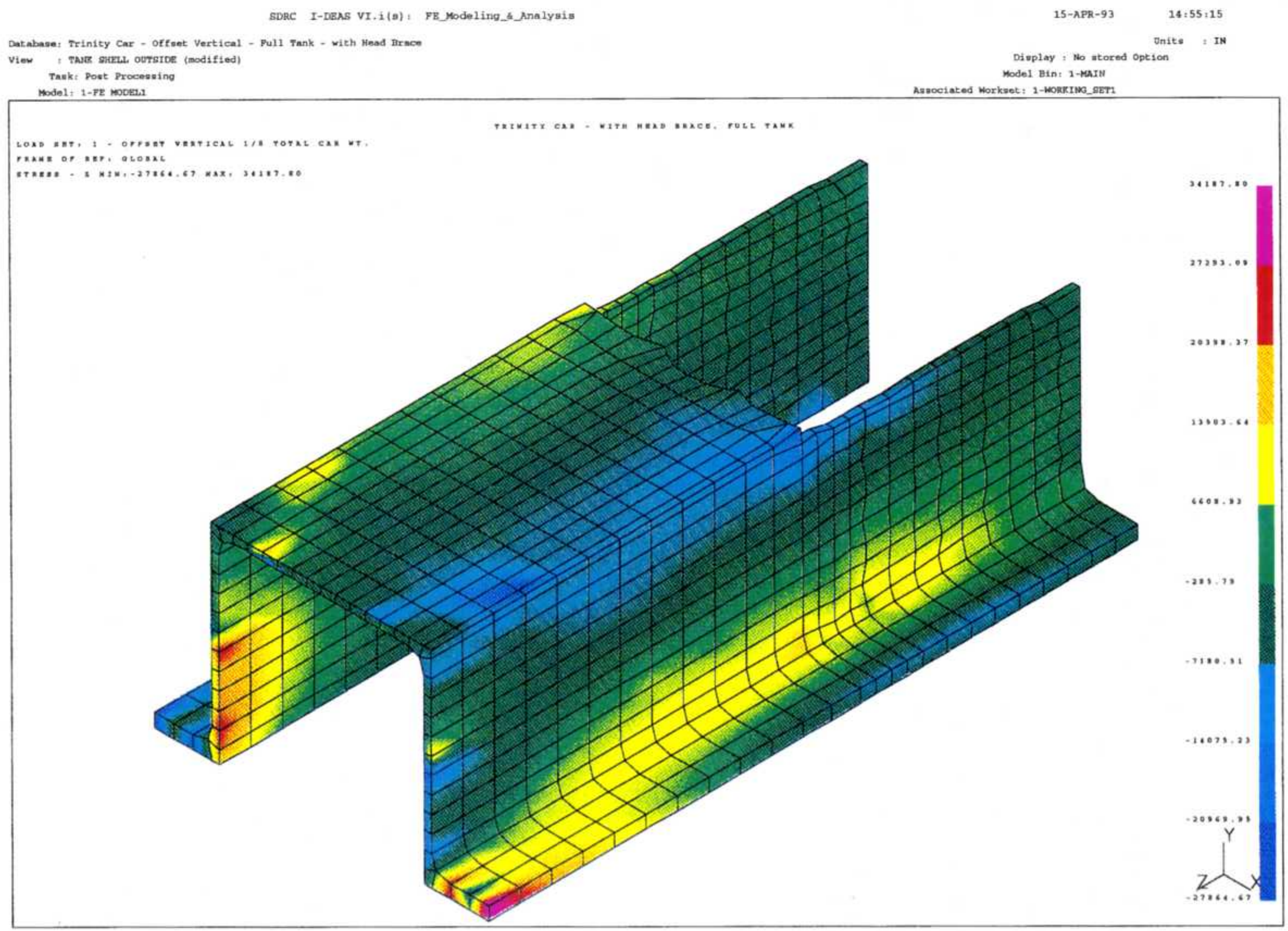

FIGURE B-53. TRINITY Z SECTION LUG AREA, LONGITUDINAL STRESS, OFFSET VERTICAL LOAD, FULL TANK, WITH HEAD BRACE; Maximum Stress = 34.2 ksi, Minimum Stress = -27.9 ksi

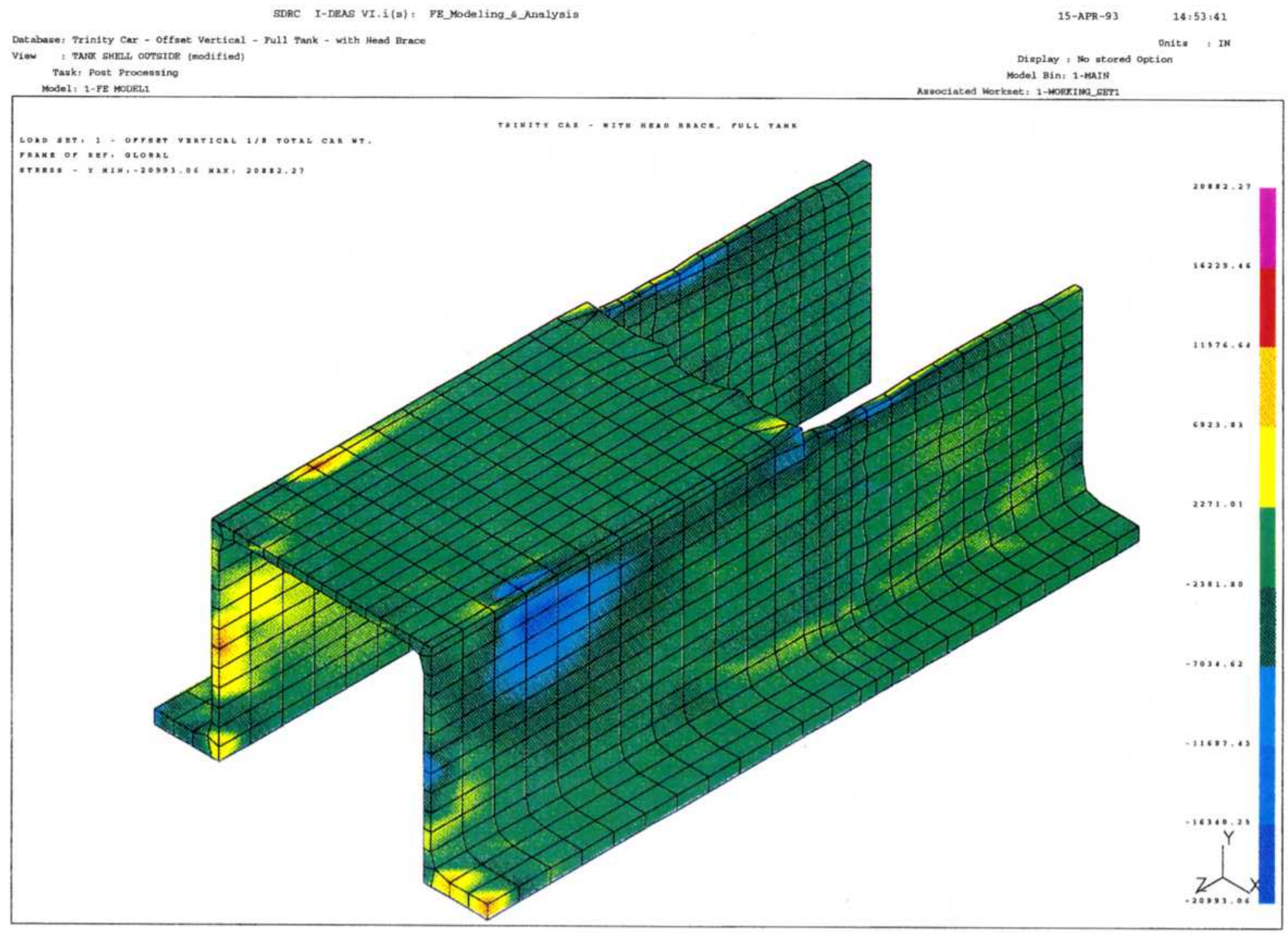

FIGURE B-54. TRINITY Z SECTION LUG AREA, VERTICAL STRESS, OFFSET VERTICAL LOAD, FULL TANK, WITH HEAD BRACE; Maximum Stress = 20.9 ksi, Minimum Stress = -21.0 ksi

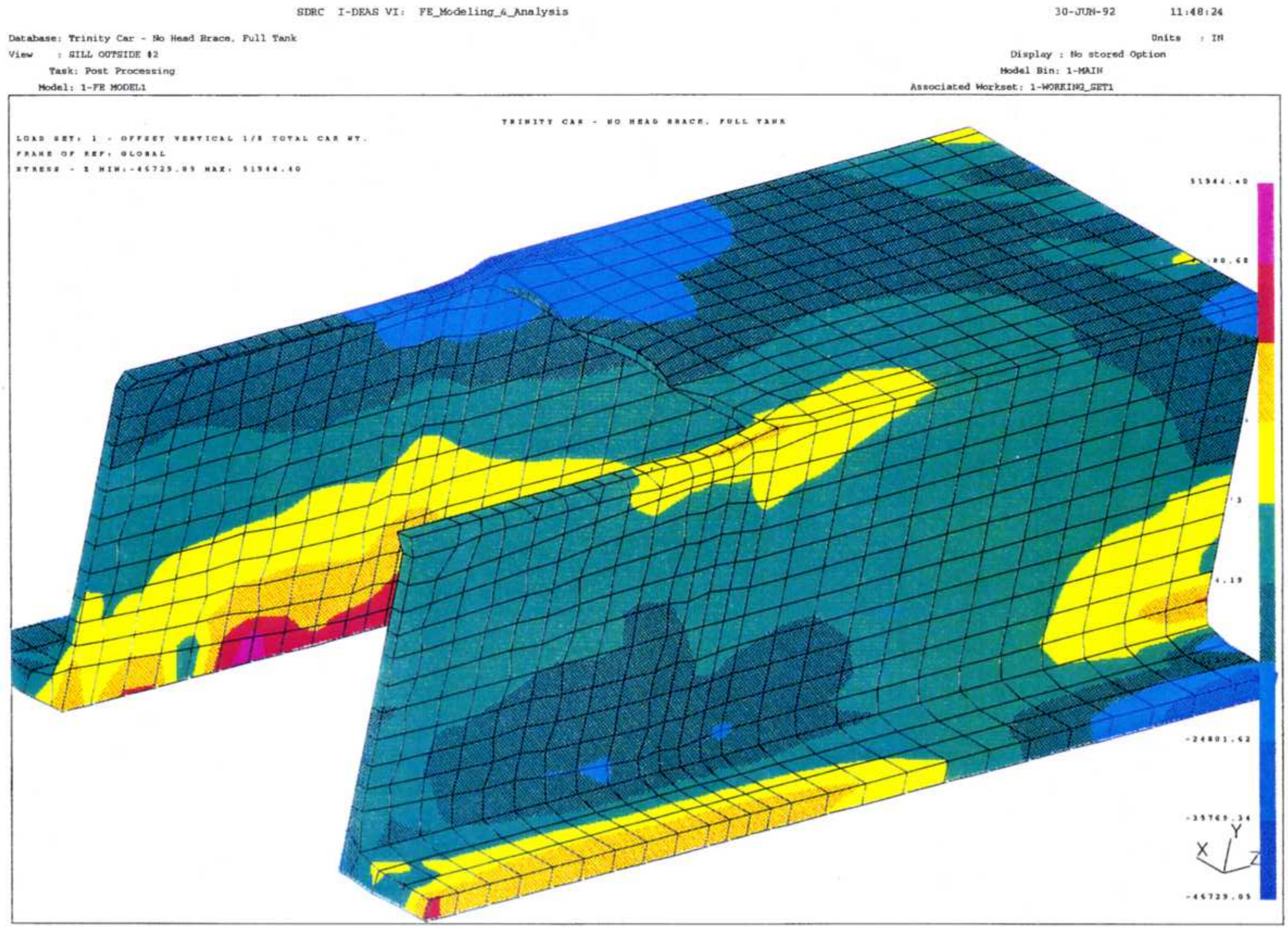

FIGURE B-55. TRINITY Z SECTION, LONGITUDINAL STRESS, OFFSET VERTICAL LOAD, FULL TANK, NO HEAD BRACE; Maximum Stress = 51.9 ksi, Minimum Stress = -46.7 ksi

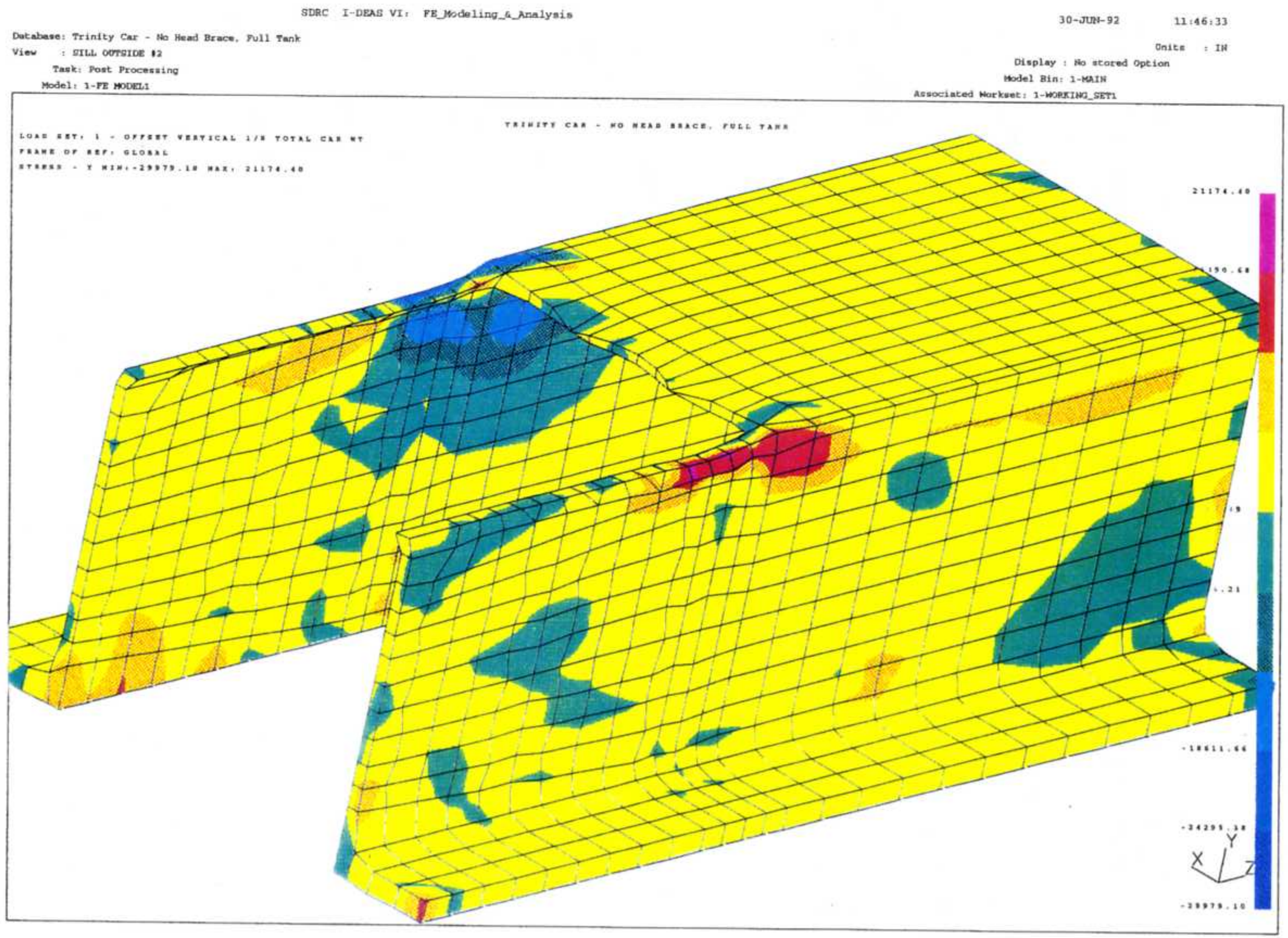

FIGURE B-56. TRINITY Z SECTION, VERTICAL STRESS, OFFSET VERTICAL LOAD, FULL TANK, NO HEAD BRACE; Maximum Stress = 21.2 ksi, Minimum Stress = -30.0 ksi

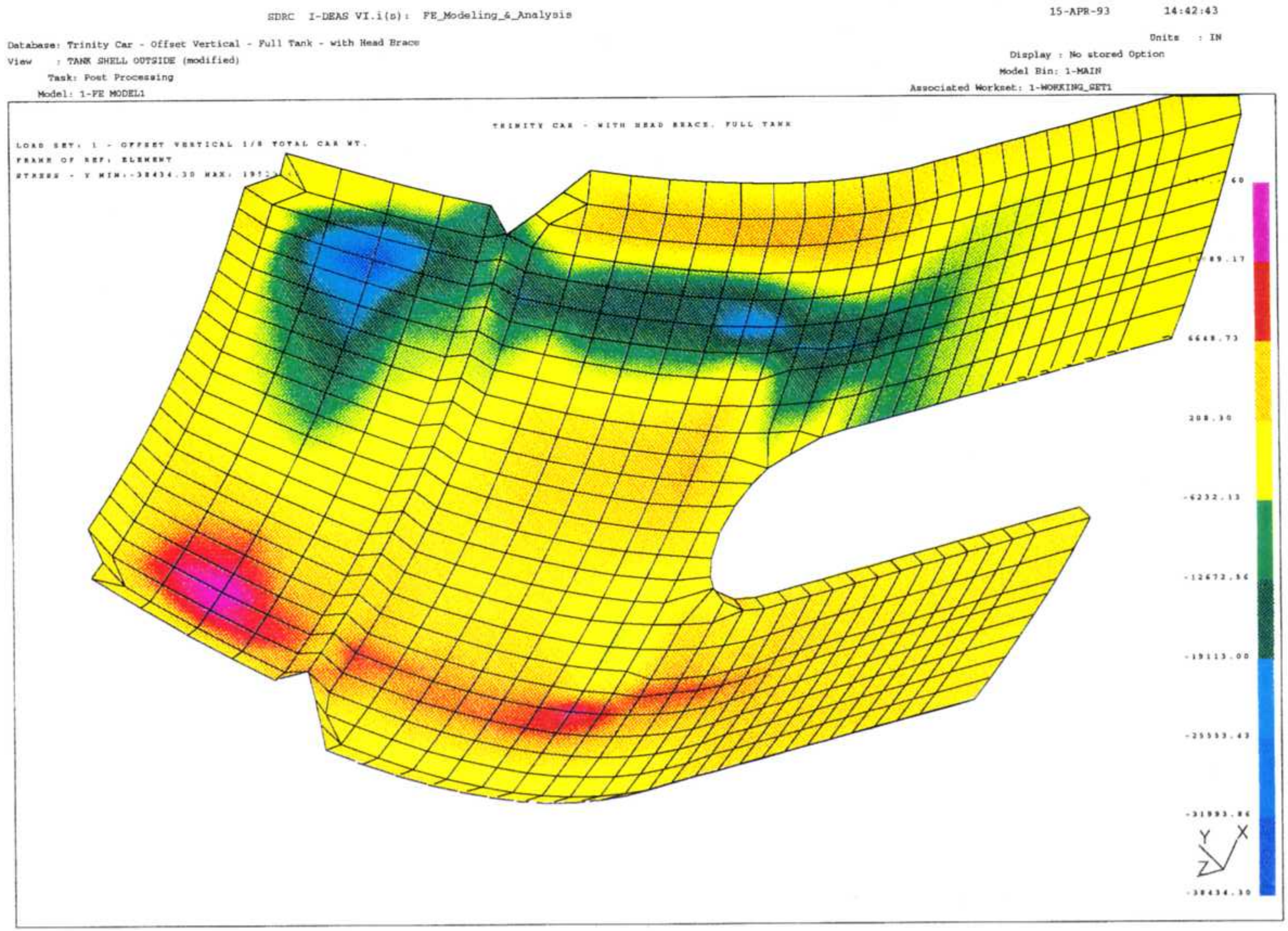

FIGURE B-57. TRINITY HEAD PAD, LONGITUDINAL STRESS, OFFSET VERTICAL LOAD, FULL TANK, WITH HEAD BRACE; Maximum Stress = 19.5 ksi, Minimum Stress = -38.4 ksi

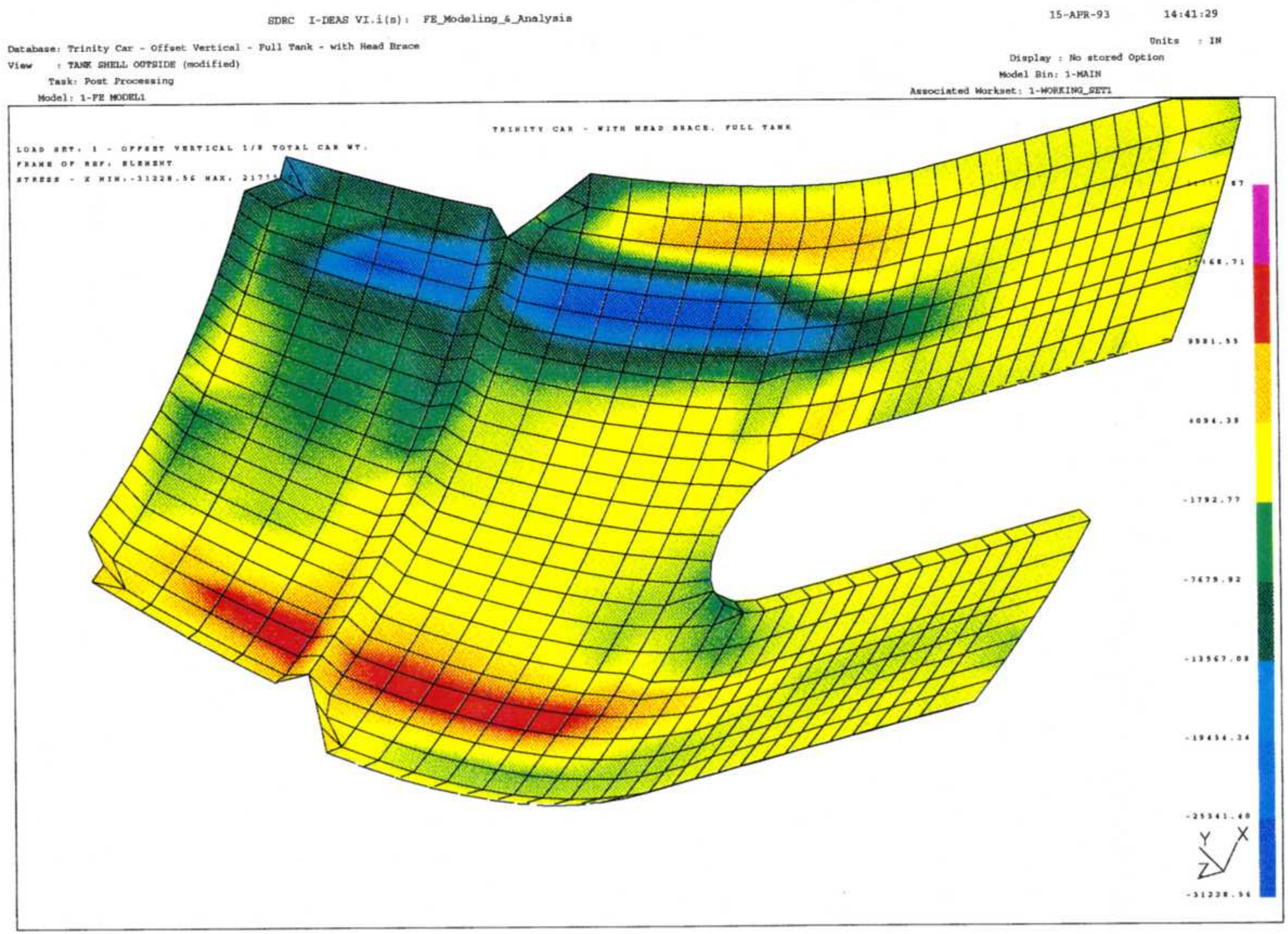

FIGURE B-58. TRINITY HEAD PAD, TRANSVERSE STRESS, OFFSET VERTICAL LOAD, FULL TANK, WITH HEAD BRACE; Maximum Stress = 21.8 ksi, Minimum Stress = -31.2 ksi

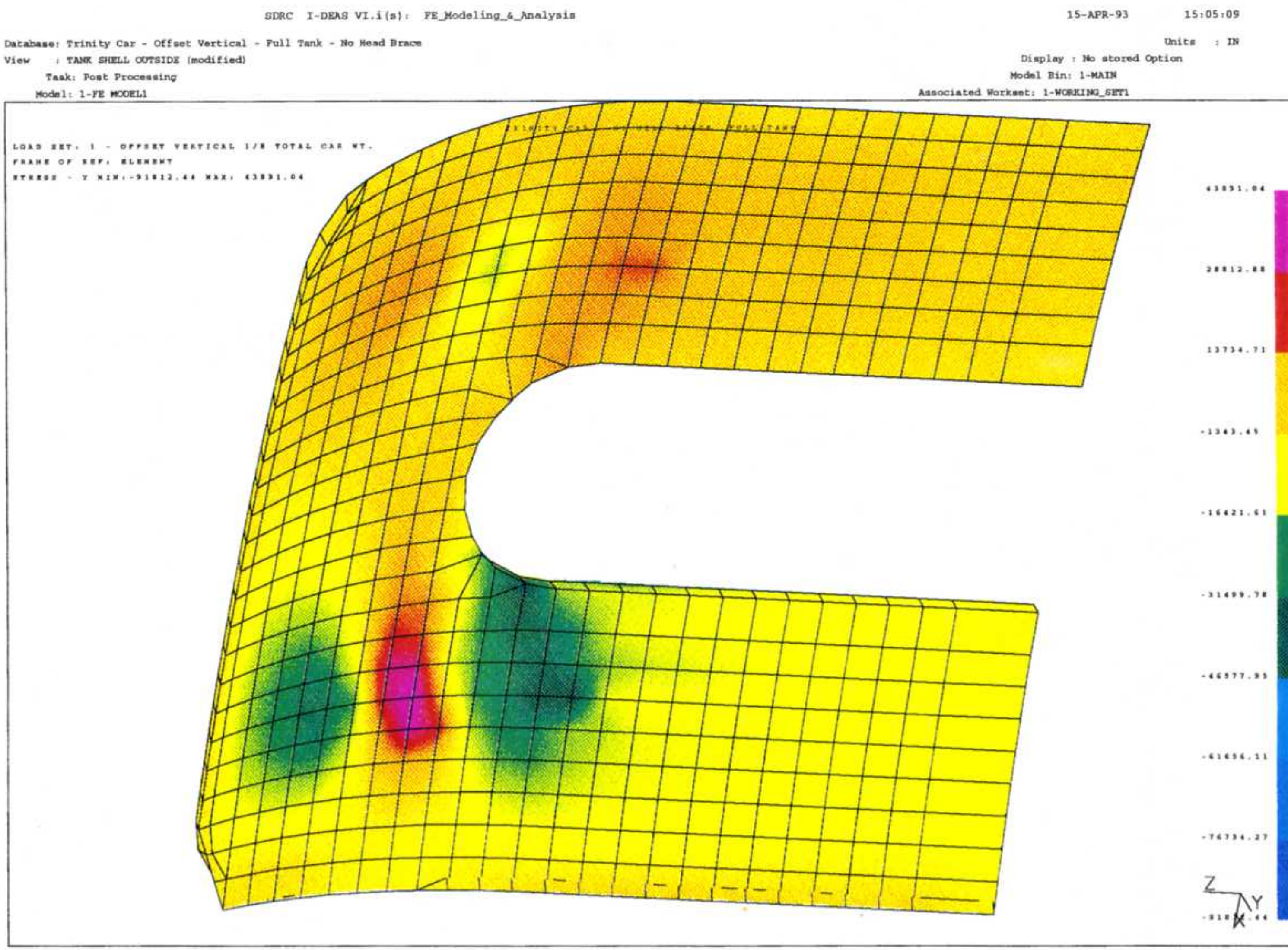

FIGURE B-59. TRINITY HEAD PAD, LONGITUDINAL STRESS (1ST VIEW) OFFSET VERTICAL LOAD, FULL TANK, NO HEAD BRACE; Maximum Stress = 43.9 ksi, Minimum Stress = -91.8 ksi

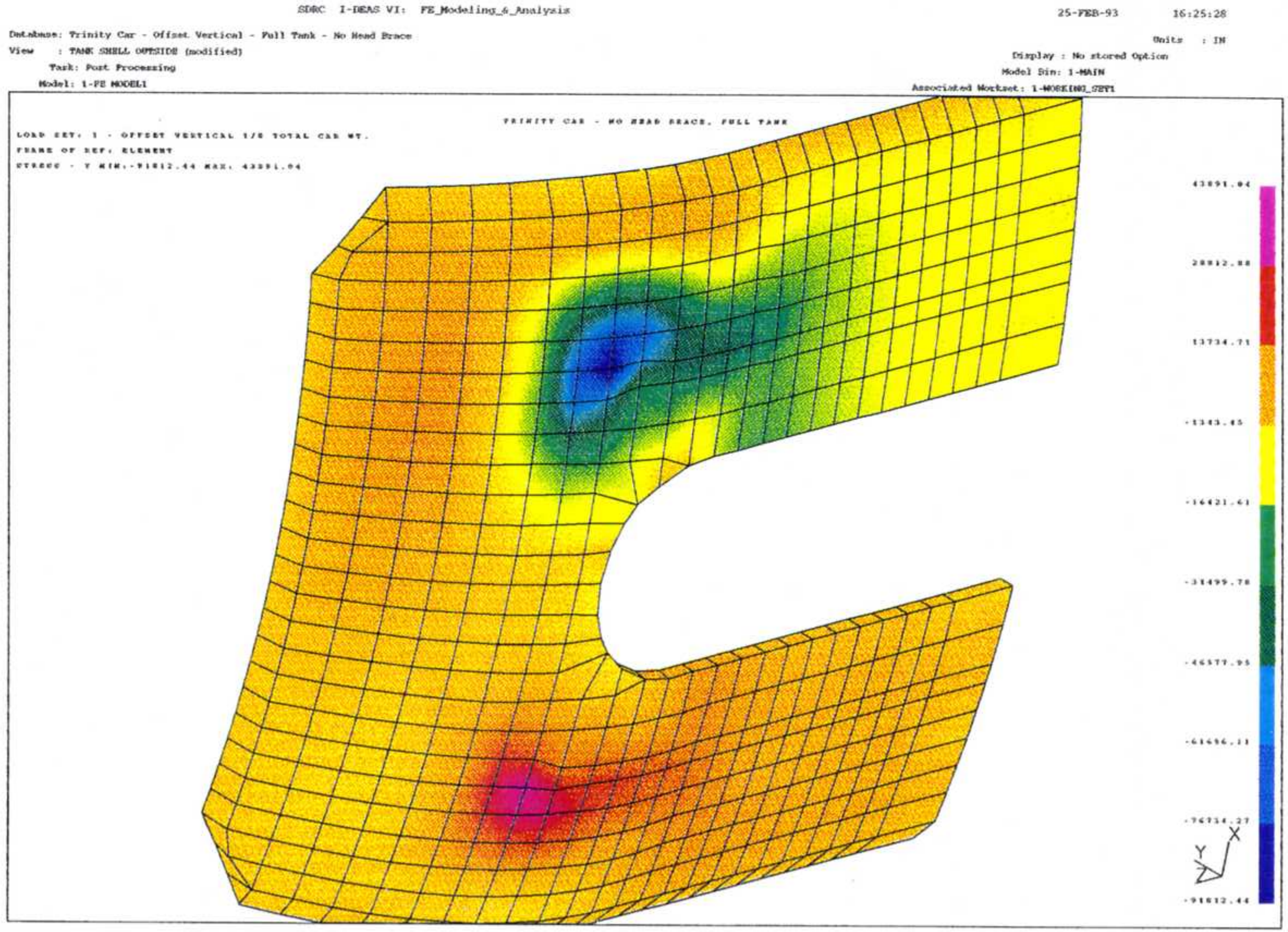

FIGURE B-60. TRINITY HEAD PAD, TRANSVERSE STRESS (2ND VIEW) OFFSET VERTICAL LOAD, FULL TANK, NO HEAD BRACE; Maximum Stress = 43.9 ksi, Minimum Stress = -91.8 ksi

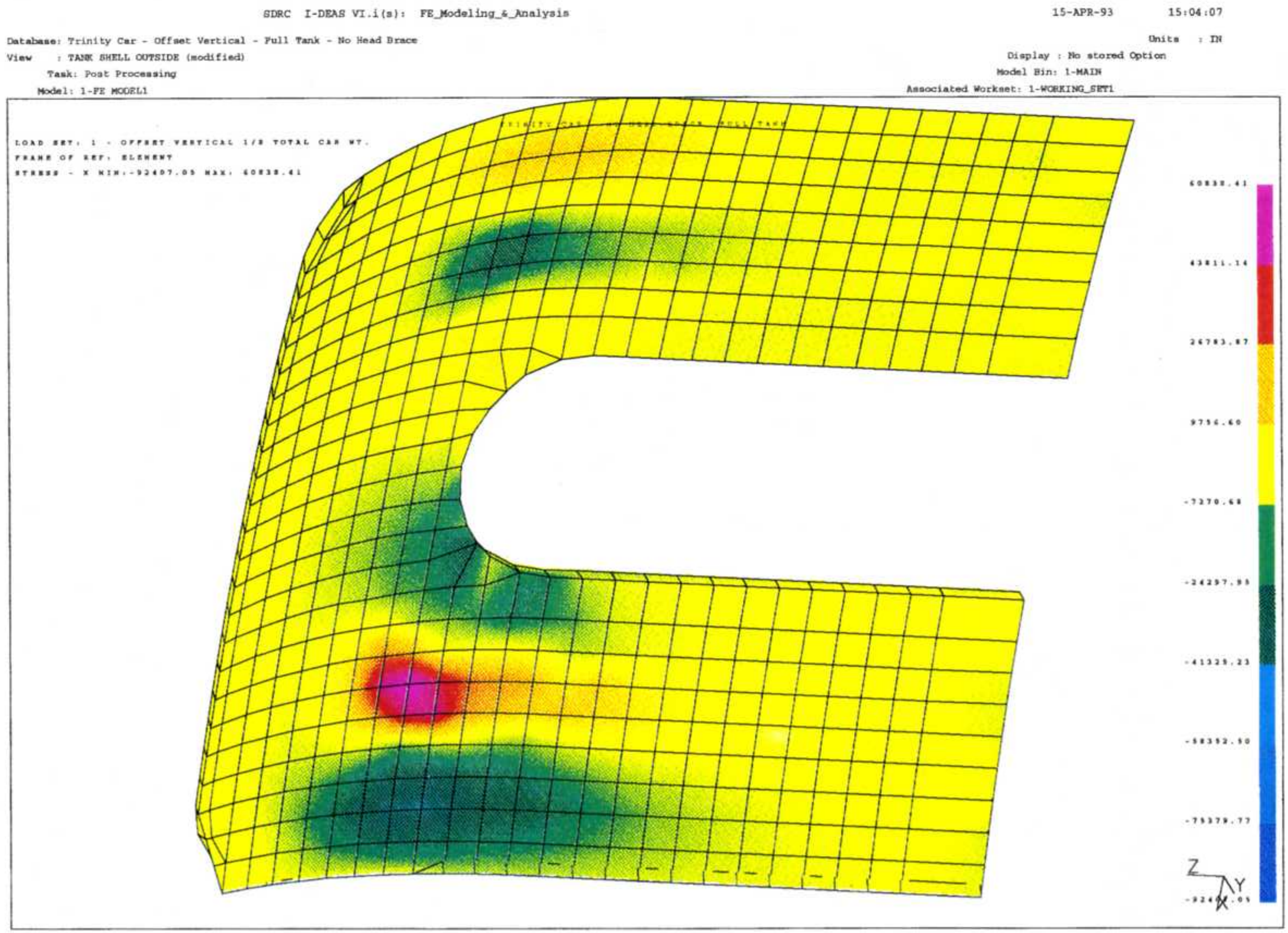

FIGURE B-61. TRINITY HEAD PAD, LONGITUDINAL STRESS, OFFSET VERTICAL LOAD, FULL TANK, NO HEAD BRACE (FIRST VIEW); Maximum Stress = 60.8 ksi, Minimum Stress = -92.4 ksi

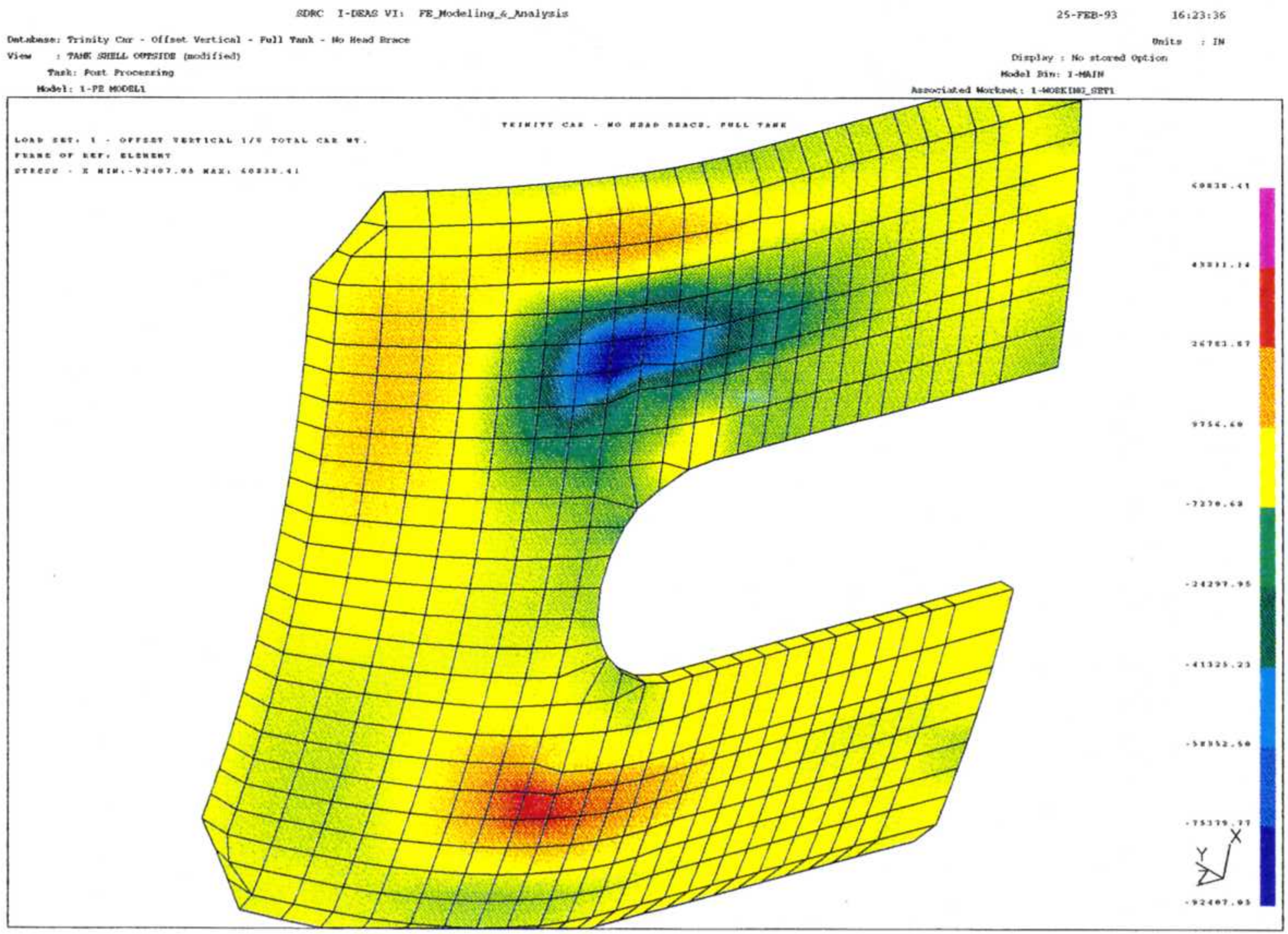

FIGURE B-62. TRINITY HEAD PAD, TRANSVERSE STRESS, OFFSET VERTICAL LOAD, FULL TANK, NO HEAD BRACE (SECOND VIEW); Maximum Stress = 60.8 ksi, Minimum Stress = -92.4 ksi

APPENDIX C

Stress Plots Supporting the Stub Sill Inspection Procedure

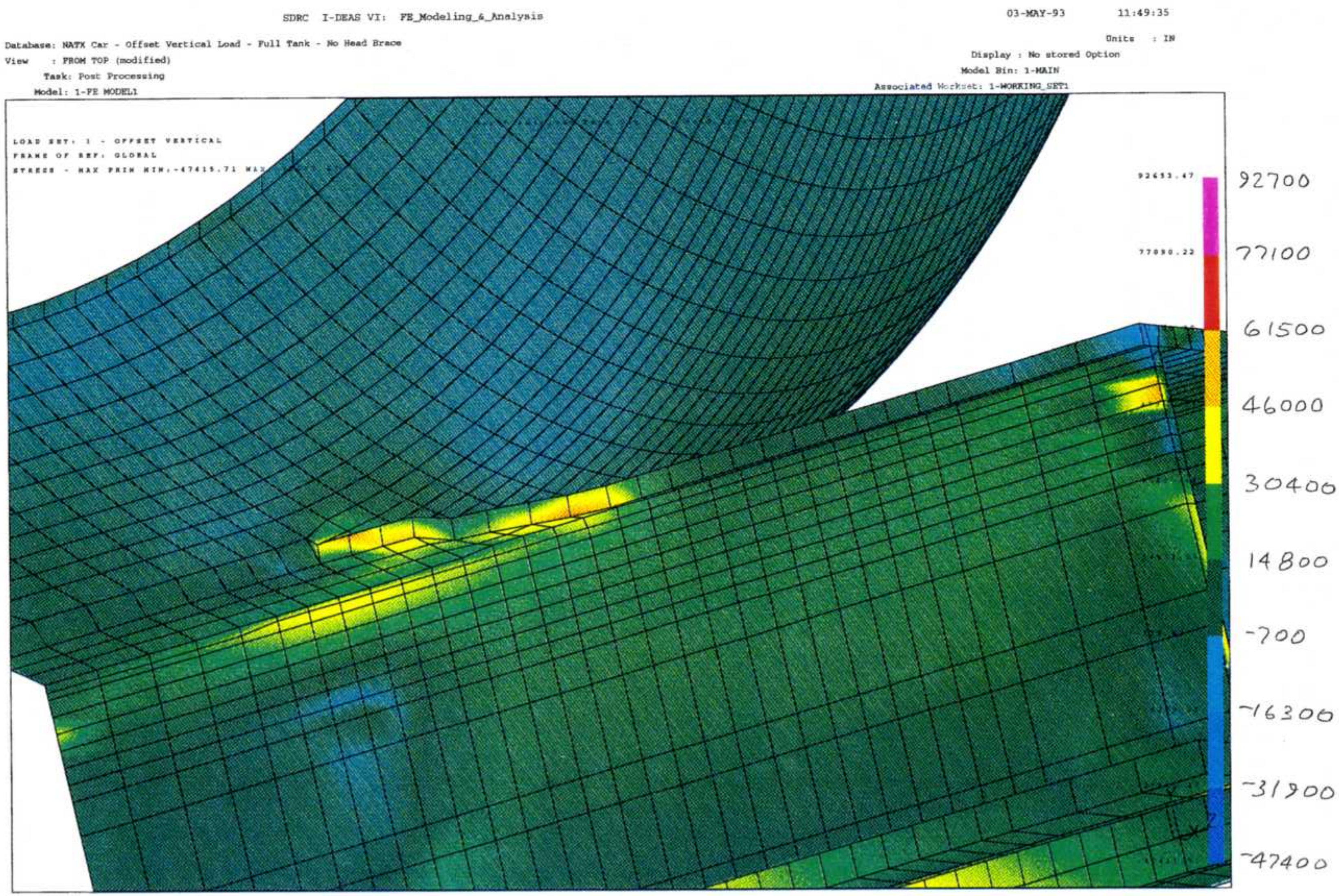

FIGURE C-1. NATX MAXIMUM PRINCIPAL STRESSES, OFFSET VERTICAL, FULL TANK, NO HEAD BRACE (-X VIEW); Maximum Stress = 92.7 ksi, Minimum Stress = -47.4 ksi

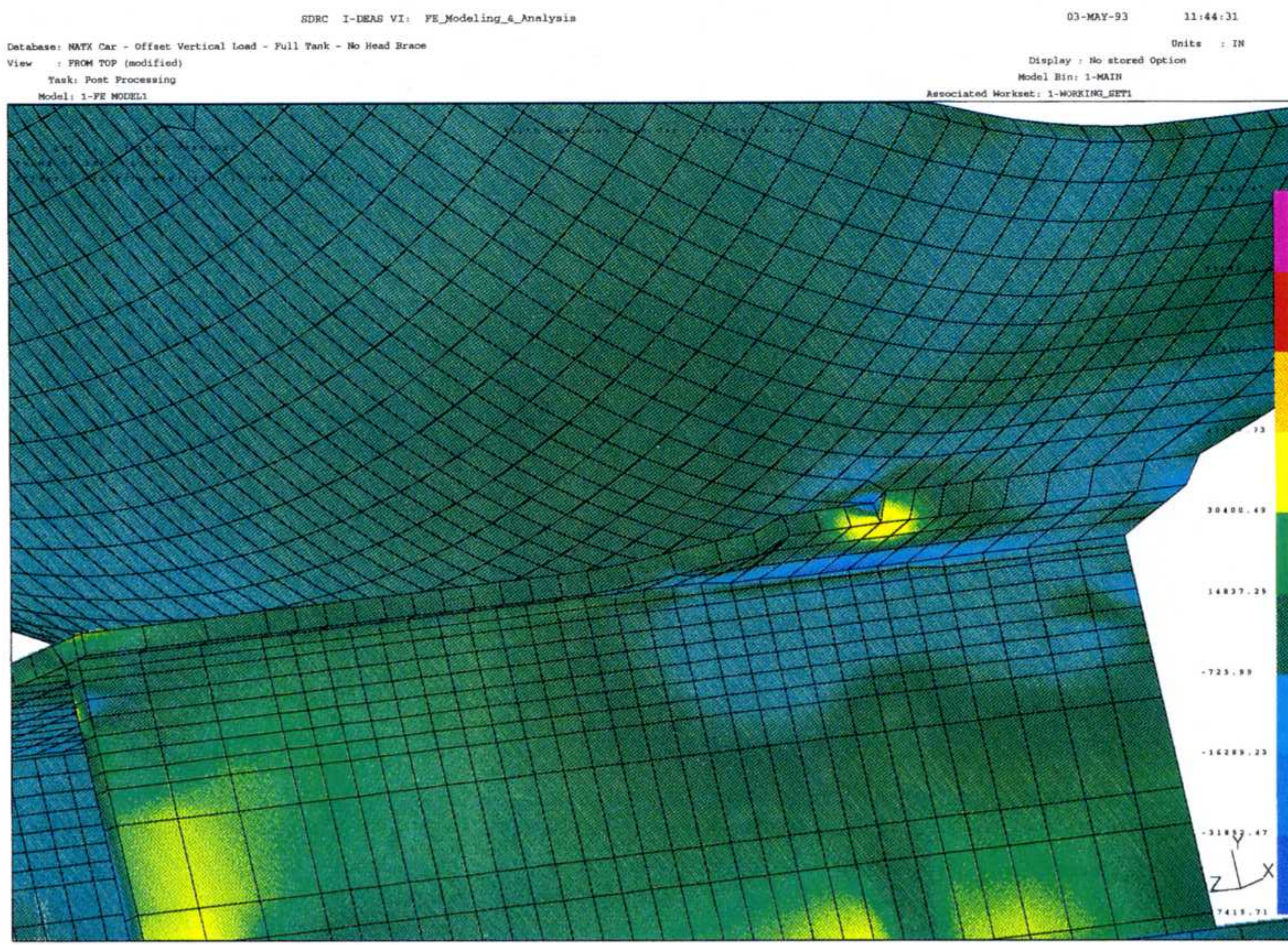

FIGURE C-2. NATX MAXIMUM PRINCIPAL STRESSES, OFFSET VERTICAL, FULL TANK, NO HEAD BRACE (+X VIEW); Maximum Stress = 92.7 ksi, Minimum Stress = -47.4 ksi

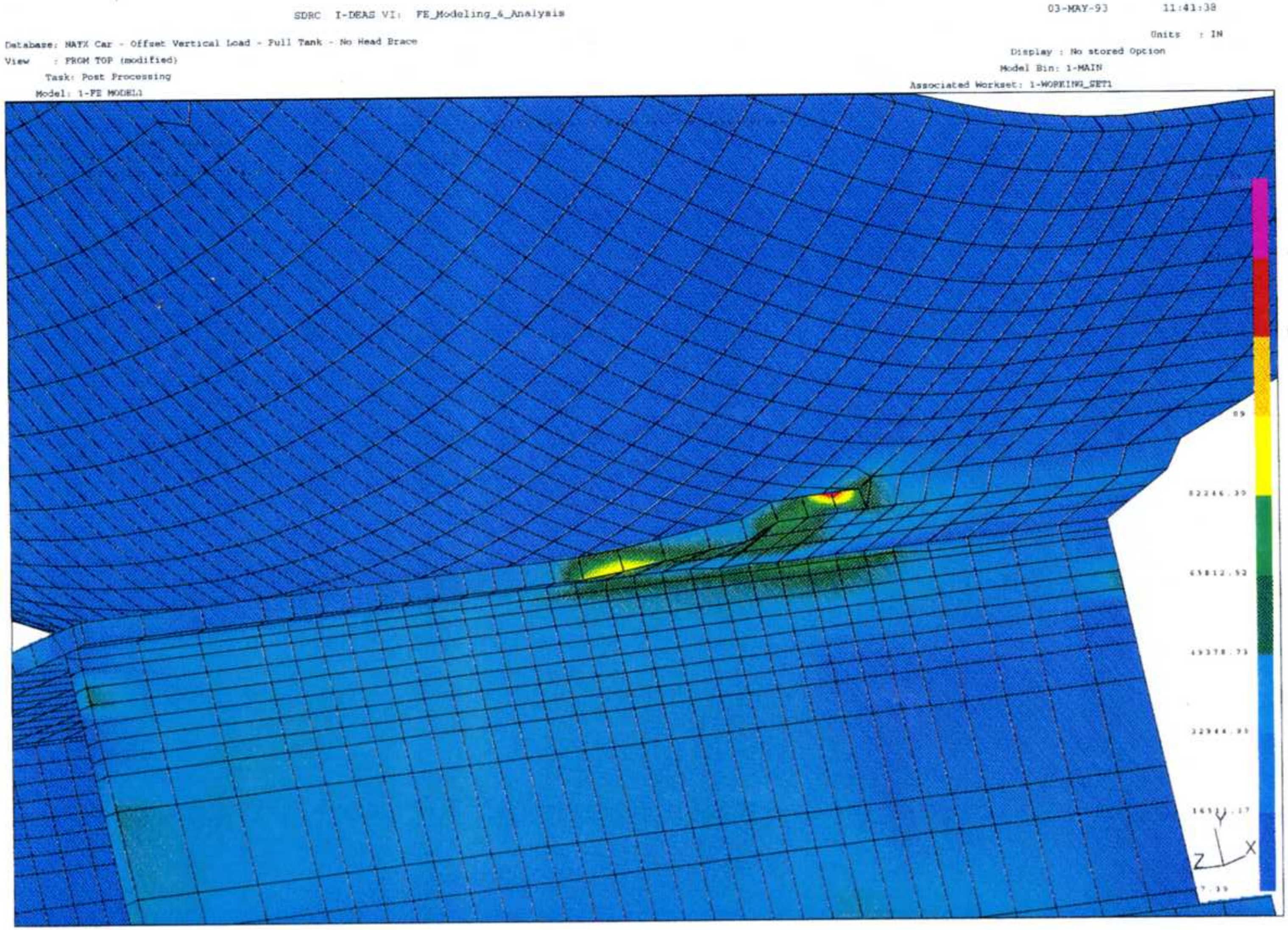

FIGURE C-3. NATX VON MISES STRESSES, OFFSET VERTICAL, FULL TANK, NO HEAD BRACE; Maximum Stress = 148.0 ksi, Minimum Stress = -0.0 ksi

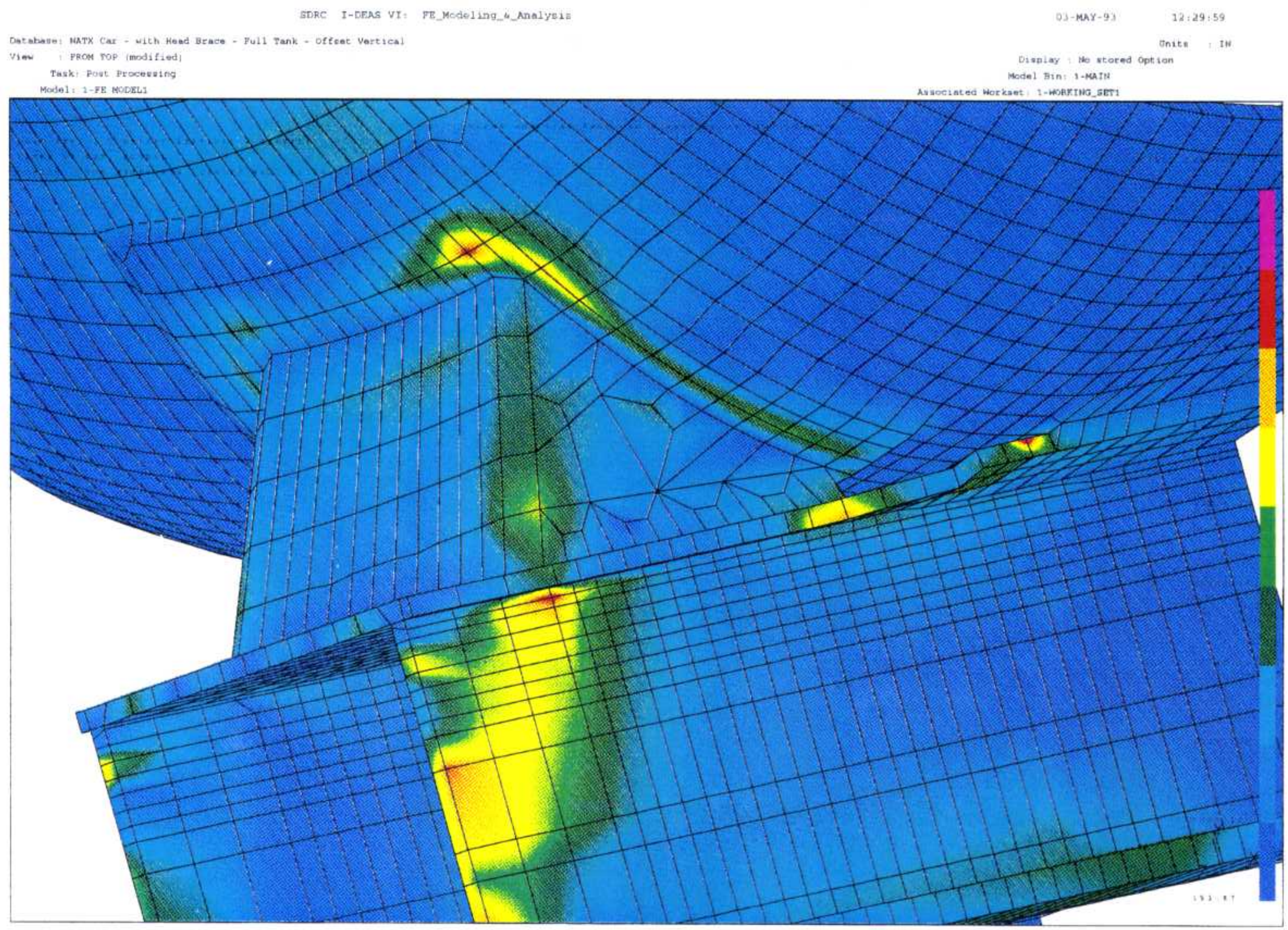

FIGURE C-4. NATX VON MISES STRESSES, OFFSET VERTICAL, FULL TANK, WITH HEAD BRACE; Maximum Stress = 61.9 ksi, Minimum Stress = 0.2 ksi

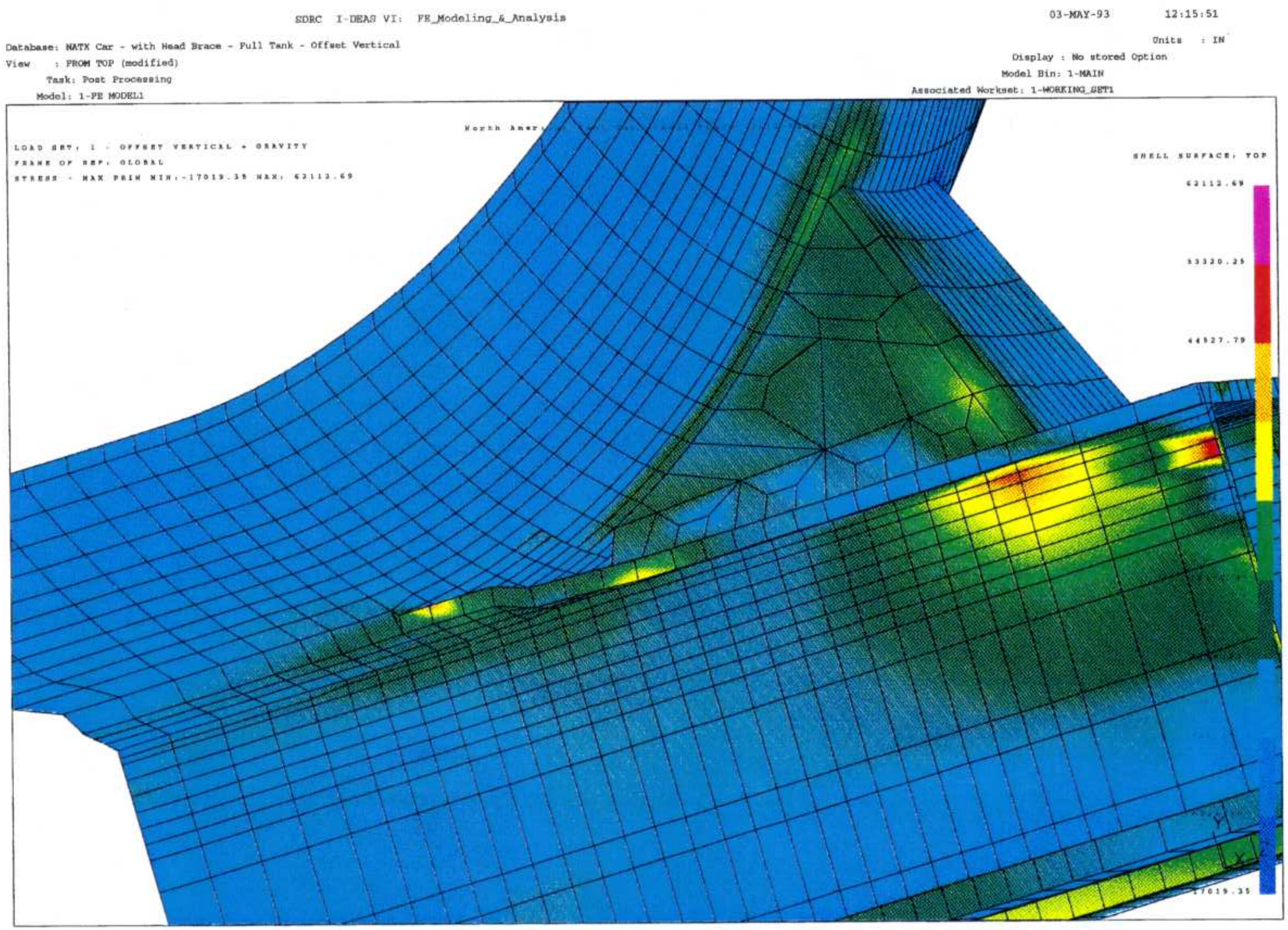

FIGURE C-6. NATX MAXIMUM PRINCIPAL STRESSES OFFSET VERTICAL, FULL TANK, WITH HEAD BRACE (-X VIEW); Maximum Stress = 62.1 ksi, Minimum Stress = -17.0 ksi

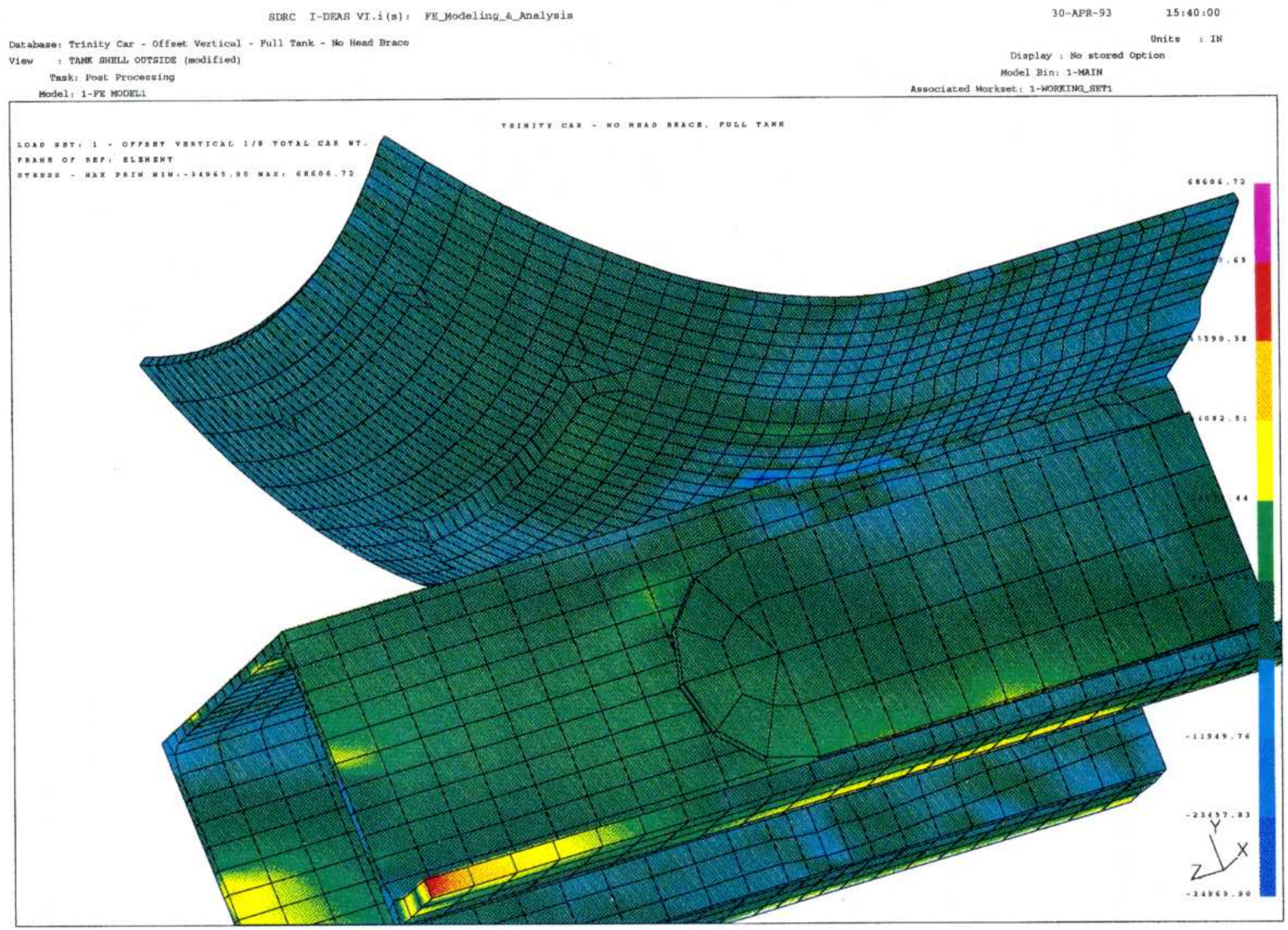

FIGURE C-7. TRINITY MAXIMUM PRINCIPAL STRESSES, OFFSET VERTICAL, FULL TANK, NO HEAD BRACE (+X VIEW); Maximum Stress = 68.6 ksi, Minimum Stress = -35.0 ksi

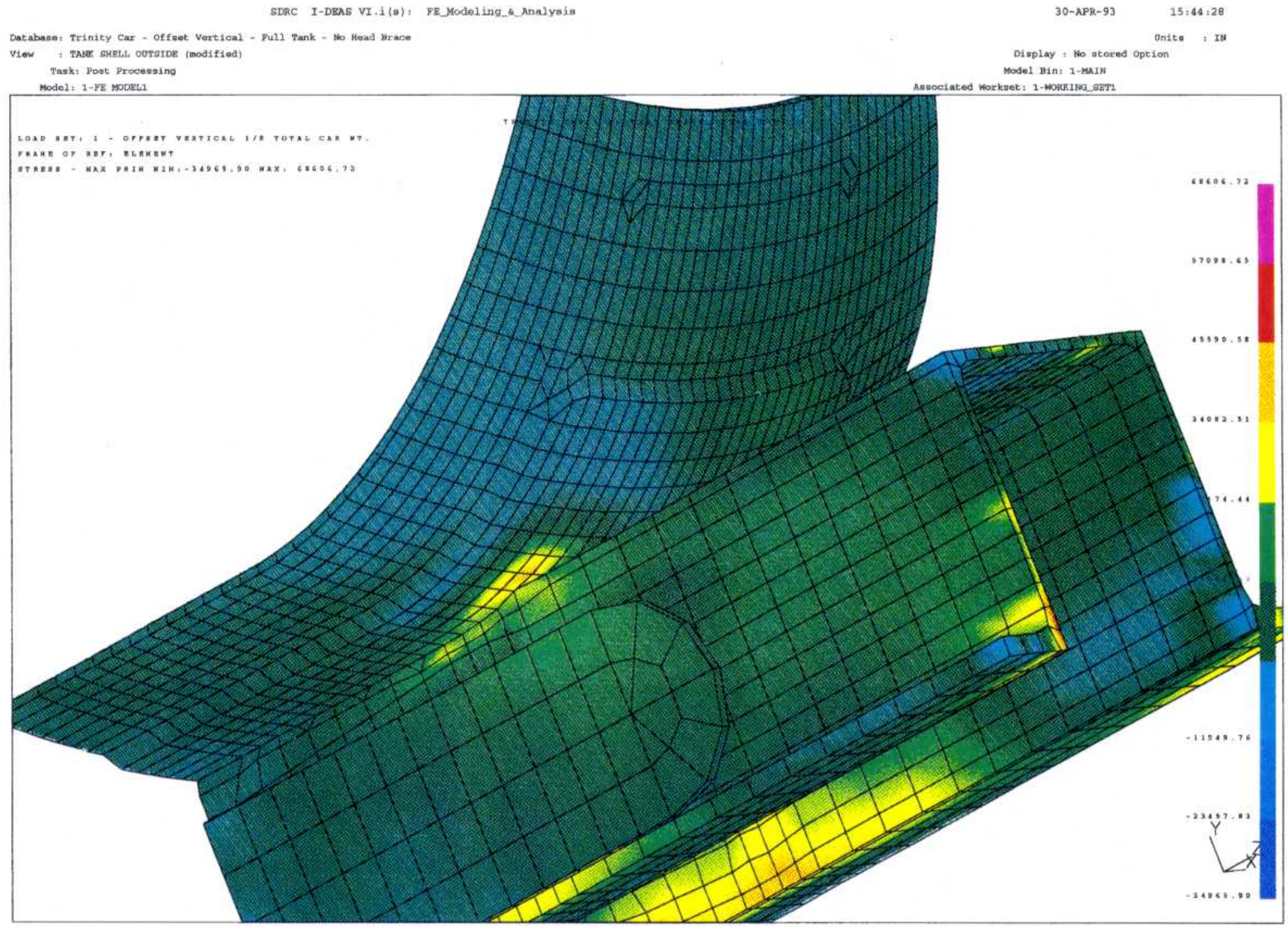

FIGURE C-8. TRINITY MAXIMUM PRINCIPAL STRESSES, OFFSET VERTICAL, FULL TANK, NO HEAD BRACE (-X VIEW); Maximum Stress = 68.6 ksi, Minimum Stress = -35.0 ksi

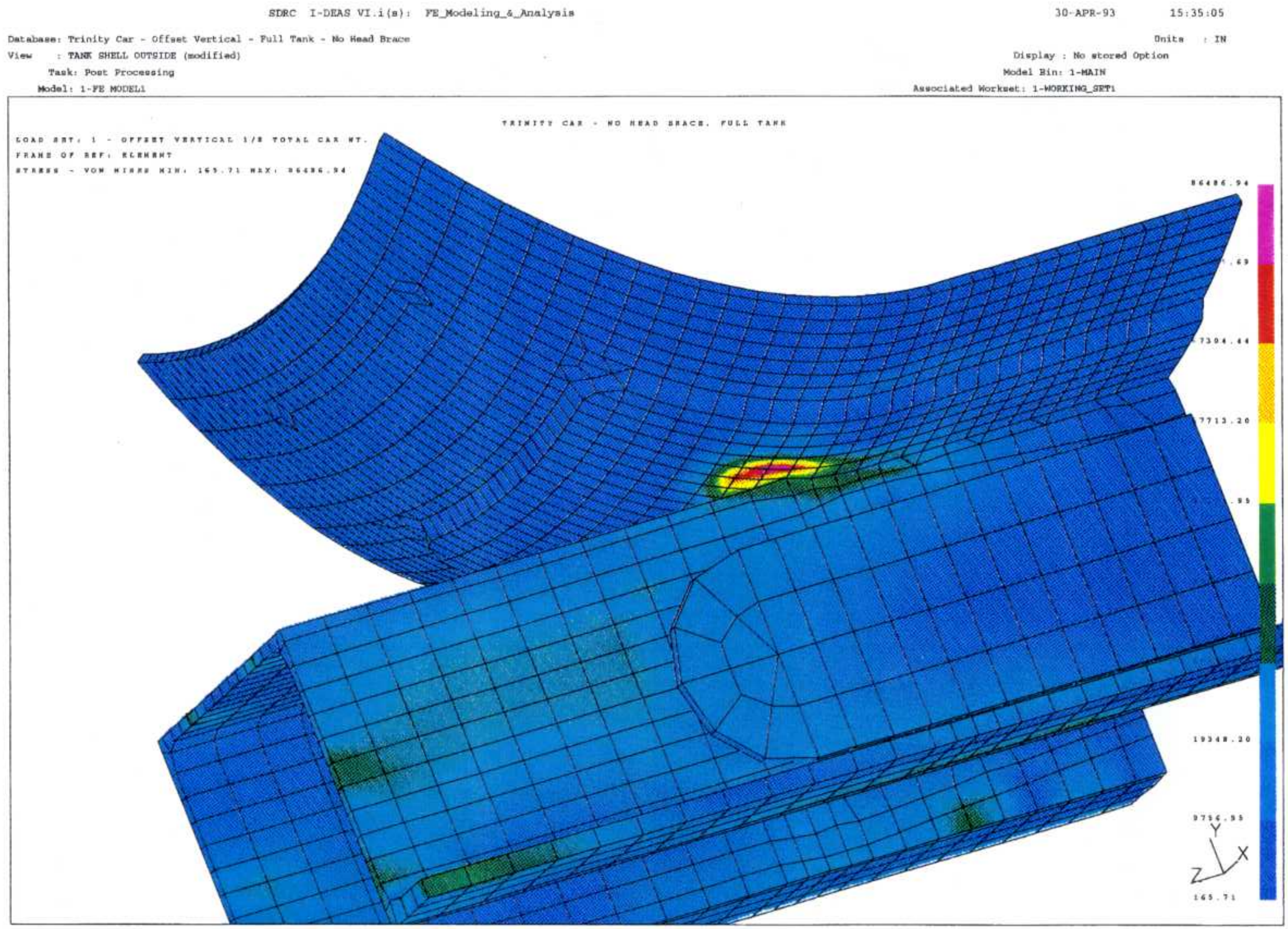

FIGURE C-9. TRINITY VON MISES STRESSES, OFFSET VERTICAL, FULL TANK, NO HEAD BRACE; Maximum Stress = 86.5 ksi, Minimum Stress = 0.2 ksi

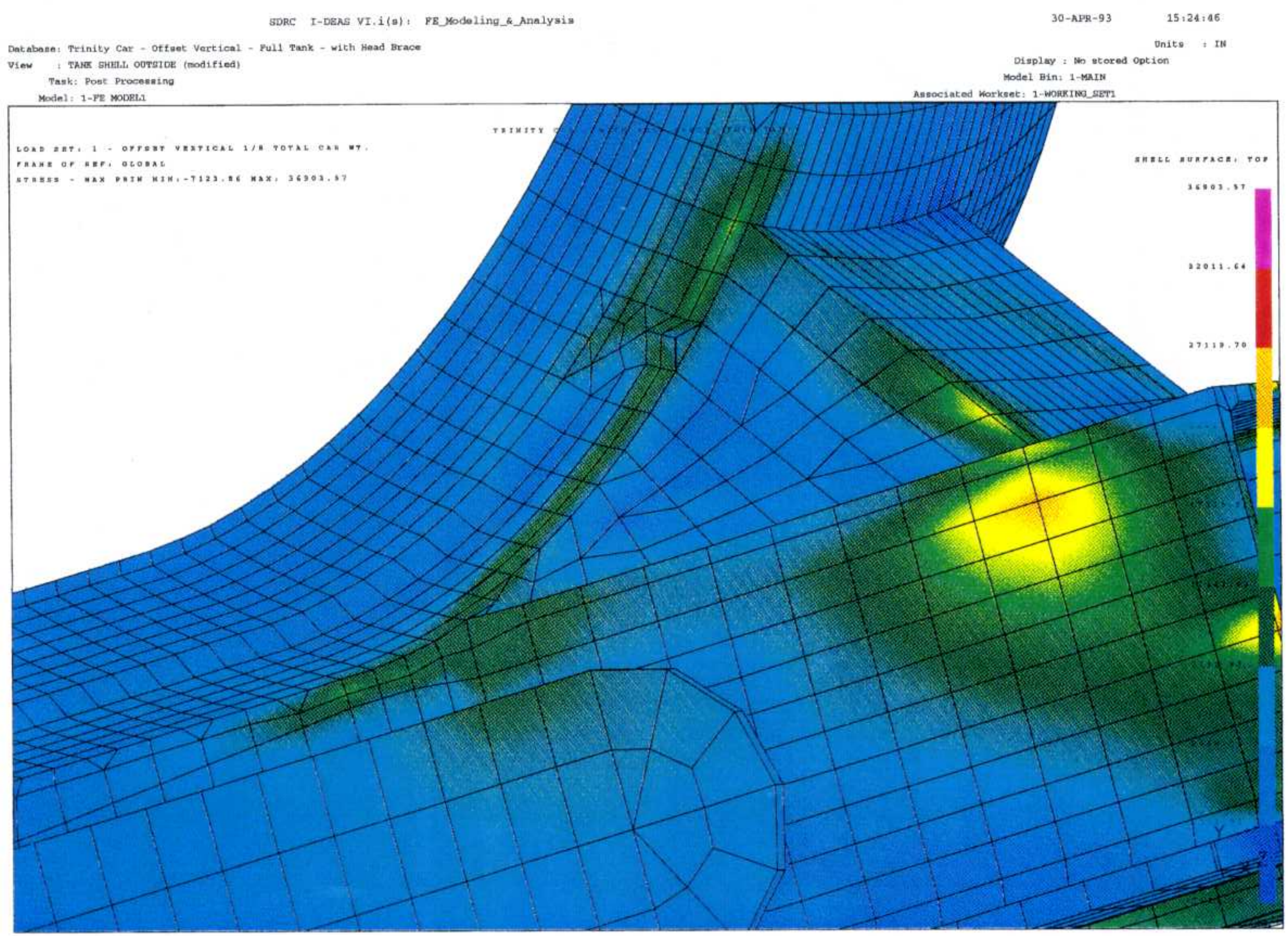

FIGURE C-10. TRINITY MAXIMUM PRINCIPAL STRESSES, OFFSET VERTICAL, FULL TANK, WITH HEAD BRACE; Maximum Stress = 36.9 ksi, Minimum Stress = -7.1 ksi

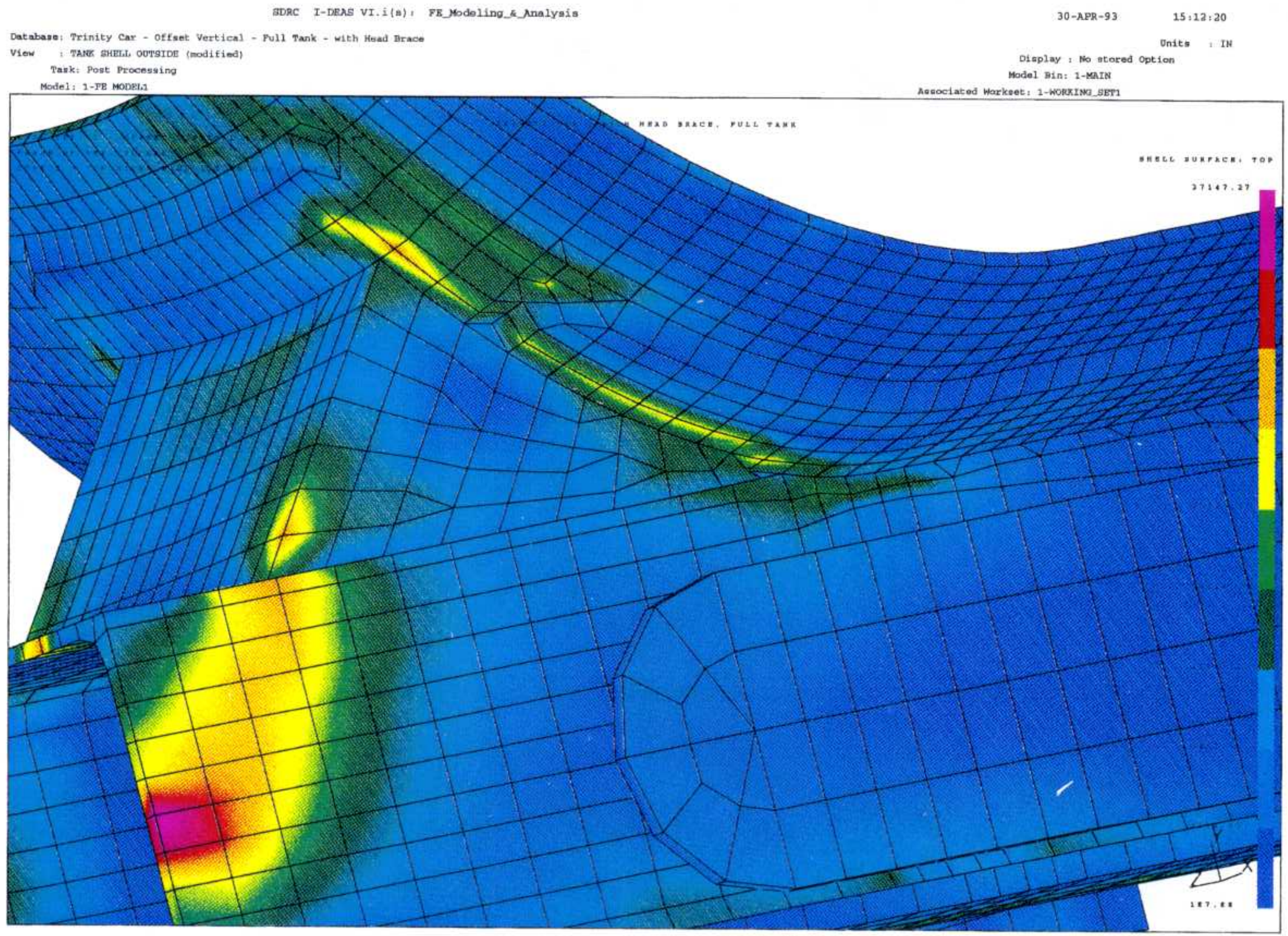

FIGURE C-11. TRINITY VON MISES STRESSES, OFFSET VERTICAL, FULL TANK, WITH HEAD BRACE; Maximum Stress = 37.2 ksi, Minimum Stress = 0.2 ksi